INDC(JPN)-172/U

NOT FOR PUBLICATION

PROGRESS REPORT

(July 1993 to June 1994 inclusive)

August 1994

Editor

Y. Nakajima

Japanese Nuclear Data Committee

Japan Atomic Energy Research Institute
Tokai Research Establishment
Tokai-mura, Ibaraki-ken, Japan

Editor's Note

This is a collection of reports which have been submitted to the Japanese Nuclear Data Committee at the committee's request. The request was addressed to the following individuals who might represent or be in touch with groups doing researches related to the nuclear data of interest to the development of the nuclear energy program.

Although the editor tried not to miss any appropriate addressees, there may have been some oversight. Meanwhile, contribution of a report rested with discretion of its author. The coverage of this document, therefore, may not be uniform over the related field or research.

In this progress report, each individual report is generally reproduced as it was received by the JNDC secretariat, and editor also let pass some simple obvious errors in the manuscripts if any.

This edition covers a period of July 1, 1993 to June 30, 1994. The information herein contained is of a nature of "Private Communication". <u>Data contained in this report should not be quoted without the author's permission.</u>

Table of Contents

ELEMENT S	A	QUANTITY	ENERGY MIN	MAX	LAB	TYPE	DOCUMENTATION REF VOL PAGE	DATE	COMMENTS
C	12	EVALUATION	2.0+7	5.0+7	JAE	EVAL-PROG	INDC(JPN)172/U	AUG 94	CHIBA+.P20.TOT,SEL,SIN,PEM,AEM. NDG
C	12	(N,2N)	1.8+7	6.5+7	TOH	EXPT-PROG	INDC(JPN)172/U	AUG 94	NAKAMURA+.P99.(N,2NA)ACT-SIG IN FIG
C	12	P EMISSION	4.0+7	6.4+7	JAE	EXPT-PROG	INDC(JPN)172/U	AUG 94	BABA+.P94.DDX.NDG
C	12	D EMISSION	4.0+7	6.4+7	JAE	EXPT-PROG	INDC(JPN)172/U	AUG 94	BABA+.P94.DDX.NDG
C	12	T EMISSION	4.0+7	6.4+7	JAE	EXPT-PROG	INDC(JPN)172/U	AUG 94	BABA+.P94.DDX.NDG
C	12	A EMISSION	1.0+7	8.0+7	KYU	EVAL-PROG	INDC(JPN)172/U	AUG 94	WATANABE+.P61.MONTE CARLO CAL.KERMA
AL	27	(N,2N)	1.8+7	6.5+7	TOH	EXPT-PROG	INDC(JPN)172/U	AUG 94	NAKAMURA+.P99.(N,2NA)ACT-SIG IN FIG
SI	28	TOTAL	2.0+7	1.0+9	JPN	EVAL-PROG	INDC(JPN)172/U	AUG 94	IKEHARA+.P123.SYSTEMATICS+OPTMDL,FIG
SI	28	NONELASTIC	2.0+7	1.0+9	JPN	EVAL-PROG	INDC(JPN)172/U	AUG 94	IKEHARA+.P123.SYSTEMATICS+OPTMDL,FIG
CR	50	A EMISSION	4.5+6	1.4+7	TOH	EXPT-PROG	INDC(JPN)172/U	AUG 94	BABA+.P93.NDG
FE		A EMISSION	4.3+6	1.4+7	TOH	EXPT-PROG	INDC(JPN)172/U	AUG 94	BABA+.P92.PUBL IN NST,31,745
FE		A EMISSION	4.5+6	1.4+7	TOH	EXPT-PROG	INDC(JPN)172/U	AUG 94	BABA+.P93.NDG
NI		A EMISSION	4.5+6	1.4+7	TOH	EXPT-PROG	INDC(JPN)172/U	AUG 94	BABA+.P93.NDG
NI		A EMISSION	4.3+6	1.4+7	TOH	EXPT-PROG	INDC(JPN)172/U	AUG 94	BABA+.P92.PUBL IN NST,31,745
NI		A EMISSION	1.4+7		OSA	EXPT-PROG	INDC(JPN)172/U	AUG 94	TAKAHASHI+.P80.DDX IN FIG
CU		A EMISSION	4.5+6	1.4+7	TOH	EXPT-PROG	INDC(JPN)172/U	AUG 94	BABA+.P93.NDG
CU	63	TOTAL	2.0+7	1.0+9	JPN	EVAL-PROG	INDC(JPN)172/U	AUG 94	IKEHARA+.P123.SYSTEMATICS+OPTMDL,FIG
CU	63	NONELASTIC	2.0+7	1.0+9	JPN	EVAL-PROG	INDC(JPN)172/U	AUG 94	IKEHARA+.P123.SYSTEMATICS+OPTMDL,FIG
SR	90	(N,GAMMA)	2.5-2		JAE	EXPT-PROG	INDC(JPN)172/U	AUG 94	HARADA+.P69.PUBL IN NST,31,173
SR	90	RES INT CAP	5.0-1		JAE	EXPT-PROG	INDC(JPN)172/U	AUG 94	HARADA+.P69.PUBL IN NST,31,173

ELEMENT S	A	QUANTITY	ENERGY MIN	MAX	LAB	TYPE	DOCUMENTATION REF VOL PAGE	DATE	COMMENTS
NB	93	N EMISSION	1.4+7	1.8+7	TOH	EXPT-PROG	INDC(JPN)172/U	AUG 94	BABA+.P92.TBP IN NST
MO		N EMISSION	1.4+7		TOH	EXPT-PROG	INDC(JPN)172/U	AUG 94	BABA+.P92.TBP IN NST
TC	99	(N,GAMMA)	2.5-2		YOK	EXPT-PROG	INDC(JPN)172/U	AUG 94	HARADA+.P67.SIG=22.7+-1.1 B
TC	99	RES INT CAP	5.0-1		YOK	EXPT-PROG	INDC(JPN)172/U	AUG 94	HARADA+.P67.RI=395+-34 B
CS	137	(N,GAMMA)	2.5-2		JAE	EXPT-PROG	INDC(JPN)172/U	AUG 94	SEKINE+.P68.PUBL IN NST,30,1099
CS	137	RES INT CAP	5.0-1		JAE	EXPT-PROG	INDC(JPN)172/U	AUG 94	SEKINE+.P68.PUBL IN NST,30,1099
TA	181	N EMISSION	1.4+7		TOH	EXPT-PROG	INDC(JPN)172/U	AUG 94	BABA+.P92.TBP IN NST
TA	181	(N,P)	1.3+7	1.5+7	OSA	EXPT-PROG	INDC(JPN)172/U	AUG 94	KASUGAI+.P70.TBP IN NST
TA	181	(N,NP)	1.3+7	1.5+7	OSA	EXPT-PROG	INDC(JPN)172/U	AUG 94	KASUGAI+.P70.TBP IN NST
W		N EMISSION	1.4+7		TOH	EXPT-PROG	INDC(JPN)172/U	AUG 94	BABA+.P92.TBP IN NST
W	184	(N,ALPHA)	1.3+7	1.5+7	OSA	EXPT-PROG	INDC(JPN)172/U	AUG 94	KASUGAI+.P70.TBP IN NST
W	186	(N,ALPHA)	1.3+7	1.5+7	OSA	EXPT-PROG	INDC(JPN)172/U	AUG 94	KASUGAI+.P70.TBP IN NST
W	188	(N,NP)	1.3+7	1.5+7	OSA	EXPT-PROG	INDC(JPN)172/U	AUG 94	KASUGAI+.P70.TBP IN NST
AU	197	(N,2N)	1.8+7	2.3+7	JAE	EXPT-PROG	INDC(JPN)172/U	AUG 94	UNO+.P26.ABSOLUTE ACT-SIG IN FIG
PB		TOTAL	2.0+0	1.5+5	KTO	EXPT-PROG	INDC(JPN)172/U	AUG 94	KOBAYASHI+.P45.TRANSMISSION EXPT.FIG
PB	208	TOTAL	2.0+0	1.5+5	KTO	EXPT-PROG	INDC(JPN)172/U	AUG 94	KOBAYASHI+.P45.TRANSMISSION EXPT.FIG
BI	209	(N,XN) X>2	1.8+7	6.5+7	TOH	EXPT-PROG	INDC(JPN)172/U	AUG 94	NAKAMURA+.P99.X=3,4,5. FIG GIVEN
BI	209	N EMISSION	1.4+7	1.8+7	TOH	EXPT-PROG	INDC(JPN)172/U	AUG 94	BABA+.P92.TBP IN NST
U	233	FRAG SPECTRA	2.5-2		KTO	EXPT-PROG	INDC(JPN)172/U	AUG 94	HAKODA+.P76.DOUBLE E METHOD.FIG GVN
U	235	FISS PROD GS	2.5-2		KTO	EXPT-PROG	INDC(JPN)172/U	AUG 94	SHIBATA+.P70.PR151 DECAY. TBP IN JPJ

ELEMENT S	A	QUANTITY	ENERGY MIN	MAX	LAB	TYPE	DOCUMENTATION REF VOL PAGE	DATE	COMMENTS
U	235	FISS YIELD	2.5-2		KTO	EXPT-PROG	INDC(JPN)172/U	AUG 94	HAKODA+.P76.DOUBLE E METHOD.FIG GVN
U	235	FRAG SPECTRA	2.5-2		KTO	EXPT-PROG	INDC(JPN)172/U	AUG 94	HAKODA+.P76.DOUBLE E METHOD.FIG GVN
U	238	TOT INELAST	NDG		KYU	EVAL-PROG	INDC(JPN)172/U	AUG 94	KANDA.P59,NDG
U	238	DIFF INELAST	NDG		KYU	EVAL-PROG	INDC(JPN)172/U	AUG 94	KAWANO+.P60.PUBL IN JAERI-M94-19,290
U	238	DIFF INELAST	NDG		KYU	EVAL-PROG	INDC(JPN)172/U	AUG 94	KAWANO+.P60.CC CALC. NDG
U	238	(N,GAMMA)	NDG		KYU	EVAL-PROG	INDC(JPN)172/U	AUG 94	KANDA.P59.NDG
PU	237	EVALUATION	1.0-5	2.0+7	JAE	EVAL-PROG	INDC(JPN)172/U	AUG 94	NAKAGAWA+.P15.ALL QUANTITIES, FIG
PU	239	FISS YIELD	2.5-2		KTO	EXPT-PROG	INDC(JPN)172/U	AUG 94	HAKODA+.P76.DOUBLE E METHOD.FIG GVN
PU	239	FRAG SPECTRA	2.5-2		KTO	EXPT-PROG	INDC(JPN)172/U	AUG 94	HAKODA+.P76.DOUBLE E METHOD.FIG GVN
PU	244	EVALUATION	1.0-5	2.0+7	JAE	EVAL-PROG	INDC(JPN)172/U	AUG 94	NAKAGAWA+.P15.ALL QUANTITIES, FIG
AM	241	FISSION	1.0-1	1.0+4	KTO	EXPT-PROG	INDC(JPN)172/U	AUG 94	KOBAYASHI+.P42.REL TO U235 NF. FIG
CF	252	FISS YIELD	SPON		OSA	EXPT-PROG	INDC(JPN)172/U	AUG 94	HAKODA+.P76.DOUBLE E METHOD.FIG GVN
CF	252	FRAG SPECTRA	SPON		OSA	EXPT-PROG	INDC(JPN)172/U	AUG 94	HAKODA+.P76.DOUBLE E METHOD.FIG GVN
MANY		EVALUATION	1.0-5	2.0+7	JAE	EVAL-PROG	INDC(JPN)172/U	AUG 94	KAWAI+.P13.FP'S FOR JENDL-3.2
MANY		EVALUATION	1.0-5	2.0+7	JAE	EVAL-PROG	INDC(JPN)172/U	AUG 94	P11.RE-EVALUATION FOR JENDL-3.2
MANY		(N,2N)	TR	2.0+7	JAE	EVAL-PROG	INDC(JPN)172/U	AUG 94	KONSHIN.P17.Z=90-98(72 NUCL), NDG
MANY		(N,XN) X>2	TR	2.0+7	JAE	EVAL-PROG	INDC(JPN)172/U	AUG 94	KONSHIN.P17.X=3.Z=90-98(72 NUCL),NDG
MANY		FISSION	1.0+6	2.0+7	JAE	EVAL-PROG	INDC(JPN)172/U	AUG 94	KONSHIN.P17.Z=90-98(72 NUCL), NDG
MANY		LVL DENSITY	/		JAE	THEO-PROG	INDC(JPN)172/U	AUG 94	MENGONI+.P22.INTERACT BOSON MDL. NDG
MANY		LVL DENSITY	/		JPN	THEO-PROG	INDC(JPN)172/U	AUG 94	NAKAMURA.P3.SHELL-PAIRING CORR. FIG

ELEMENT S A	QUANTITY	ENERGY MIN	ENERGY MAX	LAB	TYPE	DOCUMENTATION REF	VOL	PAGE	DATE	COMMENTS
MANY	LVL DENSITY	/		JAE	THEO-PROG	INDC(JPN)172/U			AUG 94	MENGONI+.P21.LDL PARAM IN FIG

The content table in the CINDA format was compiled by the JNDC CINDA group:
S.Chiba(JAERI), M.Kawai(Toshiba), H.Kitazawa(Tokyo Inst. of Technol.), H.Matsunobu(Sumitomo At. Energy Industries), T.Nakagawa(JAERI), R.Nakasima(Hosei Univ.), K.Shibata(JAERI)

I. Fuji Electric Co., Ltd.

A. Nuclear Engineering Division

I-A-1 Nuclear Level Density Formula with Shell-Pairing Correlation Terms

H.Nakamura

We are proposing a semi-empirical level density formula with the renewed systematics of its parameters. Among the simple semi-empirical models which account for the energy-dependent shell and pairing corrections of the nuclear level density, the KRK[1] model is a typical one. This model relates the shell and pairing effects on the level density to the ground state corrections

$$E_S + E_P = M_{exp} - M_{drop} \tag{1}$$

defined as the differences of the experimental mass M_{exp} and the liquid drop mass M_{drop} (gross terms). However, the above shell and pairing corrections, E_s and E_P respectively, do not take the unique contents but depend on the different mass formulas, from which the shell and pairing corrections are available. Separation of those corrections on the level density parameters is not clear in literatures. The typical correction energies are those of Meyers and Swiatecki[2] for the shell energy E_s, and of Gilbert and Cameron[3] for the pairing energy E_P. On the other hand, the shell-pairing correlation effects seems to be correctly considered only by means of the microscopic Fermi-gas model[4], which has, however, still an inaccuracy due to the formalism in the superconducting phase[5].

The purpose of the present work is to make those contents of correction clear on the level density formula and its parameters, and to obtain a new systematics. In the present model, an analytic expression similar to the previous KRK model is adopted for the single-particle states, in particular, considering the shell-pairing correlation (called as 'SPC model'). The nuclear level density formula is derived by using the Fourier expansion of single-particle state density, considering only a fundamental harmonic for the main-shell overlaped with the sub-shell due to pairing interaction :

$$g(\varepsilon) = \sum_{x} g_{ox}[1+f_x\cdot\cos\{Q(\varepsilon-\varepsilon_x)\}][1-\cos\{q(\varepsilon-\lambda)\}], \tag{2}$$

$Q = 2\pi/\hbar W$, related to the main-shell spacing $\hbar W$.

$q = 2\pi/\hbar w$, related to the pairing energy.

ε_x = main-shell position.

λ = Fermi level.

g_{ox} = average single-particle state density (2-fold degenerate).

f_x = amplitude of main-shell.

x = stand for proton(=z) or neutron(=n) shell.

After the traditional statistical process the well-known expression of the level density formula is obtained as :

$$\rho(U, J, \Pi) = \tfrac{1}{2} W(J) R(U) K_{rot}(U), \tag{3}$$

where the factor $\frac{1}{2}$ is assumed for equal probability of parity states Π, $W(J)$ and $R(U)$ are the components depending on the total spin J and the excitation energy U respectively, and K_{rot} is the rotational enhancement factor[6]. The main features different from the previous formula appear in the following factors :

$$U = a t^2 + E_S[h_1(T)h_2(T)-1] - E_P[h_1(T_P)h_2(T_P)-1] \tag{4}$$

$E_S = C_S f \cdot \cos(2\pi X)$, shell correction energy.

X = occupied fraction of the main-shell.

$E_P = C_P \delta[1 - F_P(E_S/C_S)]$, pairing correction energy

$h_1(T) = T \cdot \mathrm{cosech}(T)$, $h_2(T) = T \cdot \coth(T)$

$T \equiv \pi Q t$, $T_P \equiv \pi q t$

δ = 1(even protons or neutrons), = 0(odd)

$$S = 2 a t \text{ , entropy} \tag{5}$$

$$a = a_0 + \tfrac{1}{2} t^{-2}[E_S \cdot h_1(T)\{h_2(T)-1\} - E_P \cdot h_1(T_P)\{h_2(T_P)-1\}] \tag{6}$$

a_0 = asymptotic level density parameter

$$\sigma^2 = I t \text{ , spin cut-off factor} \tag{7}$$

I = moment of inertia of nucleus

t = thermodynamic temperature

$$I = I_0 + I_0 \delta[- h_1(T_P) + (E_S/C_S)\{h_1(T)-h_1(T_P)\}] \tag{8}$$

$I_0 = I_r$, (for spherical nuclei)

$= I_\perp^{2/3} I_\parallel^{1/3}$, (for axially symmetric deformed nuclei)

$I_r = 0.015 A^{5/3}$, Fermi-gas moment of inertia

A = mass number

$I_\perp = I_r(1 + \varepsilon/3)$, $I_\parallel = I_r(1 - 2\varepsilon/3)$

ε = a parameter of quadrupole deformation.

$$K_{rot}(U) = I_\perp t \text{ , for deformed nuclei.} \tag{9}$$

As a result of the formulation the traditional prescription of the odd-even mass difference, which is used to define the effective excitation energy, is not needed. An advantage of the present model is no use of independent shell and pairing correction tables, as used in the previous one. At the ground state the shell and pairing corrections, E_S and E_P in Eq. (4), are obtained by fitting the empirical mass excess data, assuming from Eq. (4) as,

$$[E_S]_{exp} = \{C_S \cdot X(1-X) - C_1 \cdot X - C_2\} \cdot FF, \tag{10}$$

X = occupied fraction for each shell of proton or neutron,
magic numbers are assumed as [14, 28, 50, 82, 126, 184].

$FF = \exp\{-C_3\cdot(X-X_{D1})(X_{D2}-X)\}$, for deformed regions

(D1, D2) = 58<Z<76 or Z>90,

94<N<118 or N>138.

$FF = 1.0$: for spherical regions.

$$[E_P]_{exp} = C_P\delta[1 - F_P(E_s/C_s)] \quad : \text{for proton or neutron shell} \qquad (11)$$

$[E_s]_{exp}$ and $[E_P]_{exp}$ are empirical shell and pairing energies respectively, adjusted by using the constant-shell terms and the gross term of Ref.7 as the first guess, and the empirical mass excess data of Ref.8. Free parameters included in the present formula are from Eqs.(10) and (11), C_s, $C_i(i=1,3)$ = shell correction const., C_P = pairing correction const., F_P = amplitude for shell-pairing correlation. For total 1996 nuclei, the mean deviation ΔM between the empirical and the computed masses is $\Delta M = 0.373$ MeV. This error is the σ_{th} defined by the relations[9],

$$\sigma_{th} = [\Sigma W\{(M_{th}-M_{exp})^2-\sigma_{exp}^2\}/\Sigma W]^{1/2}, \quad W = 1/(\sigma_{exp}^2 + \sigma_{th}^2) \qquad (12)$$

where the summation is over the whole empirical masses and the final σ_{th} is easily obtained within a few iterations.

For the excited states, free parameters of the present level density formula are the following 3 parameters, and its mass-dependence is assumed as respectively

$a_0 = A_0\cdot A$: asymptotic level density parameter

$W = W_0\cdot A^{1/3}$: main-shell spacing (13)

$q = q_0\cdot A^{1/2}$: related to the pairing constant C_P of Eq.(11) by a relation $C_P = g_0/q^2$.

In the above, a value of constant q_0 is estimated by assuming as[4],

$$q^2 = g_0/C_P, \quad C_P \fallingdotseq \tfrac{1}{4}g_0\Delta^2, \quad \Delta = 12/A^{1/2}$$

$$q = 2/\Delta = (1/6)A^{1/2} = 0.167A^{1/2}, \qquad q_0 = 0.167. \qquad (14)$$

The predictions of the SPC model are compared with those of other semi-empirical models, the traditional FG (Fermi-gas) model and the KRK model. A set of values (A_0, W_0) is determined for the level density formula to fit the s-wave neutron or the proton resonance spacings, which have been analyzed in the previous study[5]. The shell and pairing corrections are those of the present work described above. A measure of the quality associated with the systematics is taken as the root mean squares (rms) deviation defined for the parameter a_0 as

$$\chi^2 = \sum_i (a_{0i} - A_0\cdot A_i)^2 \quad , \text{for all nuclei.} \qquad (15)$$

The values for A_0 and W_0 of KRK and SPC models, and A_0 of FG model respectively are found by minimizing the quantity χ^2. Fig.1 shows the spread of the a_0 values for FG, KRK and SPC model respectively. The analyses using the s-wave neutron and proton resonance spacings of the mass range A = 41～67 show that the prediction of the present formula and its parameters will be superior to those of the previous models. Those systematic improvements may be due to the analytical expression for the shell-pairing correlation terms in the level density formula.

Further studies of the systematics for the mass range of A > 70, specially for deformed nuclei, will be necessary to validate the present SPC model over a wide range of nuclei.

References ;

1) Kataria S.K., Ramamurthy V.S. and Kapoor S.S.: Phys.Rev., C18, 549(1978).
2) Meyers W.D. and Swiatecki W.S.: Ark. Fys., 36, 343(1967).
3) Gilbert A. and Cameron A.W.G.: Can.J.Phys., 43, 1446(1965).
4) Moretto L.G.: Nucl.Phys.A182, 641(1972).
5) Vonach H., et al: Phys.Rev., C38, 2541(1988).
6) Ignatyuk A.V., Istekov K.K. and Smirenkin G.N.: Sov.J.Nucl.Phys.29, 450(1979).
7) Ando Y., Uno M. and Yamada M.: JAERI-M 83-025(1983).
8) Wapstra A.H., Audi G. and Hoekstra R.: Atomic Data and Nuclear Data Tables, 39 281(1988).
9) Moller P. and Nix J.R.: ibid., 39, 213(1988).

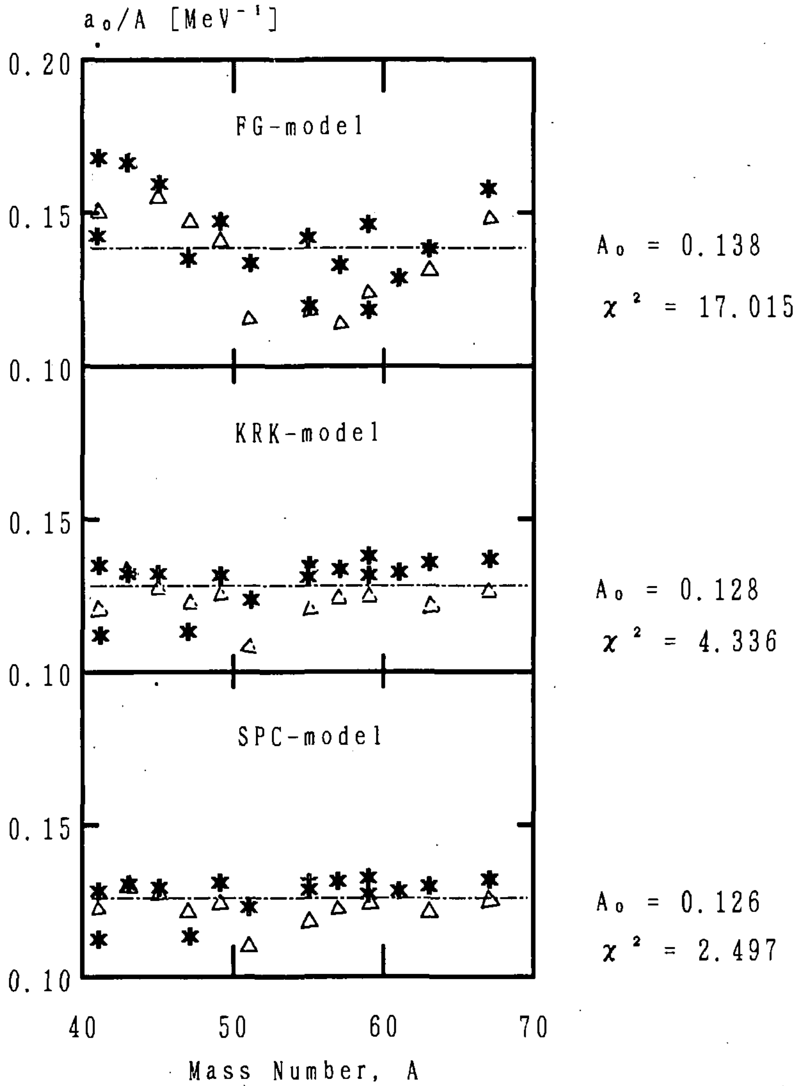

Fig. 1 Mass number A dependence of asymptotic level density parameter a_0. ✱ from neutron and Δ from proton resonances, —·—·— Results of the least-squares fits described in the text.

II. Japan Atomic Energy Research Institute

A. Nuclear Data Center and Japanese Nuclear Data Committee

II-A-1

Second Revision of JENDL-3 (JENDL-3.2)

Nuclear Data Center and Japanese Nuclear Data Committee

The third version of Japanese Evaluated Nuclear Data Library (JENDL-3)[1,2] has been updated to JENDL-3.2. This revision work started in 1992 to improve drawbacks of JENDL-3.1 which was released in 1990, and was done by the Nuclear Data Center and working groups of Japanese Nuclear Data Committee (JNDC). JENDL-3.2 provides the neutron induced reaction data for 340 nuclei in the energy range from 10^{-5} eV to 20 MeV. Among those nuclides, the data of 16 nuclei are newly added to JENDL-3, and those of more than 180 nuclei were revised from previous evaluation. Main aspects of the present revision are summarized below:

Resonance Parameters of Important Actinides

The resolved resonance parameters of ^{233}U, ^{235}U, ^{238}U, ^{239}Pu and ^{241}Pu were updated with new evaluation based on the Reich-Moore formula. The energy range of the resolved resonance region was expanded to higher energies than JENDL-3.1. For example, the parameters of ^{239}Pu were evaluated by Derrien[3] by means of SAMMY code[4] and recent measurements of fission and total cross sections. Its resonance region was extended from 1 keV of JENDL-3.1 to 2.5 keV. The unresolved resonance parameters were modified for ^{235}U and ^{238}U. The fission and capture cross sections of ^{235}U were re-evaluated in the unresolved resonance region and the unresolved resonance parameters were determined to reproduce the new cross-section data. For ^{238}U, the upper boundary of the unresolved resonance region was changed from 50 keV of JENDL-3.1 to 150 keV.

Inelastic Scattering Cross Sections of ^{233}U and ^{238}U

After careful recalculation with sophisticated theoretical calculation method, these cross sections were slightly modified from JENDL-3.1.

Fission spectra of ^{233}U, ^{235}U, ^{238}U and ^{239}Pu

These data were newly calculated with non-equitemperature Madland-Nix model proposed by Ohsawa[5], which takes account of different temperatures for two fission fragments and multi-chance fission process. Their spectra became softer than those in JENDL-3.1.

Total Cross Sections of Structural Material

The total cross sections of ^{14}N, ^{23}Na and Fe were reevaluated. Their drawbacks were revealed by benchmark calculation[6] to Broomstick experiments. In the case of natural Fe, JENDL-3.1 was evaluated from fine resolution experimental data. However, the experimental data are broadened with a finite experimental resolution even in the very fine resolution experiments. The total cross section of Fe given in JENDL-3.1 was unfolded by considering the experimental resolution. Those of Cr and Ni were also modified with the same method. The total cross sections of ^{14}N and ^{23}Na were reevaluated by taking more reasonable data. Revised data are in very good agreement with the benchmark experiments.

Double Differential Cross Sections

The double differential cross sections (DDX) are important for fusion neutronics. To improve the DDX, JENDL Fusion File[7] is being provided, in which the DDX data are represented in MF6 of ENDF-6 format. The modified data for JENDL Fusion File were adopted in JENDL-3.2 by approximately transforming the MF6 representation to the conventional MF4-MF5 format. By the adoption of JENDL Fusion File, the data of the inelastic scattering, (n,2n), and other neutron emission cross sections and the angular and energy distributions of secondary neutrons were remarkably improved. Even in the conventional representation, JENDL-3.2 reproduces quit well the experimental DDX data measured at Osaka and Tohoku universities for many nuclides.

Fission Product Nuclei

The resonance parameters and capture cross sections of many nuclei in the fission product region (from As to Tb) were modified. New experimental data reported after the previous evaluation were taken into consideration. The inelastic scattering cross sections of even mass isotopes of Sm were updated by adding the contributions from the direct process. The data of As, Zr, Mo and Sb were taken from JENDL Fusion File.

Gamma-ray Production Data

New evaluation was made for seven nuclei. JENDL-3.2 contains, therefore, the γ-ray production data for 66 nuclei. The γ-ray spectra in the low energy region were calculated with CASTHY[8], and energy balance was carefully checked. The discrete γ-rays from the inelastic scattering of natural elements were separated from continuum spectra.

Preliminary benchmark calculations for JENDL-3.2 were made by working groups of JNDC for LWR, FBR and shielding of JNDC. It has been confirmed that JENDL-3.2 improves the drawbacks found in JENDL-3.1, and JENDL-3.2 provides the reliable neutron nuclear data for wide region of applications.

References

1) Shibata K., et al.: "Japanese Evaluated Nuclear Data Library, Version 3, - JENDL-3 -", JAERI 1319 (1990).
2) Kawai M., et al.: J. Nucl. Sci. Technol., 29, 195 (1992).
3) Derrien H.: J. Nucl. Sci. Technol., 30, 845 (1993).
4) Larson N.M.: "Updated Users' Guide for SAMMY: Multilevel R-Matrix Fits to Neutron Data Using Bayes' Equations", ORNL/TM-9179/R1 (1985).
5) Ohsawa T. and Shibata T.: "Analysis of Fission Neutron Spectra by Non-Equitemperature Madland-Nix Model", Proc. of Int. Conf. on Nuclear Data for Science and Technology, Juelich, 13-17 May, 1991, p.965 (1992).
6) Kawai M., et al.: "Shielding Benchmark Tests of JENDL-3", JAERI 1330 (1994).
7) Chiba S., Yu B. and Fukahori T.: "Evaluation of JENDL Fusion File", JAERI-M 92-027, p. 35 (1992).
8) Igarasi S. and Fukahori T.: "Program CASTHY - Statistical Model Calculation for Neutron Cross Sections and Gamma Ray Spectrum -", JAERI 1321 (1991).

II-A-2

NEANSC International Evaluation Cooperation SG10 Activities on Inelastic Scattering Cross Sections for Weakly Absorbing Fission Product Nuclides

M. Kawai[1], S. Chiba, T. Nakagawa, Y. Nakajima, T. Watanabe[2], A. Zukeran[3]
H. Gruppelaar[4], A. Hogenbirk[4], M. Salvatores[5], K. Dieze[5], R.Q. Wright[6]
and R.E. Schenter[7]

The integral tests of the evaluated fission product nuclear data libraries such as JENDL-3 and JEF-1 revealed a trend of underestimation of the reactivity worths for weak absorbers measured at STEK. H. Gruppelaar and H.A.J. van der Kamp pointed out that such underestimation came from uncertain inelastic scattering cross sections: for most FP nuclide data in the current evaluated data libraries, direct inelastic scattering cross sections are disregarded. The subgroup 10 has been organized since 1991 in NEANSC Evaluation Cooperation Working Party in order to review the inelastic scattering cross sections for weakly absorbing FP nuclides (e.g. even mass isotopes of Zr, Mo, Ru, Pd, Nd and Sm) which show anomalous behavior in the integral data on the sample reactivity worth measured at STEK, to recommend methods and model parameters for evaluation of the inelastic scattering cross sections of FP nuclides and to examine the reliability of the STEK neutron spectra which were adjusted to reproduce the worth of standard samples.

In the subgroup, the applicability of the DWBA calculations, which were used for the evaluation of direct inelastic scattering cross section for even mass fission product nuclides of JENDL-3, was investigated by comparison with the experimental data and with coupled channel calculations for isotopes of Zr, Mo, Pd, Cd, Ba, Nd and Sm. As a result, it turned out applicable for estimating the cross sections for one-phonon vibrational levels. The coupled channel theory estimates well the excitation functions for both vibrational and rotational levels of deformed nuclei and for the mass range around 100.

Neutron spectra of the STEK cores were calculated on the basis of JENDL-3 with the vectorized pointwise Monte Carlo code, MVP, using a three dimensional homogeneous model of the STEK reactor and corrected for a heterogeneous effect according to diffusion calculations. The results were compared with the original spectra reported from Petten and employed to the sample worth calculations. The calculated spectra give appreciable improvement of sample worth of the weak absorbers. In the lower energy range in which neutrons much contribute to worth of the strong absorbers in a large core, the Monte Carlo calculation with the correction for the heterogeneous effect supports the original spectra.

Intercomparison of integral tests with measured sample worths and capture rates has been made for JENDL-3.1, JENDL-3.2, JEF-1 and JEF-2. The discrepancies of the measured and calculated sample worths in the STEK experiments are partially attributed to the unreasonable inelastic scattering cross sections. Modification of the inelastic scattering cross sections reduces the discrepancies in some degree. However, there are discrepancies for some strong absorbers and the standard samples such as carbon and oxygen whose cross sections are rather accurate this suggests that there remain yet other factors such as errors in the adjoint spectra and resonance self-shielding effects.

(Presented at Int. Conf. on Nuclear Data for Science and Technology, Gatlinburg, USA., 9-13 May 1994)

---

1. Toshiba Corporation, 2. Kawasaki Heavy Industries, Ltd. 3. Hitachi Ltd.
4. ECN Petten, Netherlands, 5. CEA-Cadarache, France, 6. ORNL, 7. HEDL

II–A–3

Revision of Fission Product Nuclear Data Library For JENDL–3.2

M. Kawai[1], S. Chiba, H. Matsunobu[2], T. Nakagawa, Y. Nakajima, T. Sugi
T. Watanabe[3] and A. Zukeran[4]
JNDC Fission Product Nuclear Data Working Group

Reevaluation of the nuclear data for about 60 fission product nuclides has been made for JENDL–3.2, taking account of new experimental data and results of integral tests for JENDL–3. Integral tests of the revised data were made with the STEK experiments.

The thermal capture cross sections of Sr–90, Cs–137, Eu–154 and Eu–155 were revised on the basis of the recent measurements at JRR–4 of JAERI. A major part of the revision of the resonance parameters were made according to the renormalization of the experimental capture area data of ORNL. Capture cross sections above the resonance region were modified so as to reduce the discrepancies between the differential and the integral data. For As–75, Mo–98, Mo–100 and Rh–103, the optical model parameters were revised to improve the energy dependence of the total cross sections. Direct inelastic components and threshold reaction cross sections were revised with the DWUCK–4 and GNASH code calculations for the isotopes of As, Zr, Nb, Mo and Sb. As for deformed nuclides such as Sm and Nd isotopes, the direct inelastic scattering contributions calculated with the coupled channel theory were taking into consideration.

Integral tests for the revised data with the STEK experiments show that the worth calculated from JENDL–3.2 generally gives a better agreement with the measured data than JENDL–3. However, as for some strong absorbers such as Tc–99, Ag–109 and La–139, the worths are underestimated. This discrepancy may come from uncertainties of resonance self-shielding calculations or of the integral experiments.

(Presented at Int. Conf. on Nuclear Data for Science and Technology, Gatlinburg, U.S.A., 9 – 13 May 1994)

1. Toshiba Corporation
2. Sumitomo Atomic Energy Industries, Inc.
3. Kawasaki Heavy Industries, Ltd.
4. Hitachi Ltd.

II-A-4

Evaluation of Neutron Nuclear Data of ^{244}Pu and ^{237}Pu

T. Nakagawa and V. Konshin

The evaluation of neutron nuclear data of ^{244}Pu and ^{237}Pu was done in the neutron energy range from 10^{-5} eV to 20 MeV. Quantities evaluated are the total, elastic and inelastic scattering, capture, fission, (n,2n) and (n,3n) reaction cross sections, the angular and energy distributions of secondary neutrons, and number of neutrons emitted per fission. Figures 1 and 2 show the cross section data. Mean values are shown in the resonance region of ^{244}Pu.

^{244}Pu

The resolved resonance parameters were given in the energy range up to 290 eV on the basis of experimental data by Auchampaugh et al.[1] The thermal fission and capture cross sections calculated from the resonance parameters are 0.0017 b and 1.68 barns. Their resonance integrals are 5.07 barns and 50 barns, respectively. Above the resonance region, theoretical calculation was made with ECIS[2], STAPRE[3] and CASTHY[4]. The ECIS calculation was adopted for the total, shape elastic and direct inelastic scattering cross sections, and their angular distributions. The (n,2n), (n,3n) and fission cross sections, and energy distributions of neutrons due to the continuum inelastic scattering, (n,2n) and (n,3n) reactions were calculated with STAPRE. The fission cross sections below 8 MeV were determined from existing experimental data[1),5] which are in agreement with the STAPRE calculation. The CASTHY was used to calculate the capture and compound scattering cross sections to discrete levels. The continuum inelastic scattering cross section was determined by subtracting a sum of the other partial cross sections from the total cross section.

The number of prompt neutrons per fission (ν_p) was estimated as: $\nu_p = 2.79 + 0.163\times E(MeV)$. The number of delayed neutrons is 0.03 in the thermal energy region and 0.019 in the MeV region.

^{237}Pu

No resonance parameters were given. The thermal fission cross section was taken from Mughabghab's recommendation[6] (2455±295 barns). The capture cross section was assumed to be 500 b at 0.0253 eV, which is about 1/5 of the fission cross section. The resonance integral calculated from the present evaluated cross section is 816 barns for the fission and 142 barns for the capture.

No experimental data are available for the cross sections of ^{237}Pu. The fission cross section was assumed to be $\sigma_R\times0.85$ where σ_R is the total reaction cross section calculated with CASTHY and the factor of 0.85 was estimated at 100 keV by assuming the cross section is almost the same as ^{239}Pu. Other quantities were estimated with ECIS, STAPRE and CASTHY in the same manner as ^{244}Pu.

The number of prompt neutrons per fission was estimated as: $\nu_p = 2.863 + 0.123\times E(MeV)$. The number of delayed neutrons is 0.002 in the thermal energy region and 0.0014 in the MeV region.

References

1) Auchampaugh G.F., Farrell J.A. and Bergen D.W.: Nucl. Phys., A171, 31(1971).
2) Raynal J.: unpublished.
3) Uhl M. and Stromaier B.: Report IRK-76/10 (1976).

4) Igarasi S. and Fukahori T.: "Program CASTHY – Statistical Model Calculation for Neutron Cross Sections and Gamma Ray Spectrum –", JAERI 1321 (1991).
5) Moore M.S., et al.: Proc. Int. Conf. on Nuclear Data for Science and Technol., Antwerp, 6–10 Sep. 1982, p.74 (1983).
6) Mughabghab S.F.: "Neutron Cross Sections, Vol. 1, Part B", Academic Press Inc. (1984).

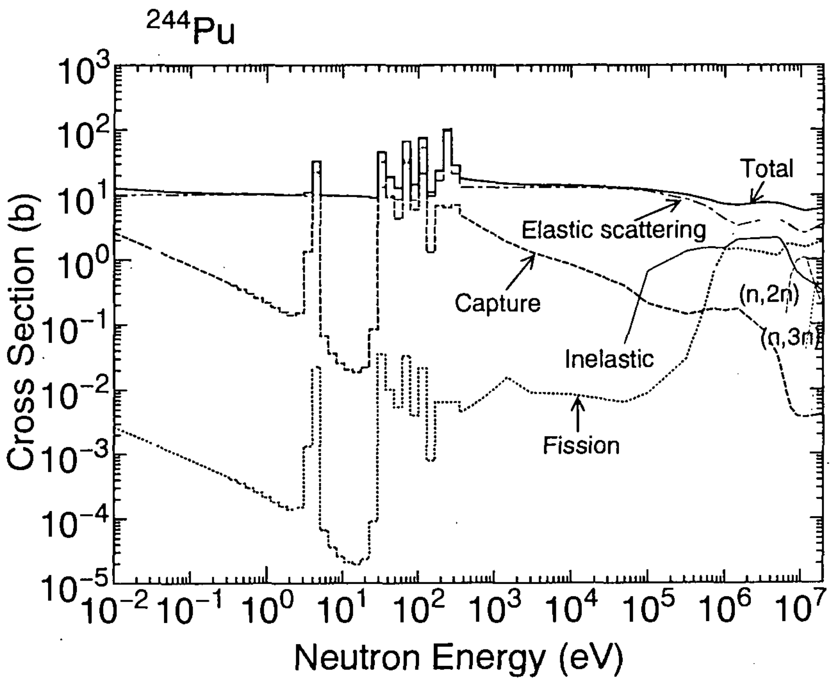

Fig. 1 Evaluated cross sections of ^{244}Pu

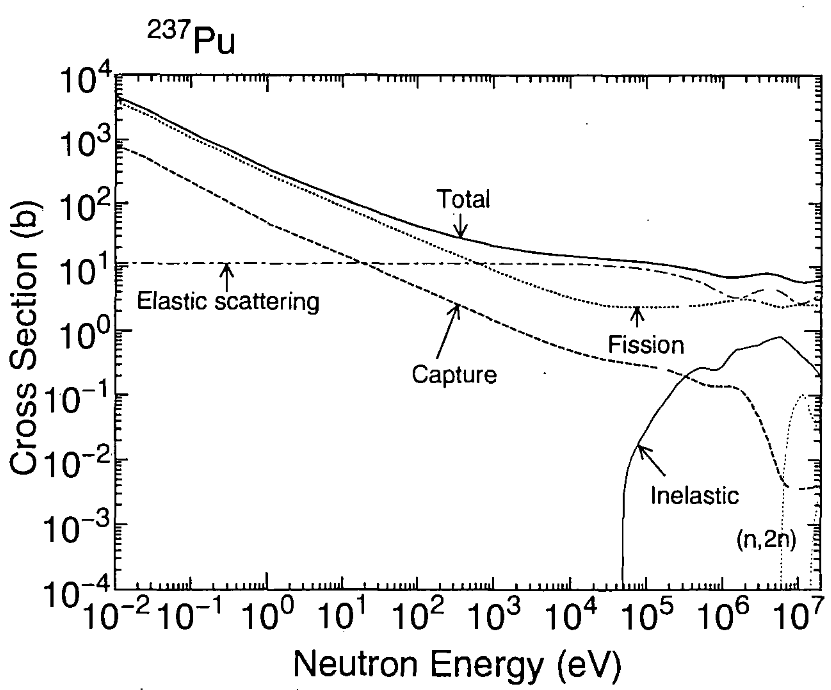

Fig. 2 Evaluated cross sections of ^{237}Pu

II–A–5

Consistent Calculations of Fast Neutron Induced Fission, (n,2n) and (n,3n) Cross–Sections for 71 Isotopes of Th, Pa, U, Np, Pu, Am, Cm, Bk and Cf

V.A. Konshin

A paper on this subject will be submitted as a JAERI–M report with the following abstract:

The neutron cross–sections for fission, (n,2n) and (n,3n) reactions have been calculated consistently for $^{227\sim234}$Th, $^{229\sim233}$Pa, $^{230\sim240}$U, $^{235\sim239}$Np, $^{236\sim247}$Pu, $^{239\sim245}$Am, $^{238\sim251}$Cm, $^{245\sim249}$Bk and $^{249\sim252}$Cf using the Hauser–Feshback statistical model code STAPRE, in the neutron energy range from 1 to 20 MeV. The main parameters of the pre–equilibrium exciton model was tested against the experimental data for the inelastically scattered neutron spectra of ^{238}U. Shell, superfluid and collective effects in nuclear level density have been taken into account. Neutron transmission coefficients were calculated using the coupled–channel code ECIS. All experimental data available for fission and (n,2n) reactions for the above isotopes have been used for model testing. Due to a lack of experimental data for the majority of the nuclei considered, theoretical prediction of neutron cross–sections has been made.

II–A–6

Status of Nuclear Data Evaluation for JENDL High Energy File

Tokio FUKAHORI, Satoshi CHIBA, Yasuyuki KIKUCHI,
Masayoshi KAWAI and Norio KISHIDA

A paper on this subject will be published in Proc. of the Int. Conf. on Nuclear Data for Science and Technology, May 9–13, 1994, at Gatlinburg, Tennessee, U.S.A. with the following abstract:

The present status of the JENDL High Energy File is reported. The PKA/KERMA File and the Photonuclear Data File are also introduced briefly as related topics with the JENDL High Energy File.

II–A–7 Status of Intermediate Energy Nuclear Data

Tokio FUKAHORI

A paper on this subject have been published in Proc. of the First Symposium on Simulation of Hadronic Many–body System, Oct. 18–20, 1993, at Tokai, Ibaraki, Japan with the following abstract:

One of the recent interests of nuclear physicists is to analyze phenomena such as multi–fragmentation and particle emission from the heavy ion interaction in the intermediate energy region. Some models and theories, for example, the VUU theory, quantum molecular dynamics (QMD), antisymmetrized molecular dynamics (AMD), etc., have been developed as tools to perform above. On the other hand, intermediate energy nuclear data (IEND) are required from many nuclear engineering fields, especially accelerator applications. Therefore, IEND can become an interface between nuclear physicists and nuclear engineers. A few of review papers are available for requirements and status of IEND for accelerator systems[1,2]. However, no such review for wide range applications has been performed yet. In this paper, requests and present status of IEND is reported from an engineering side, and needs of IEND are described from a view point of several applications. Present conditions on experimental databases and calculation codes for evaluation in the intermediate energy region are introduced. For the future work, a project of the evaluated intermediate energy nuclear data file is reported.

II–A–8 A Code Guidance System for Integrated Nuclear Data Evaluation System on the Basis of Knowledge Engineering Technology

Tokio FUKAHORI and Tsuneo NAKAGAWA

A paper on this subject will be published in Proc. of the Second Specialist Meeting on Application of Artificial Intelligence and Robotics to Nuclear Plants (AIR '94), May 30 – Jun. 2, 1994, at Tokai, Ibaraki, Japan with the following abstract:

The integrated nuclear data evaluation system (INDES) is being made in order to support the nuclear data evaluation work. A guidance system in INDES, '*Evaluation Tutor* (ET)', is under development in order to support users in selecting the most suitable set of theoretical calculation codes by applying knowledge engineering technology and the experiences of evaluation work for JENDL–3. In this paper, the function of ET is introduced as well as the functions and databases of INDES. An example run of ET for ^{56}Fe in the 1–20 MeV neutron energy region is also explained.

II-A-9 QMD Calculation of Nucleon-Nucleus Reaction Cross Sections

Satoshi Chiba

A paper on this subject was published as JAERI-M 94-028(1994), p.111, with the following introduction:

In the field of heavy-ion physics, the method of microscopic simulation has turned out to be extremely powerful in describing the experimentally observed information. Among theses approaches, the Quantum Molecular Dynamics (QMD) and its improved versions (AMD. FMD) have been currently the most elaborate approach which, not only the one-body observable (e.g., inclusive nucleon spectra), could give quantitative picture of the correlation of many nucleons, i.e. the fragmentation. This success of QMD has lead to various important understanding of the reactions between heavy-ions. Even though the ultimate goal of fixing the nuclear equation-of-state (eos) seems to be still too far, the QMD (and its relatives) seems to be an attractive tool for calculation of the nuclear cross sections.

In spite of its success, however, the QMD has not been applied to nucleon(N)-nucleus(A) collisions extensively. Peilert et al. have applied QMD in calculating the double-differential (p,xn) cross sections of Al, Zr and Pb at several incident energies, and the predictions were favorably compared with the data. Although this is an encouraging results, the applicability of QMD to N-A reactions is still an open question.

The purpose of this work is to give our first (and mostly preliminary) result on the applicability of QMD to nucleon-nucleus reactions. This paper gives a simple explanation of the concept and typical examples of the calculation carried out in the energy region from 26 to 60 MeV.

II-A-10 Applicability of the Quantum Molecular Dynamics to Nucleon-Nucleus Collisions

S. Chiba, T. Fukahori, H. Takada, T. Maruyama, K. Niita and A. Iwamoto

A paper on this subject was presented at Int. Conf. on Nuclear Data for Science and Technology, May 9-13, 1994, Gatlinburg, Tennessee U.S.A, with the following abstract:

The Quantum Molecular Dynamics (QMD) theory is applied to nucleon(N)-induced nuclear reactions. It was found that results of the QMD can give a remarkable agreement with the data of the (N,xN') type reactions over the energy region from several tens MeV to several GeV. The QMD gives a unified picture on the 3 major reaction mechanisms (i.e., compound, pre-equilibrium and spallation) without any adjusting parameters.

II-A-11 Evaluation of Neutron Cross Sections of ^{12}C up to 50 MeV

S. Chiba, T. Fukahori, Y. Watanabe and Y. Koyama

A paper on this subject was published as JAERI-M 94-019(1994), p.300, with the following abstract:

The neutron cross sections of ^{12}C have been evaluated in the energy range of 20 to 50 MeV. The total cross section was determined by the generalized least-squares method taking account of the available experimental information. Other quantities are evaluated with the aid of theoretical calculations. The spherical optical model was employed to evaluate the reaction and elastic scattering cross sections. The inelastic scattering to the first excited 2^+ state was calculated based on the DWBA. The optical potentials used in these calculations were obtained in a microscopic way. The double-differential data for neutron, proton, deuteron, triton, ^3He and α-particle emissions and recoil spectra are evaluated based on the Monte-Carlo method.

II-A-12

Far from Stability: Evaluation of Properties of Nuclear Excited States

A. Mengoni†, G. Maino†† and Y. Nakajima

A paper on this subject was submitted to the Proceedings of the International Conference on Nuclei in the Cosmos, held at L'Aquila, Italy on July 8 - 13, 1994 with the following abstract:

We propose as integrated technique for evaluation of nuclear excitation properties using a model(based on the Fermi gas with pairing and shell correction) for the level density in the continuum and the Interacting Boson Model for the calculation of the discrete spectra of nuclei far from the stability line. An example is shown relevant to the calculation of the excitation energies of the Cd isotopes in the N = 50 - 82 shell.

---

†ENEA, Bologna, Italy

††ENEA, Bologna and INFN, Firenze, Italy

II-A-13

The Systematics of Nuclear Level Density Parameters Revisited: Nuclear Deformation Effects

A. Mengoni† and Y. Nakajima

A paper on this subject was published in the Proceedings of the 1993 Symposium on Nuclear Data, JAERI-M 94-019, February 1994, p. 337.

We have recently derived a systematics of level density parameters based on the Fermi-gas model(FGM).[1] In particular we have concentrated on deriving a reliable systematics of the level density parameter a. In doing this, we have corrected the FGM for paring and shell effects. The correction for taking into account shell effects is based on the Ignatyuk prescription[2]. Following this approach, the strong fluctuation on the a-parameter are removed by using the relation

$$a = a(*) \left[1 + \frac{E_{sh}}{U} \left(1 - e^{-\gamma U} \right) \right]$$

where U is the excitation energy, γ a damping parameter. In this relation the shell correction energy, E_{sh}, is assumed to be just the difference between the experimental mass of the nuclide in question and the smooth part of a liquid drop-like(LDM) mass-formula: $E_{sh} = M_{exp} - M_{LDM}$. Because in the LDM it is possible to separate between a *shell* and a *deformation* contributions, we can look at these two effects separately. The results of our analysis is shown in the figure below. The curves labelled by (a) are obtained using only shell part in the LDM. The curves labelled by (b) are obtained including the shell and deformation energies. The experimental points are derived as usual from the s-wave neutron level spacings at the neutron separation energy[3].

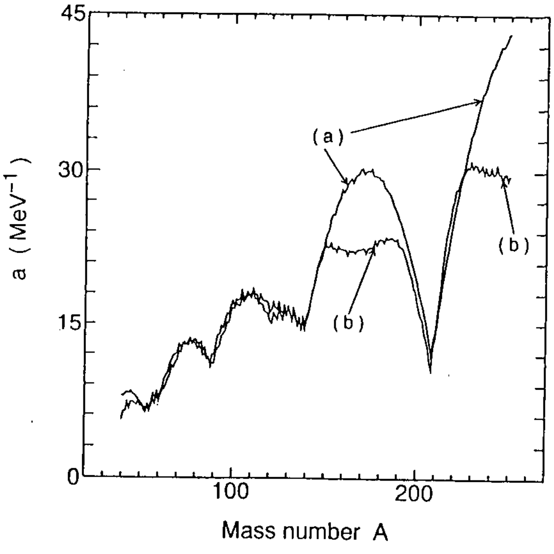

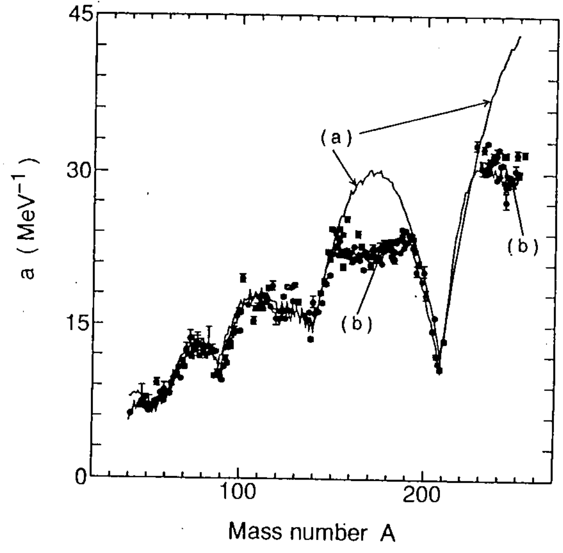

†ENEA, Bologna, Italy

The results show a clear agreement of the experimental with the calculated level density parameters for the case in which deformation energy is included in the LDM.

References:

1) A. Mengoni and Y. Nakajima: J. Nucl. Sci. Technol., **31**, 151(1994); A. Mengoni and Y. Nakajima: JAERI–M 93–177(1993).
2) A.V. Ignatyuk, K.K. Istekov and G.N. Smirenkin: Sov. J. Nucl. Phys., **29**, 450(1979).
3) S.F. Mughabghab, M. Divadeenam and N.E. Holden: "Neutron Cross Sections", Volume 1, Part A, Academic, New York, (1981); S.F. Mughabghab: ibid., Part B, Academic, New York, (1984).

II–A–14

Algebraic and Geometric Approaches to the Collective Enhancement of Nuclear Level Densities

A. Mengoni[††], G. Maino[†††], A. Ventura[†††] and Y. Nakajima

A paper on this subject was submitted to the Proceedings of the International Conference on Perspectives for the Interacting Boson Model on the Occasion of its 20th Anniversary, held at Padova, Italy on June 13 – 17, 1994 with the following abstract:

The Interacting Boson Model(IBM) has been employed in the evaluation of the collective contribution to nuclear level density. Previous calculations have been extended to transitional nuclei in the framework of the neutron–proton version of the model(IBM–2). The results are shown in comparison with the predictions of geometric models.

[††]ENEA, Bologna, Italy

[†††]ENEA, Bologna and INFN, Firenze, Italy

B. Fusion Neutronics Laboratory

II–B–1 Benchmark Experiment on Copper Slab Assembly Bombarded by D-T Neutrons and the Experimental Analysis

F. Maekawa, Y. Oyama, C. Konno, Y. Ikeda, K. Kosako* and H. Maekawa

Copper is a very important material for fusion reactor because it is used in superconducting magnets or first walls and so on. To verify nuclear data of copper, a benchmark experiment [1-3] was performed using the D-T neutron source of the FNS facility in Japan Atomic Energy Research Institute. A cylindrical experimental assembly of 629 mm in diameter and 608 mm in thickness made of pure copper was located at 200 mm from the D-T neutron source. In the assembly, the following quantities were measured; i) neutron spectra in energy regions of MeV and keV, ii) neutron reaction rates, iii) prompt and decay gamma-ray spectra and iv) gamma-ray heating rates.

Cross section data of copper in JENDL-3.1 were verified through analyses of the experiment with the MCNP and DOT codes. The analyses suggested that neutron data were almost appropriate except some small problems. The self-shielding correction should be considered in group constants for DOT calculations. As for secondary gamma-ray data in JENDL-3.1, the data for threshold reactions are good. Probability of direct transitions from the capture state to the ground state for keV neutron capture should be increased. It is also found that energy valance of secondary gamma-ray data for the neutron capture reaction is inconsistent in an incident neutron energy range between 0.01 and 10 keV. Excess of released gamma-ray energy in JENDL-3.1 resulted in larger gamma-ray heating rates.

References:

1) F. Maekawa, Y. Oyama, C. Konno, Y. Ikeda, K. Kosako and H. Maekawa: "Benchmark Experiment on a Copper Slab Assembly Bombarded by D-T Neutrons", JAERI-M 94-38 (1994).
2) C. Konno, F. Maekawa, Y. Oyama, Y. Ikeda and H. Maekawa: "Benchmark Experiment on Copper with D-T Neutrons for Verification of Neutron Transport and the Related Nuclear Data of JENDL-3.1," Submitted to Third International Symposium on Fusion Nuclear Technology, UCLA, Los Angeles, June 27 - July 1, 1994, to be published in Fusion Technol.
3) F. Maekawa, Y. Oyama, C. Konno, Y. Ikeda and H. Maekawa: "Benchmark Experiment on Copper with D-T Neutrons for Verification of Secondary Gamma-Ray Data in JENDL-3.1," ibid.

* : Nuclear Energy Data Center (Present Affiliation: Sumitomo Atomic Energy Industries, Ltd.)

II–B–2 Measurement of Low Energy Neutron Spectrum in Iron Assembly in eV Energy Region for Validation of Evaluated Nuclear Data

F. Maekawa, Y. Oyama and C. Konno

Iron is the most essential structural material for fusion and fission applications. For verifying nuclear data of iron, benchmark experiments have been carried out for an iron cylindrical assembly utilizing the Fusion Neutronics Source (FNS) facility. Neutron spectra above 3 keV and activation reaction rates were measured[1-2] so far in the assembly. In such a benchmark experiment, however, neutron spectrum below 3 keV was usually not measured. Hence measurement of neutron spectra below 3 keV was attempted in the iron assembly.

The experimental assembly of 1000 mm in diameter and 950 mm in thickness made of iron was placed at 200 mm from the tritium target of FNS. The neutron slowing down time method[3] was adopted to measure neutron spectra below 3 keV. Measurement positions were at 110, 210, 310, 410, 610 and 810 mm from the front surface.

Benchmark calculations of the experiment were performed by using MCNP-4 with cross section libraries based on JENDL-3.1, -3.2 and ENDF/B-IV. Neutron spectra at 210 mm and 810 mm measured in the present experiment and those by Konno, et al. are shown in Fig. 1 in comparison with MCNP calculations. It is clearly seen that agreements between the calculated spectra with JENDL-3.2 and the measured ones are fairly good not only for their shapes but also their absolute values. As for the energy range below 1 keV, the JENDL-3.2 calculation agrees with the experiment within about 10 % at all measurement positions. On the other hand, the calculation with JENDL-3.1 underestimates the flux by a few tens of percentage near the front surface of the assembly, and the ENDF/B-IV calculation is smaller than the experiment by about 30 % at all positions.

References:
1) K. Oishi, et al.: Proc. 7th Int. Conf. on Radiation Shielding, Bournemouth, 9331-340 (1988).
2) C. Konno, et al.: Fusion Eng. Des., 18, 297-303 (1991).
3) F. Maekawa and Y. Oyama: "Development of Measurement Technique for Neutron Spectrum in Energy Region of eV in Large Assemblies", JAERI-M 93-181, pp. 96-98 (1993).

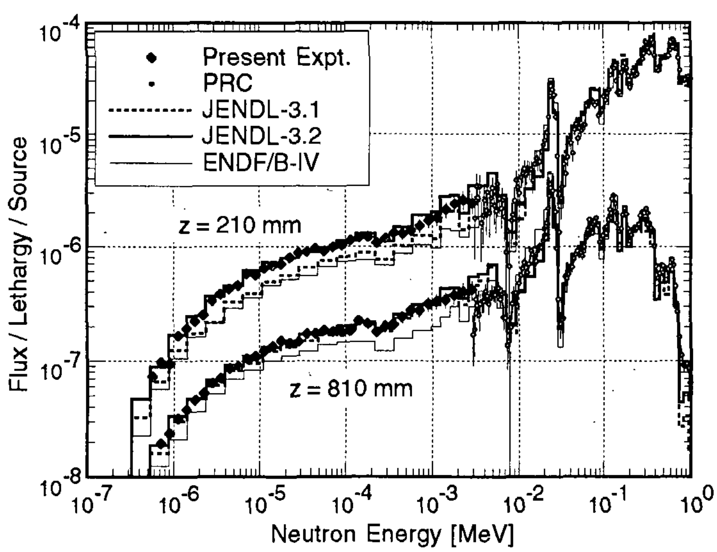

Fig. 1 Measured neutron spectra in the iron assembly in comparison with MCNP calculation.

II–B–3 Verification of Secondary Gamma-Ray Data in JENDL-3 through Analysis of Benchmark Experiments at FNS and OKTAVIAN

F. Maekawa, Y. Oyama and K. Kosako*

As an activity of Shielding Integral Working Group of Japanese Nuclear Data Committee, secondary gamma-ray data in JENDL-3.1 and -3.2 were tested [1] by benchmark calculations of existing experiments. Two series of integral experiment with D-T neutron source were selected for the data testing; i) FNS/JAERI clean benchmark experiments with three experimental assemblies of Cu, W and type 316 stainless steel (SS316) and ii) OKTAVIAN/Osaka University pulse sphere experiments for LiF, CF_2, Al, Si, Ti, Cr, Mn, Co, Cu, Mo, W and Pb.

The continuous energy Monte Carlo code MCNP-4 was used for the calculations. Through comparisons between the experimental and calculated gamma-ray spectra, while some of the secondary gamma-ray data in JENDL-3.2 still included inadequate data in some cases, validity of the data was confirmed for most of the materials.

References:

1) F. Maekawa, K. Kosako and Y. Oyama: "Verification of Gamma-ray Data in JENDL-3.1 through Analysis of OKTAVIAN Experiment," Proc. Int. Conf. on Nucl. Data for Sci. and Technol., Gatlinburg, USA, May 9-13, 1994.

* : Nuclear Energy Data Center (Present Affiliation: Sumitomo Atomic Energy Industries, Ltd.)

II-B-4 Measurements of Activation Cross Sections at 18-30 MeV by Using the ^{7}Li(p,n) Quasi-monoenergetic Neutron Source at JAERI-TANDEM

Y. Uno, S. Meigo, S. Chiba, T. Fukahori, Y. Kasugai* and Y. Ikeda

The demands for the neutron cross section date above 20 MeV have been increased recently. The experiment of neutron activation cross section measurement by using the ^{7}Li(p,n) quasi-monoenergetic neutron source at 18-30 MeV was started at the TANDEM accelerator facility of JAERI.

The 20 and 25 MeV protons bombarded the thin ^{7}Li target. There is the cooling water layer separated by a 0.1-mm-thick aluminum plate and the protons passing through the ^{7}Li target are fully absorbed in this water. The neutron energy spectrum in the forward direction was measured by the TOF method by using an NE213 liquid scintillation detector. The measured neutron energy spectra are shown in Fig. 1. A quasi-monoenergetic peak produced by the ^{7}Li(p,n)^{7}Be[0.0, 0.429MeV] reaction is observed. There are low energy neutron tails corresponding to the breakup of higher excitation states of ^{7}Be, and to the interaction of protons with the cooling water and the structural materials of the target. The absolute flux of peak neutrons was measured by the proton recoil counter telescope. The characteristics of the p-Li neutron source are tabulated in the Table 1. The angular distributions of the peak neutron yield were also measured with the NE213 detector.

The samples of Co, Nb, Cu, Y, Tm, Ti, Ni, Fe, Zr, W, Au and Al were irradiated at the distance of 10 cm from the Li target. After the irradiation, the gamma-rays of each samples were measured by HP-Ge detectors and the reaction rates were derived from the measured induced activities. The obtained reaction rates include the contribution from the low energy neutrons. Therefor the correction for this low energy neutrons is necessary. The cross section for the effective peak energy, σ, is calculated as follows,

$$\sigma = R \cdot \frac{\int_{E_{min}}^{E_{max}} \sigma_0(E) \cdot \phi(E)\, dE}{\int_{E_{th}}^{E_{max}} \sigma_0(E) \cdot \phi(E)\, dE} \cdot \frac{1}{\phi_{peak}} , \qquad (1)$$

where R is the obtained reaction rate, $\sigma_0(E)$ is the cross section data cited from the literature, $\phi(E)$ is the neutron spectra, E_{th} is the threshold energy of the reaction, E_{max} and E_{min} are the highest and the lowest energy of the peak neutrons respectively, and ϕ_{peak} is the absolute peak neutron yield. The measured cross sections of ^{197}Au(n,2n)^{196}Au reaction are shown in Fig. 2. The cross section data evaluated by M. Wagner et al[1]. were used as $\sigma_0(E)$ in the eq. (1). The presently derived cross sections are in good agreements with the evaluated data. This result demonstrated the adequacy of the method.

Reference
1) M. Wagner et al. : PHYSICS DATA No. 13-5 (1990)

*Department of engineering, Nagoya University

Table 1 The characteristics of the p-Li neutron source

Proton energy [MeV]	Thickness of Li [mm]	Effective energy of peak neutrons [MeV]	Peak neutron yield in the forward direction [#/Sr/μC]
20	1.8	17.6	6.05×10^8
25	1.45	22.7	9.49×10^8

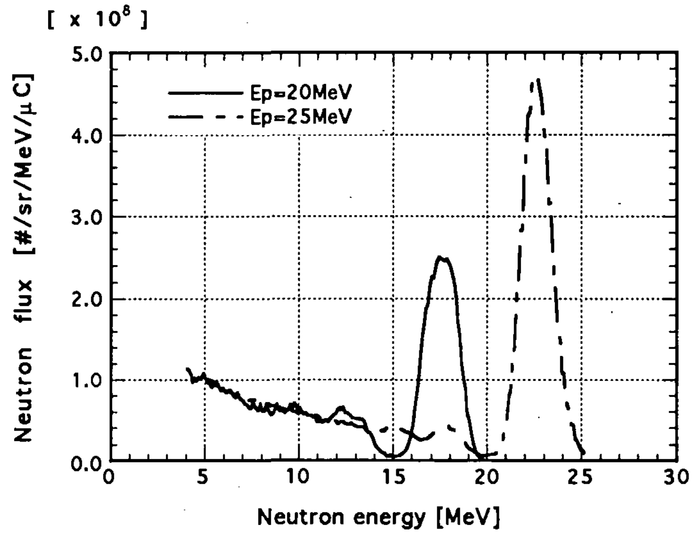

Fig. 1 Neutron spectra of 20 and 25 MeV proton

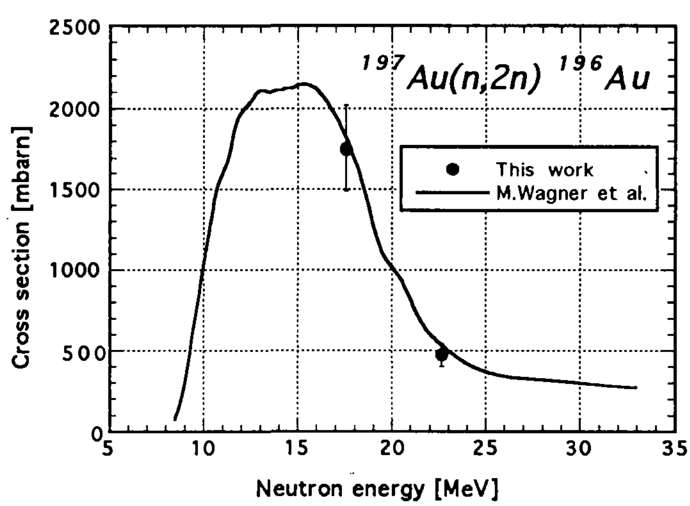

Fig. 2 Cross section of $^{197}Au(n,2n)^{196}Au$

C. Isotope Research and Development Division

II–C–1 Decay of the New Isotope ^{127}Pr

T. Sekine, A. Osa, M. Koizumi, S. Ichikawa,* M. Asai,* H. Yamamoto,* and K. Kawade*

A paper on this subject was submitted to the Z. Phys. A.[1)]

As results, a new isotope, ^{127}Pr, has been identified and its decay has been studied using on-line isotope separation of $^{94}Mo(^{36}Ar,p2n)$ reaction products. The half-life of the isotope was determined to be 7.7(6) s, and a γ/X-ray spectrum has been obtained. A partial level scheme is proposed for ^{127}Ce on the basis of γ-singles, β-gated γ and $\gamma\gamma$-coincidence data.

References:

1) T. Sekine, A. Osa, M. Koizumi, S. Ichikawa, M. Asai, H. Yamamoto, and K. Kawade, Z. Phys. A, in press.

---

*School of Engineering, Nagoya University, Nagoya 464-01, Japan

D. Fuel Cycle Safety Evaluation Laboratory

II-D-1 Isotopic Composition of Spent Fuel in Light Water Reactors

Y. Naito, M. Kurosawa, and T. Kaneko*

In the framework of the activity of the working group on Evaluation of Nuclide Generation and Depletion in the Japanese Nuclear Data Committee, we summarized the assay data of the isotopic composition of LWR spent fuels in order to verify the accuracy of the burnup calculation codes. A report on this subject was published in JAERI-M 94-034(1994)

The report contains the data collected from the 13 light water reactors (LWRs) including the 9 LWRs(5 PWRs and 4 BWRs) in Europe and USA, the 4 LWRs(2 PWRs and 2 BWRs) in Japan. Summary of these reactors is shown in Table 1.

The assay data include the burnup in the unit of GWD/t and the isotopic compositions of fuel samples; U component , Pu component and Am, Cm, Np contents(TRU), and Cs, Nd, Kr, Xe etc.(FP).

The collected data were sorted into the isotopic composition of the fuel samples, the irradiation history of the fuel samples, the composition of the fuel assemblies and the sampling position for benchmark calculation.

Finally, we studied on burnup characteristics of the fuels using these data. Several groups of isotopic composition data were chosen to study the dependence of the isotopic compositions of U and Pu on burnup in the followings.

1) Obligheim	PWR	initial enrichment 3.00 wt.%
2) Obligheim	PWR	initial enrichment 2.83 wt.%
3) Gundremmingen	BWR	initial enrichment 2.53 wt.% axially lower part
4) Gundremmingen	BWR	initial enrichment 2.53 wt.% axially upper part
5) Mihama-3(Japan)	PWR	initial enrichment 3.24 wt.%
6) Genkai-1 (Japan)	PWR	initial enrichment 3.42 wt.%

We tried to express U and Pu components of spent fuel as function of flux time which is a parameter related to burnup.

---

* The Japan Research Institute, Ltd

The relation between flux time ($x=\phi t$) and burnup (B) is given by the following equation.

$$B = ({}^{235}\sigma_f\,{}^{235}N + {}^{239}\sigma_f\,{}^{239}N + {}^{241}\sigma_f\,{}^{241}N)\ \phi t$$

where N is an atomic number of each nuclide per ton of initial U, σ_f is microscopic fission cross section (barn), Suffixes 235, 239, 241 show U-235, Pu-239 and Pu-241 respectively.

The following values are used as microscopic cross section at 2200m/s of each nuclide.

$$^{235}\sigma_f = 584$$
$$^{239}\sigma_f = 746.7$$
$$^{241}\sigma_f = 1015$$

Then, if the seven functions:

$\Delta^{238}U/^{238}U_{init} = f_1(x)$,

$(^{235}U/^{total}U)/\varepsilon = f_2(x)$, ε ; initial enrichment

$^{total}Pu = f_3(x)\ ^{total}U$,

$^{239}Pu = f_4(x)\ ^{total}Pu$,

$^{240}Pu = f_5(x)\ ^{total}Pu$,

$^{241}Pu = f_6(x)\ ^{total}Pu$,

$^{242}Pu = f_7(x)\ ^{total}Pu$

can be determined, the amounts of U-235,-238, Pu-239,-240,241 and Pu-242 can be estimated by indicating the flux time x. The fitting curves were obtained using the assay data. We supposed each curve an approximation of each function. The curve of $(^{235}U/.^{total}U)/\varepsilon$ as a function of flux time is shown in Fig.1, and the data plotted as a function of burnup is shown in Fig.2. Comparing these plots including other cases, it is seen in most cases that the plots using flux time have smaller scattering of data.

Therefore, the flux time is able to trace the burnup characteristics of U, Pu isotopes better than burnup in the unit of GWD/t.correctness of the data here of.

Reference:

1) Y. Naito, M. Kurosawa and T. Kaneko:"Data Book of the Isotopic Composition of Spent Fuel in Light Water Reactors", JAERI-M 94-034(1994).

Table 1 Core Composition and Performance

Reactor Name	Yankee	Trino Vercellese		Obrigheim	Garigliano		Gundremmingen	Monticello
	Core I	Cycle I	Cycle II		Cycle I	Cycle II		
Reactor Type	PWR	PWR		PWR	BWR		BWR	BWR
Fuel Pellet								
Diameter (cm)	0.74676	0.89	0.89	0.904	1.191	1.290	1.224	1.057
Length of pellet stack in fuel rod (cm)	230.05	264.1	264.1	295.6	267.72	271.8	330.2	365.76
Fuel Clad								
Material	SUS348	SUS304	SUS304	Zircaloy-4	Zircaloy-2	Zircaloy-2	Zircaloy-2	Zircaloy-2
Square fuel assembly								
Rod array	18 × 18	15 × 15	15 × 15	14 × 14	9 × 9	8 × 8	6 × 6	8 × 8
Number of rods	304/305	208	208	180	81	64	36	63
Fuel rod pitch (cm)	1.07188 1.15824	1.303	1.303	1.430	1.73	1.93	1.78	
Initial enrichment (%) (reloaded assembly+)	3.4	2.72/3.13/ 3.90	2.72/3.13 3.90/4.00+	2.5/2.8/ 3.1	1.6/2.1	1.83/2.41	1.87/2.53	1.45/1.87/ 2.14/2.87
Control rod								
Absorbing material	Ag-In-Cd	Ag-In-Cd	Ag-In-Cd	Ag-In-Cd	B_4C Powder	B_4C Powder	B_4C Powder	B_4C Powder
Core								
Equivalent diameter (cm)	190.75	249.9	240.0	250.0	291.084	291.084	274.8	
Active height (cm)	233.4	264.9	264.9	275.0	267.72	271.8	330.2	365.76
No. of square assemblies	76	120	112	121	208	208	368	
Power (MWth)	392	825	825	907.5	506	506		
(MWe)				350			250	536

Table 1 Core Composition and Performance (continue-1)

Reactor Name	Mihama-3	Genkai-1	Tsuruga-1	JPDR	TMI	Robinson-2	Quad Cities-1
Reactor Type	PWR	PWR	BWR	BWR	PWR	PWR	BWR
Fuel Pellet							
Diameter (cm)	0.929	0.929	1.237	1.25	0.94	0.93	1.24
Length of pellet stack in fuel rod (cm)	366	366	365.7			386.1	366
Fuel Clad							
Material	Zircaloy-4	Zircaloy-4	Zircaloy-2	Zircaloy-2	Zircaloy-4	Zircaloy-4	Zircaloy-2
Square fuel assembly							
Rod array	15 × 15	14 × 14	7 × 7	6 × 6		15 × 15	7 × 7
Number of rods	204	179		36	208	204	49
Fuel rod pitch (cm)	1.43	1.41		1.956	1.36		
Initial enrichment (%)	3.24	3.42	1.40/1.80/2.10/2.79	2.6	2.29/2.64/2.90	1.85/2.55/3.10	1.20/1.69/2.44
Control rod							
Absorbing material							
Core							
Equivalent diameter (cm)	304	246		127	328	304	463
Active height (cm)	366	366	365.7	147	366	366	366
No. of square assemblies	157		308		177	157	724
Power (MWth)	2440	1650	1064	45	2772	2200	2511
(MWe)	826	559	357		907	700	809

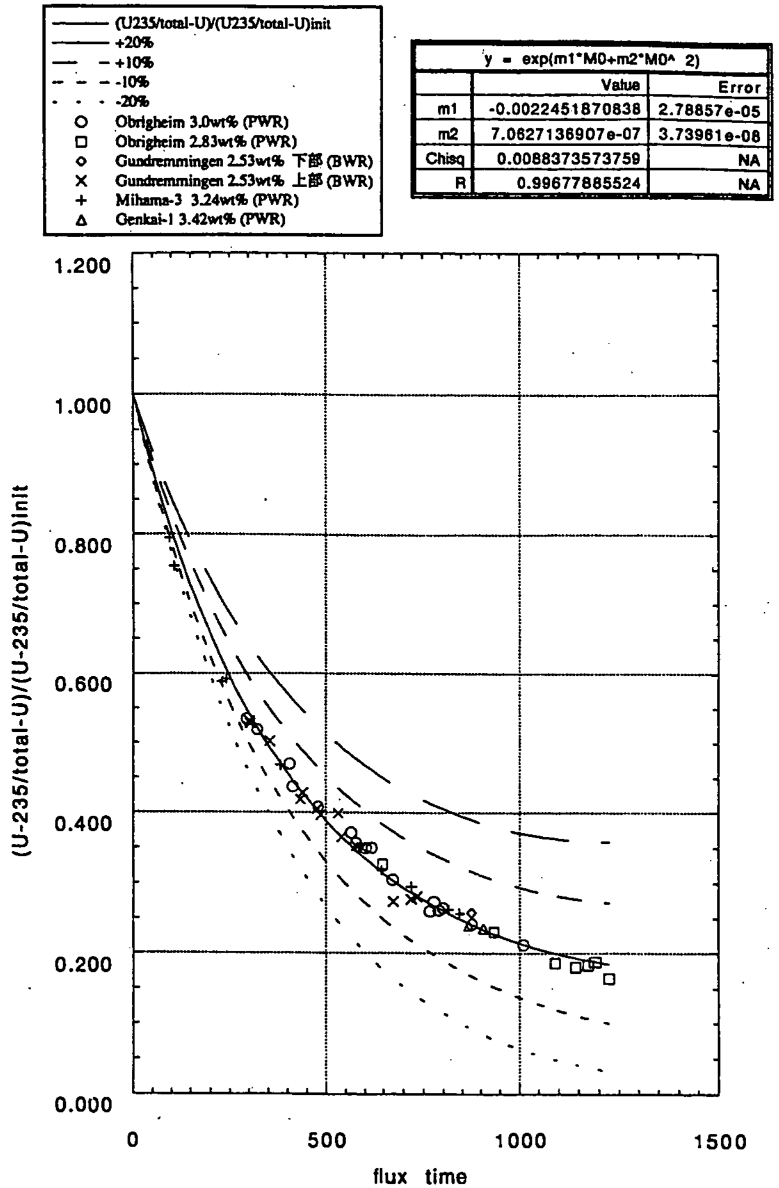

Fig. 1. (U-235/total-U)/(U-235/total-U)init vs. flux time

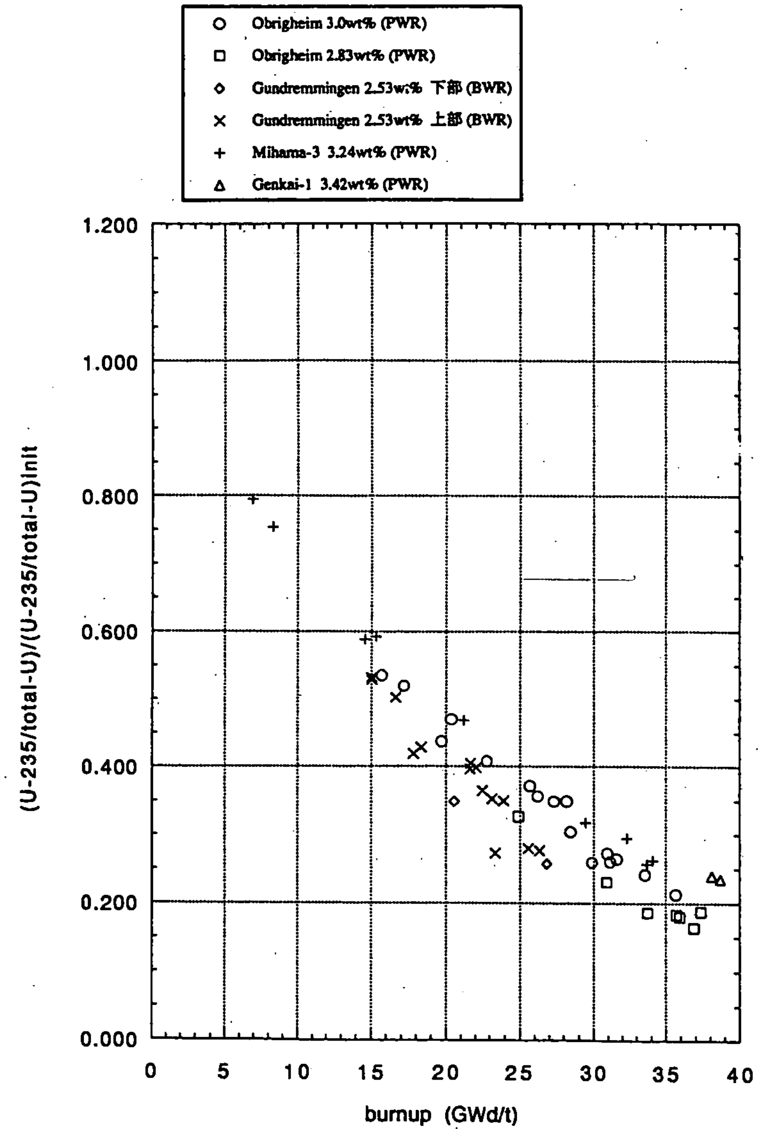

Fig. 2 (U-235/total-U)/(U-235/total-U) init vs. burnup

III. Kyoto University

A. Research Reactor Institute

III-A-1 **The half-Life of ^{148}La**

K. Okano, A. Taniguchi*, Y. Kawase and S. Yamada

The half-lives of a lot of short-lived neutron-rich nuclei produced by fission are not determined to a sufficient degree of accuracy. We are planning to determine rather precisely these short half-lives by using KUR-ISOL. As a first step towards this study, the half-life of ^{148}La has been measured.

The values of half-life of ^{148}La hitherto reported do not agree with each other. They are widely scattered as shown in Table 1. Although the recent value of 1.05(1)s reported by Gill et al.[4] is usually adopted, the value may not be so precise because it is deduced from a growth-decay curve of a ^{148}La γ-ray generated from the decay of ^{148}Ba. In the case of KUR-ISOL, ^{148}La is directly produced and no ^{148}Ba nuclei are produced by an oxidation method.

The γ-ray spectra following the decay of ^{148}La have been measured by using a 230cc HPGe detector and a low-energy photon spectrometer which were shielded by lead blocks 10cm thick. The spectra were taken by using two SMS-48 multispectrum scaling PHAs in a 16×0.35s scaling mode. The measurements were started about 0.5s after 2s irradiation. The half-lives of six strong γ-transitions determined following the decay for four half-lives are listed in Table 1, together with the averaged value of 1.38(1)s thus obtained.

References

1] K.-E. Seyb, Report BMFT-FBK-73-22 (1973) 131.
2] S. Amiel, G. Engler, Y. Nir-El and M. Shmid, CERN Report 76-13 (1976).
3] B. Pffeiffer, E. Koglen, E. Monnand, G. Jung and J. Münzel, Annex to Ann. Rep. Grenoble (1981).
4] R. L. Gill, M. Shmid, R. E. Chrien, Y. Y. Chu, A. Wolf, D. S. Brenner, K. Sistemich, F. K. Wohn, H. Yamamoto, C. Chung and W. B. Walters, Phys. Rev. C, 27 (1983) 1732.

*Faculty of Engineering, Nagoya University

Table 1. Half-life of ^{148}La and measuring instruments used

Present results			Previous results			
			Ref. (1)	Ref. (2)	Ref. (3)	Ref. (4)
	γ-ray (keV)					
Half-life	158.5	1.38(1)				1.05(1)
(s)	295.1	1.40(2)				
	387.9	1.32(6)				
	601.9	1.40(3)				
	760.3	1.37(3)				
	989.9	1.36(4)				
	mean	1.38(1)	1.7(5)	2.62(61)	1.55(3)	1.05(1)
Detector	HPGe detector		γ-detector	Si β-detector	γ-detector	HPGe detector
ISOL	KUR-ISOL		Chemical separation	SOLIS	OSTIS	TRISTAN

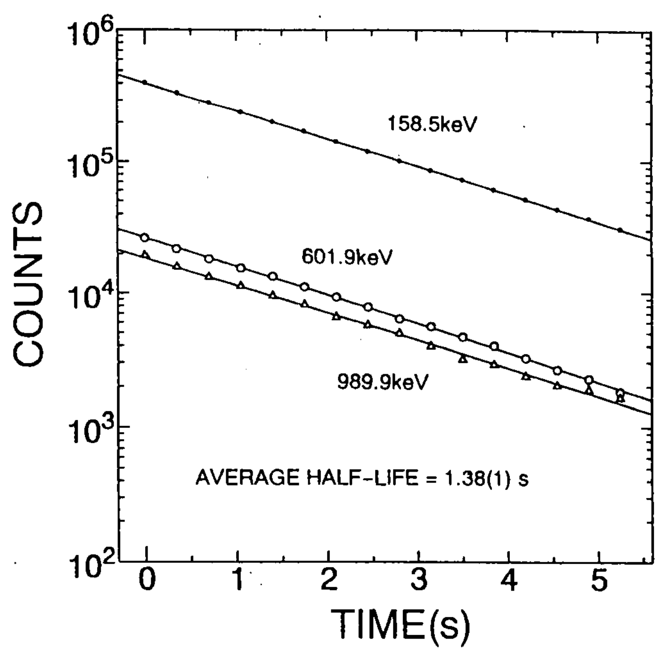

Fig. 1. Decay curves of γ-ray lines from ^{148}La.

III-A-2 Gamma-rays following the decay of ^{152}Ce

K. Okano, A. Taniguchi* and S. Yamada

The heaviest isotopes of Ce, ^{152}Ce, has previously been reported to decay with the half-life of 1.4(2) s emitting 97.8 and 114.8 keV γ-rays.[1] Additional transitions have recently been identified as shown in Table 1, utilizing mass separated beam from KUR-ISOL.

The lines decaying with the half-life of about 1.4s have been assigned to originate from ^{152}Ce, although many transitions following the decay of 3.8s ^{152}Pr have been observed simultaneously. The half-life of ^{152}Ce has been determined as 1.40(6)s from the decay curve of 97.8 and 114.8 keV lines.

The 114.8 keV transition has been asserted to be an isomeric transition with a half-life of 1.0(3)μs.[1] From the present β-γ coincidence measurements with a three dimensional list-mode data taking system, the half-life was measured to be about 4μs. Other transitions were found to have no such a long life-time. The construction of a decay scheme of ^{152}Ce including the above information is now in progress analyzing the results of γ-γ coincidence measurements.

Reference:
1) I. Tago, Y. Kawase and K. Okano, Z. Phys. A Atomic Nuclei 335 (1990) 447.

Table 1. Energies and relative intensities of γ-rays following the decay of ^{152}Ce.

$E\gamma$ (keV)	$I\gamma$
97.8(1)	52(5)
114.8(1)	100
316.6(1)	12(1)
456.7(1)	7(1)
570.1(1)	29(2)
773.7(1)	9(1)
812.7(2)	17(2)
843.9(2)	14(2)

*Faculty of Engineering, Nagoya University

III-A-3 Characteristics of Fe-Filtered Neutron Field

K. Kobayashi, T. Yoshimoto, M. Saito, T. Sato,
Y. Fujita, M. Utsuro and H. Utsumi

Some materials have sharp minima, which are often called as neutron window, in the neutron total cross section in the resonance energy region. By placing thick filters of the material into a white neutron source beam, only neutrons near the minimum can be transmitted as filtered neutrons, and the background due to the off-minimum neutrons and gamma-rays can be considerably reduced[1]. Since natural iron has a deep minimum of cross section of about 0.4 barn near 24 keV, while the average cross section value is about 5 barns except for 24 keV region, thick Fe-filters can produce quasi-monochromatic neutrons of about 24 keV.

In the present study, we have installed an Fe-filtered beam facility at the B-1 experimental hole of the Kyoto University Reactor (KUR) at the Research Reactor Institute, Kyoto University (KURRI). The experimental arrangement of the facility is shown in Fig. 1. Total thickness of the Fe-filters is 45 cm and that of the additional filters of Al is 35 cm, respectively. Collimation/shielding materials for neutrons and gamma-rays are mainly made of heavy concrete and lead. In front of the facility, a small house (1.5 m height, 1.6 m width and 2 m depth) of heavy concrete is established for the experimental space.

The characteristics of neutron spectrum were investigated by transport calculations with the MCNP and DOT 3.5 codes and by measurements using a spherical proton recoil counter 5 cm in diameter filled with H_2 gas at 1 atm. Figure 2 shows the neutron spectrum calculated with the MCNP code just behind the last filter. One can see not only 24 keV neutrons but also higher energy neutrons which penetrated a little through the thick Fe- and Al-filters. With the detection efficiency of the proton recoil counter calculated by the H(n,p) cross section, preliminary result of the neutron flux for 24 keV neutrons was estimated to be about 1.2×10^6 n/cm^2/s at the position A in Fig. 1 (45 cm from the last filter) by normalizing the KUR power to 5 MW.

The gamma–dose distribution at the Fe–filtered beam facility was also measured with thermo–luminescence dosimeters (TLDs) made of $Mg_2Si_4(Tb)$. The absorbed dose measured at the position A was 7 cGy/h, and 100 cGy/h behind the last filter, respectively.

REFERENCE:

1) R.C.Block, et al.: J. Nucl. Sci. Technol., **12**, 1 (1975).

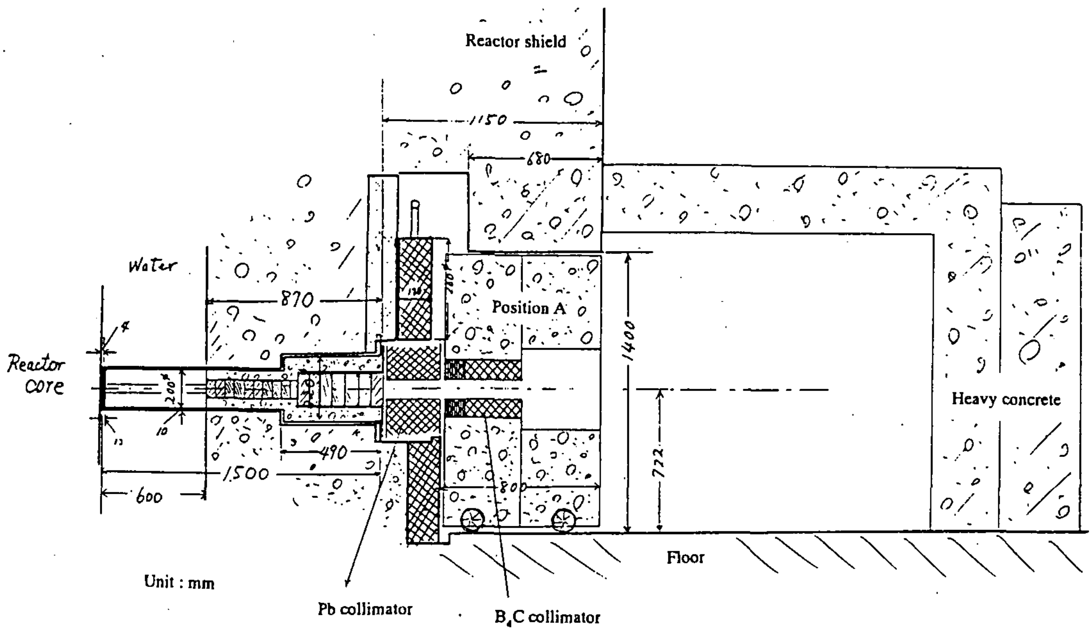

Fig. 1 Experimental arrangement for the Fe–filtered neutron field.

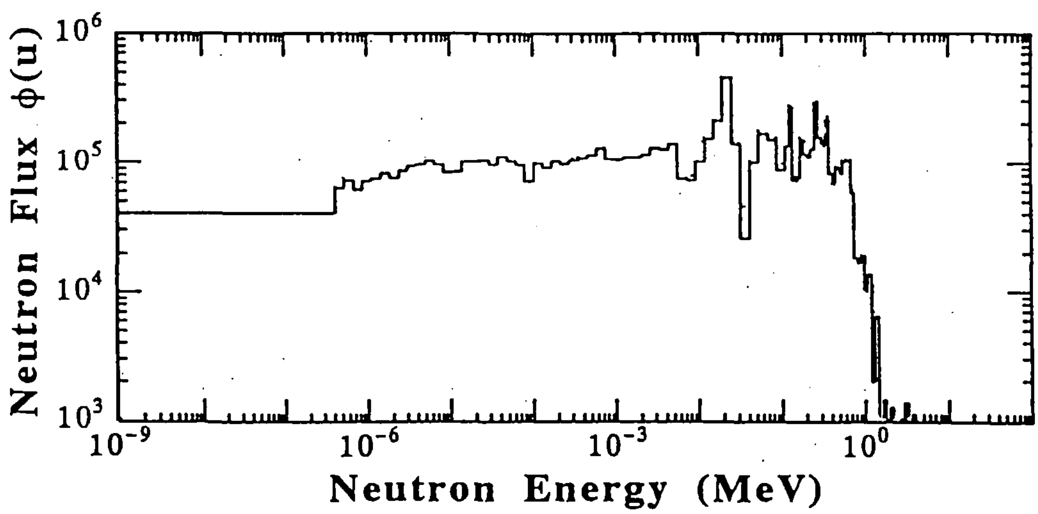

Fig. 2 Neutron spectrum behind the last filter calculated with the MCNP code.

III–A–4 Fission Cross Section Measurement of Am–241 between 0.1 eV and 10 keV with Lead Slowing–Down Spectrometer

K. Kobayashi, M. Miyoshi*, S. Yamamoto, Y. Fujita,
I. Kimura*, I. Kanno* and S. Kanazawa*

Numerous measurements of the fission cross section of ^{241}Am have been made previously and often confronted with the difficulty by the extremely large alpha–particle activity due to its short half–life of 432 years as alpha–decay. In addition, the fission cross section of ^{241}Am is relatively low (0.02 to 0.5 b) over the neutron energy range between 100 eV and 300 keV. Several groups have measured the fission cross section below about 100 keV.[1–5] However, discrepancy can be seen between the data there, although the data measured at MeV energies show good agreement with each other.[6] Two newly evaluated data files of JENDL–3[7] and ENDF/B–VI[8], which may mainly refer to the experimental data by Dabbs et al.[5], are in disagreement with the earlier data by Bowman et al.[1], Seeger et al.[2], Gayther et al.[3], and Knitter et al.[4] in the energy region above about 30 eV.

In the present measurement, the fission cross section for the ^{241}Am(n,f) reaction is measured relative to that for ^{235}U by making use of back–to–back type double fission chambers and a lead slowing–down spectrometer[9,10] coupled to 46 MeV electron linear accelerator (linac) of Research Reactor Institute, Kyoto University (KURRI). The experimental technique is the same as that of the fission cross section measurement of ^{237}Np.[9] The measured result is compared with the evaluated data in JENDL–3 and ENDF/B–VI, and with the existing experimental data.

The present result is shown in Fig. 1, and compared with the evaluated cross sections in JENDL–3 and ENDF/B–VI. Both of the evaluated data are about 3 times smaller than the present values. We processed the evaluated data by multiplying a resolution

* Department of Nuclear Engineering, Kyoto University

function of which shape is assumed to be a Gaussian with 40 % of its full width at half maximum.[9,10] From the figure, it can be seen that the shape of the energy dependent cross section is close to that of the files except for the energy regions at 3 large peaks.

The present result is also compared with the existing experimental data in Fig. 2. The data by Dabbs et al.[5] are about 3 times smaller than the present measurement. The data by Seeger et al.[2] are much larger than the present ones above 100 keV, but those by Knitter et al.[4] are much smaller there. The fission cross sections by Gayther et al.[3] and Bowman et al.[1] are rather close to our measurement in the relevant energy range.

For the investigation of the discrepancies between the earlier and the present data, we have measured the ^{241}Am sample with the α–ray and γ–ray spectrometers. The impurity in the sample was not found from the measurements. In addition, making use of the heavy water thermal neutron facility of the Kyoto University Reactor (KUR), we have also measured the thermal neutron fission cross section of ^{241}Am with the same experimental method as the case with KULS. The measured result shows good agreement with the value extrapolated from the data by KULS, as shown in Figs. 1 and 2. It may be useful, in future, to try to analyze the isotopic composition in the ^{241}Am sample with a mass spectrometer or to use another sample deposit, to investigate the discrepancies between the present and the earlier measurements.

REFERENCES

1. C. D. Bowman, et al., Phys. Rev., **137**, B326 (1965).
2. P. A. Seeger, et al., Nucl. Phys., **A96**, 605 (1967).
3. D. B. Gayther and B. W. Thomas, "Measurement of the Neutron Capture and Fission Cross Sections of ^{241}Am," Proc. of the 4th All–Union Conf. on Neutron Phys., Kiev, Part 3, p.3 (1977).
4. H. H. Knitter and C. Budtz–Jorgensen, Atomkernenergie–Kerntechnik, **33**, 205 (1979).
5. J. W. T. Dabbs, et al., Nucl. Sci. Eng., **83**, 22 (1983).
6. V. McLane, et al., "Neutron Cross Sections," Vol.2, Neutron Cross Section Curves, Academic Press, Inc., London, 1988.

7. K. Shibata, et al., "Japanese Evaluated Nuclear Data Library, Version-3, JENDL-3," JAERI 1319, JAERI, 1990.

8. R. F. Rose (Ed.), "ENDF/B Summary Documentation," BNL-NCS-17541, 4th Ed. (ENDF/B-VI) 1991.

9. A. Yamanaka, et al., J. Nucl. Sci. Technol., **36**, 863 (1993).

10. K. Kobayashi, et al., "Characteristic Behavior of Neutrons in the Lead Slowing-down Spectrometer Coupled to Electron Linac," JAERI-M 93-046, p.360, JAERI, 1993.

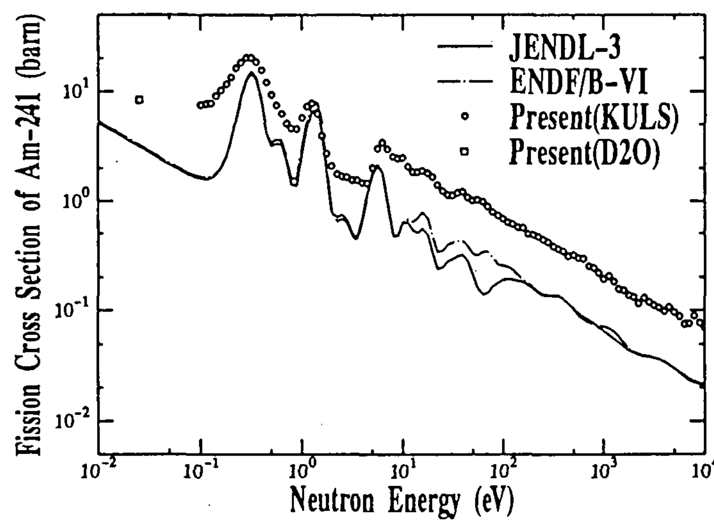

Fig. 1 Comparison of the measured fission cross section of ^{241}Am with those in evaluated data files.

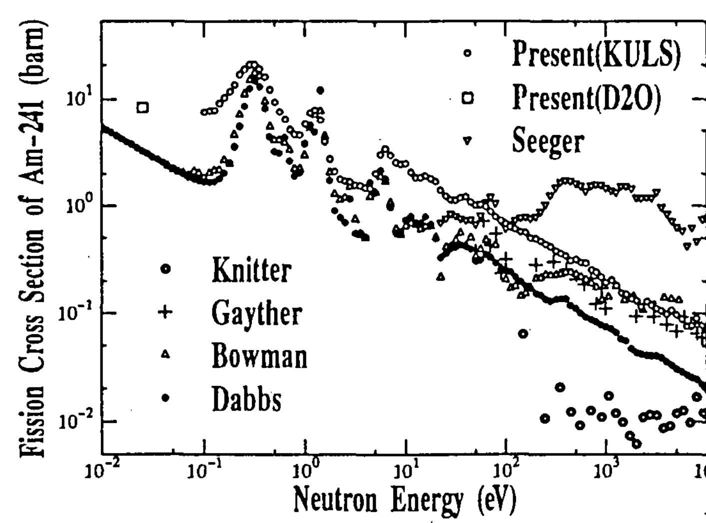

Fig. 2 Comparison of the measured fission cross section of ^{241}Am with earlier experimental data.

III-A-5 Precise Measurement of Neutron Total Cross Sections of Pb-208 and Pb-nat

K. Kobayashi, S. Yamamoto, Y. Fujita
O. A. Shcherbakov* and A. B. Laptev*

In recent years, a great interest has been focused on the precise measurement of neutron total cross section of lead, for the study of electric polarizability of neutron.[1-3] One of the characteristics of neutron is the electric polarizability α_n due to an induced electric dipole moment. It is said that the α_n value can be obtained from the high precision measurements of neutron total cross sections of heavy nuclei.[4] Correcting the measured cross sections for Schwinger, neutron-electron scattering, and resonance contributions, the α_n values are deduced.[1-4] The first resonance of ^{208}Pb is 43.3 keV and higher than that appearing in natural lead (^{nat}Pb). Moreover, as the capture cross section is pretty low, the ^{208}Pb data may be more appropriate for the investigation of α_n in the expanded energy region.

In the present work, neutron transmission measurements of ^{208}Pb and ^{nat}Pb are made (1) in the energy region from 4 to 180 eV by a resonance capture detector[5] with Ta and Sb samples, (2) in the continuous energy range from 2 eV to 2 keV, and (3) at 24, 55 and 145 keV with Fe- and Si-filtered neutrons[6] by a ^{10}B capture detector, making use of 46 MeV linac at the Research Reactor Institute, Kyoto University (KURRI). The experimental arrangement is shown in Fig. 1. The measured results are compared with the recent evaluated data in JENDL-3[7] and ENDF/B-VI[8]. The present results are also compared with the recent data measured by Alexandrov et al.[1], Schmiedmayer et al.[2], and Granada et al.[3]

The present results of ^{208}Pb and ^{nat}Pb are shown in Fig. 2 and compared with the evaluated data in both files, JENDL-3[7] and ENDF/B-VI[8]. Total amount of the experi-

* Petersburg Nuclear Physics Institute, Gatchina, Russia

mental uncertainties are 0.17–0.65 % from 4 to 180 eV, 0.13–0.66 % from 2 eV to 2 keV, 0.55–0.62 % at 24 keV, about 0.42 % at 145 keV, and about 1.3 % at 55 keV, respectively. From the figure, it can be seen that both results are almost constant below 2 keV and the ^{208}Pb data are larger by about 0.25 b than the ^{nat}Pb values. Although the shape of both energy dependent cross sections in ENDF/B–VI is similar to the present measurements, the absolute values for both cross sections are lower by about 1.5 % than the present values in the relevant energy region. The evaluated cross section of ^{nat}Pb in JENDL–3 is in good agreement with the measured data, although the evaluated data of ^{208}Pb are lower by 2 % than the measured ones. At tens of keV energies with filtered neutrons, the JENDL–3 data are much lower than the present measurements.

The present data of ^{208}Pb show very good agreement with the recent results by Alexandrov et al.[1] and Schmiedmayer et al.[2] with each other. Very recent data of ^{nat}Pb measured by Granada et al.[3] are also in good agreement with the present values.

REFERENCES

1. Y. A. Alexandrov, et al., "Measurement of the neutron Total Cross Sections for Bi and Pb: Estimate of the Electric Polarizability of the Neutron," *Proc. Int'l Conf. on Nucl. Data for Sci.*, Springer–Verlag, p.160, 1992.
2. J. Schmiedmayer, et al., "Electric properties of the neutron from Precision Cross Section Measurements," *ibid.*, p.163, 1992.
3. J. G. Granada, et al., *Physica* **B 190**, 259 (1993).
4. Y. A. Alexandrov, *Yadernaya Fizika*, **37**, 253 (1983), and **38**, 1100 (1983).
5. K. Kobayashi, et al., *Nucl. Instr. Neth.*, **A 287**, 570 (1990).
6. K. Kobayashi, et al., "Measurement of Capture cross Sections for ^{238}U and Sb," *Proc. Int'l Conf. on Nucl. Data for Sci.*, Springer–Verlag, p.65, 1992.
7. K. Shibata, et al., "*Japanese Evaluated Nuclear Data Library, Version–3, JENDL–3*," JAERI 1319, JAERI, 1990.
8. R. F. Rose (Ed.), "*ENDF/B Summary Documentation*," BNL–NCS–17541, 4th Ed. (ENDF/B–VI) 1991.

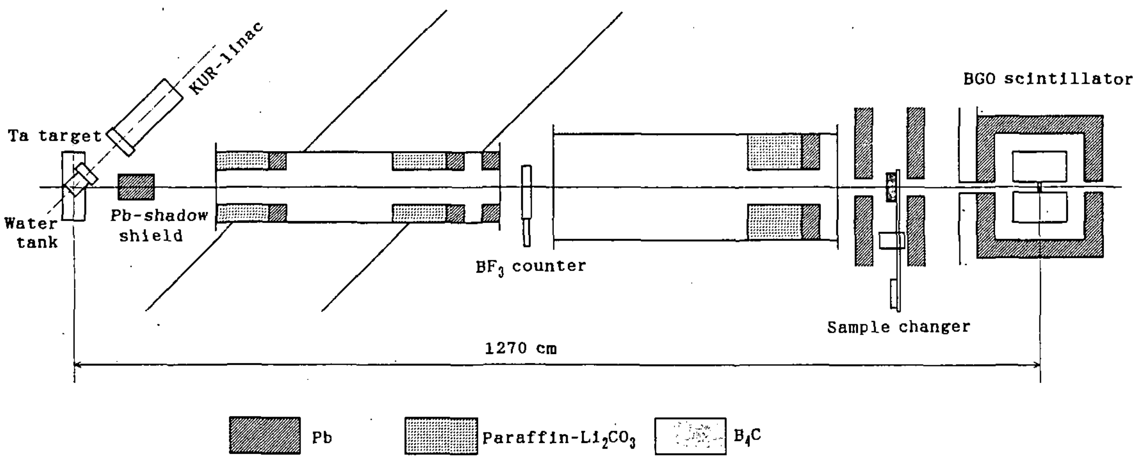

Fig. 1 Experimental arrangement for the transmission measurement.

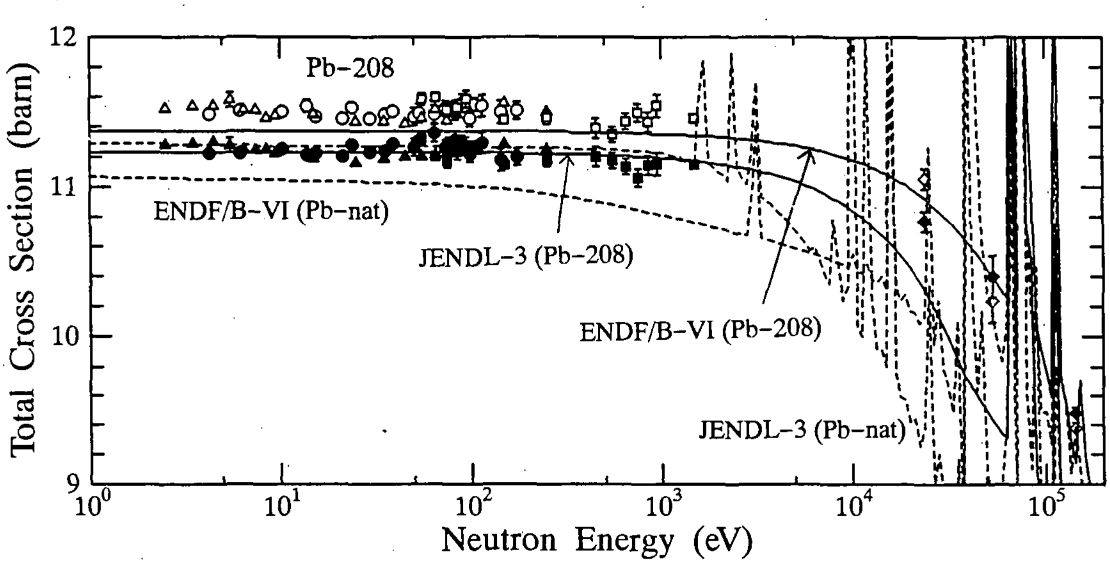

Fig. 2 Comparison of the measured neutron total cross sections of Pb-208 and Pb-nat with the evaluated data in JENDL-3 and ENDF/B-VI.

IV. Kyushu University

IV-A-1 Neutron bound sate complex potentials

O. Iwamoto, A. Nohtomi, Y. Uozumi, T. Sakae, and M. Matoba

Single particle / hole states of medium weight nuclei were studied using polarized proton / deuteron beams at the Research Center for Nuclear Physics (RCNP). Real and imaginary parts of neutron bound state potentials have been calculated from single particle / hole energies and spreading widths of the particle / hole states. They are compared with optical potentials obtained by the dispersion relation approach to neutron scattering cross section. These potentials show good agreement and it is found that the imaginary parts of the bound state potentials exhibit a symmetrical behavior with respect to the Fermi surface. A paper on this subject will be published in Nucl. Phys. A.

The ^{40}Ca,$^{58\text{-}64}$Ni(p,d) and ^{40}Ca,^{58}Ni(d,p) reaction experiments with polarized 65 MeV proton and 56 MeV deuteron beams were carried out at the AVF cyclotron facility of RCNP to study the neutron hole and particle states. Angular distributions of the cross sections and

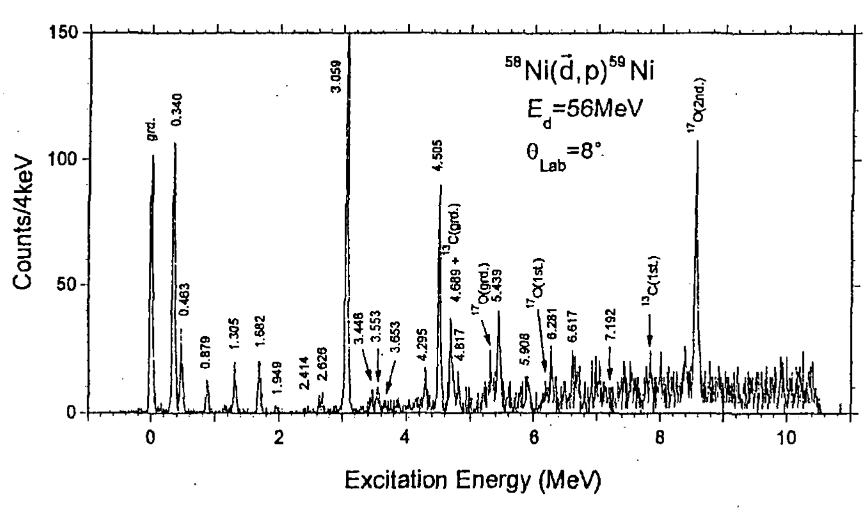

Fig.1. Typical energy spectrum of protons from ^{58}Ni(d,p)^{59}Ni reaction at 56 MeV for deuteron-spin up; θ_{Lab}=8°

analyzing powers were measured at 5° to 45° laboratory angles. The measured excitation energy region was 0-10 MeV. Figure 1 shows a typical energy spectrum from the $^{58}Ni(d,p)^{59}Ni$ reaction at 56 MeV in the excitation energy region of 0-10 MeV at 8° laboratory angle. The overall energy resolution was 40-50 keV.

Characteristics of single particle and hole states are often compared with theory in terms of integrated properties such as single particle / hole energies and spreading widths. The single particle / hole energy for nlj state is obtained by calculating the center of gravity of the spectroscopic strength function or spectroscopic factor $C^2S_{nlj}(E_i)$ as a function of energy. The width Γ_{nlj} is obtained from the second moment of the spectroscopic strength function, which is regarded as the spreading width in the present work.

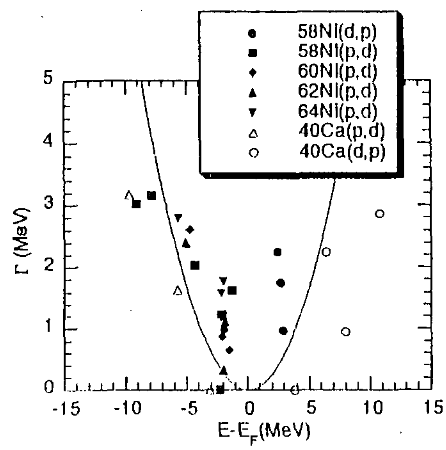

Fig. 2. Energy dependence of spreading widths for $^{58-60}Ni$ and ^{40}Ca. Solid line shows a prediction of infinite Fermi system.

The energy dependence of the spreading widths are shown in fig. 2 as a function of the energy difference from the Fermi surface, E_{nlj}-E_F. The spreading widths located above the Fermi surface are for the single particle state from stripping reactions and below the Fermi surface are for the single hole states from pickup reactions. A prediction of the infinite Fermi system[1)] is shown by a solid line. The gross feature is in agreement with the infinite model prediction. Symmetrical behaviors with respect to the Fermi surface are observed.

The potential depths of real and imaginary parts for nlj state are calculated using a complex potential parameter search code CXBOUND[2] that solves the complex eigenvalue equation,

$$\left\{-\frac{\hbar^2}{2m}\frac{d^2}{dr^2}+\frac{\hbar^2}{2m}\frac{l(l+1)}{r^2}+V(r)+iW(r)+V_{ls}(r)l\cdot s+V_C(r)\right\}u_{nlj}(r)$$
$$=\left(E_{nlj}+i\frac{\Gamma_{nlj}}{2}\right)u_{nlj}(r)$$

where E_{nlj} and Γ_{nlj} are the single particle energy and the spreading width for the nlj state, respectively. V(r) and W(r) are the real and imaginary parts of the nuclear potential, respectively. $V_C(r)$ is the coulomb potential and $V_{ls}(r)$ is the spin orbit potential. The $u_{nlj}(r)$ is the single particle radial wave function. The volume type contribution to the imaginary potential was disregarded, since the volume type contribution is negligible in this energy region near Fermi surface. The geometrical parameters used were assumed to be constant of r_0=1.25 fm, a_0=0.65 fm for all central potentials.

The volume integrals of the real and the imaginary parts of the neutron potentials for ^{40}Ca are shown as a function of the neutron energy in fig. 3. The general tendency of both the

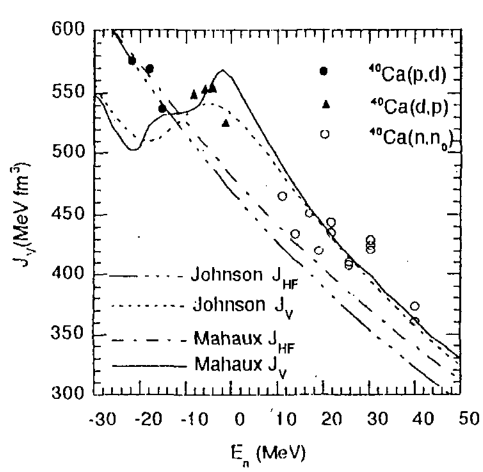

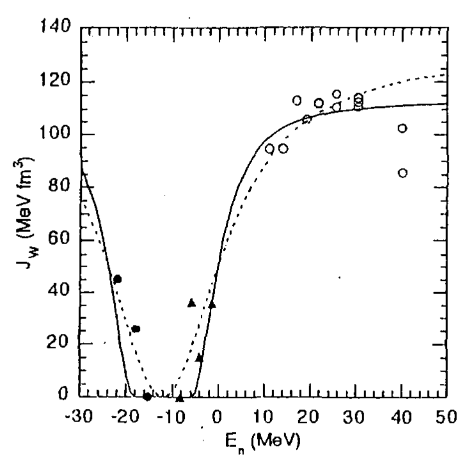

Fig. 3. Volume integral of real (left) and imaginary (right) parts of neutron bound state potential of ^{40}Ca obtained by single particle energy and dispersion relation approaches of Johnson et al.[3] and Mahaux et al.[4] J_{HF} and J_V show volume integrals of Hartree-Fock components and full potentials (HF + dispersion-contribution), respectively.

real and imaginary parts of the bound state potentials is in agreement with ones obtained by dispersion relation approaches[3,4]. Optical potentials may be connected to bound state potentials smoothly for both real and imaginary parts. The energy dependence of bound state potentials for Ni isotopes exhibits almost same tendency as for Ca isotopes except the imaginary parts near Fermi surface. The imaginary parts for Ca vanish near Fermi surface but for Ni isotopes. The symmetric behavior of the imaginary parts against the Fermi surface is also seen as in the spreading widths.

Neutron bound state complex potentials for Ca and Ni isotopes are calculated from the data of ^{40}Ca, $^{58\text{-}64}$Ni(p,d) and ^{40}Ca, ^{58}Ni(d,p) reaction. The real and the imaginary part of the potential are almost consistent with the optical potentials obtained by dispersion relation approach to neutron scattering cross section.

References:

1). G. F. Bertsch, P. F. Bortignon, R. A. Broglia, Rev. Mod. Phys. **55**, 287 (1983)

2). Y. L. Luo, M. Kawai, code CXBOUND, Kyushu University, private communication.

3). C. H. Johnson, C. Mahaux, Phys. Rev. **C38**, 2589 (1988)

4). C. Mahaux, R. Sartor, Nucl. Phys., **A528**, 253 (1991)

IV–A–2 Response of NaI(Tl) crystals to medium-energy protons

M. Yamashita[1], H. Yoshida[1], Y. Uozumi[1], S. Budihardjo[1], O. Iwamoto[1], A. Nohtomi[1], T. Sakae[1], M. Matoba[1], N. Koori[2], and T. Maki[3]

We have been interested in studying medium-energy $(p, p'x)$ preequilibrium reactions at the ring-cyclotron facility of the Research Center for Nuclear Physics (RCNP). A full energy detector which consists of five NaI(Tl) crystals has been developed [1)] to measure wide energy range of proton spectra. It is necessary in using any stopping detector to know the counter response being principally due to the certain probability that an incident particle will undergo a nuclear reaction in the detector material with losing part of its energy, or that a particle will scatter out of the detector before being stopped by the ionization process. The response is usually understood in terms of the peak-to-total ratio. In the present report, we discuss cross-section data at medium energies in comparing the ratio between experimental and calculated values.

A Monte Carlo simulation code has been developed to estimate the peak-to-total ratio of this detector. It is very important to use reliable data of nuclear reactions. In calculating the ratio, an incident particle was assumed to be lost by a nuclear reaction. The total reaction cross-section σ_R [2)] is given empirically by

$$\sigma_R = 0.045A^{0.7}f(A)g(E_p) \qquad [barn],$$

with

$$f(A) = 1 + 0.016\sin(5.3 - 2.63\ln A),$$

$$g(E_p) = 1 - 0.62\exp(-E_p/200)\sin(10.9E_p^{-0.28}),$$

where E_p is the proton energy and A the mass number of the material. As shown in Fig. 1, larger cross-section values on Sodium and Iodine are given at around $E_p = 20$ MeV with this formula than experimental values [3)]. This difference, however, has little effect on the resulted efficiency. In the case of very large detectors, the peak-to-total

[1] Faculty of Engineering, Kyushu University
[2] Tokushima University
[3] University of Occupational and Environmental Health

ratio is determined by sole the reaction loss . The peak efficiency by reaction loss is estimated with a formula of Green et al.[4]:

$$F(E_p) = \frac{1}{1 + (E_p/354)^{1.8}} \qquad : E_p < 280 \text{ MeV}.$$

In Fig. 2, results are compared with experimental data [5].

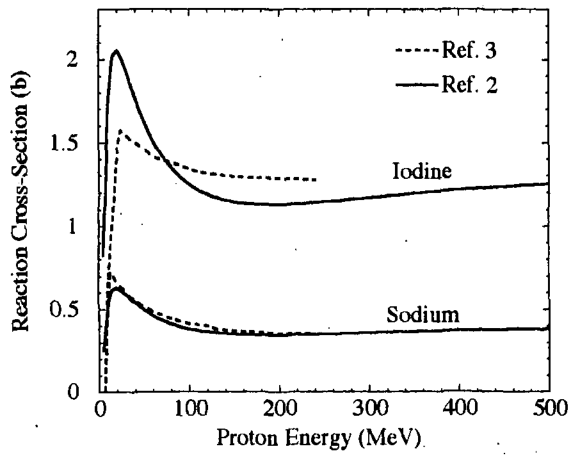

Fig. 1 Total reaction cross-section of p+Na and p+I as a function of incident energy

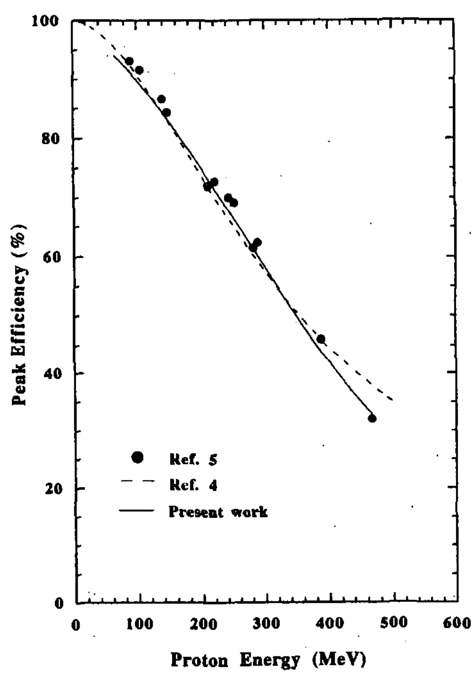

Fig. 2 Proton peak efficiency due to nuclear reactions in NaI

In the case of relatively small detectors, the out-scattering will be caused by the elastic and the multiple coulomb scattering. An empirical formula of elastic scattering cross-section was given in ref.[2]. The formula was modified mainly for simplifying the computation procedure to be

$$\frac{d\sigma_E}{d\Omega} = W\left\{\frac{R}{2\sin(\theta/2)}\right\}^2 \exp\left\{-c_p x\left(1+\frac{x}{40}\right)\right\} \qquad [cm^2/sr]$$

with

$$R = \left\{0.014A^{1/3} + \frac{0.122(A+1)}{A}\right\} \times 10^{-12},$$

$$x = 2kR\sin(\theta/2),$$

$$c_p = 0.2(208/A),$$

where W is the normalization factor as a function of E_p, and k the relativistic wave number in cm^{-1}. The calculated cross sections are displayed in Fig. 3, together with experimental cross-sections and those using the original equation. The inclination of trajectory due to the multiple coulomb scattering was calculated by a fast algorithm[6] of the Molière's formula.

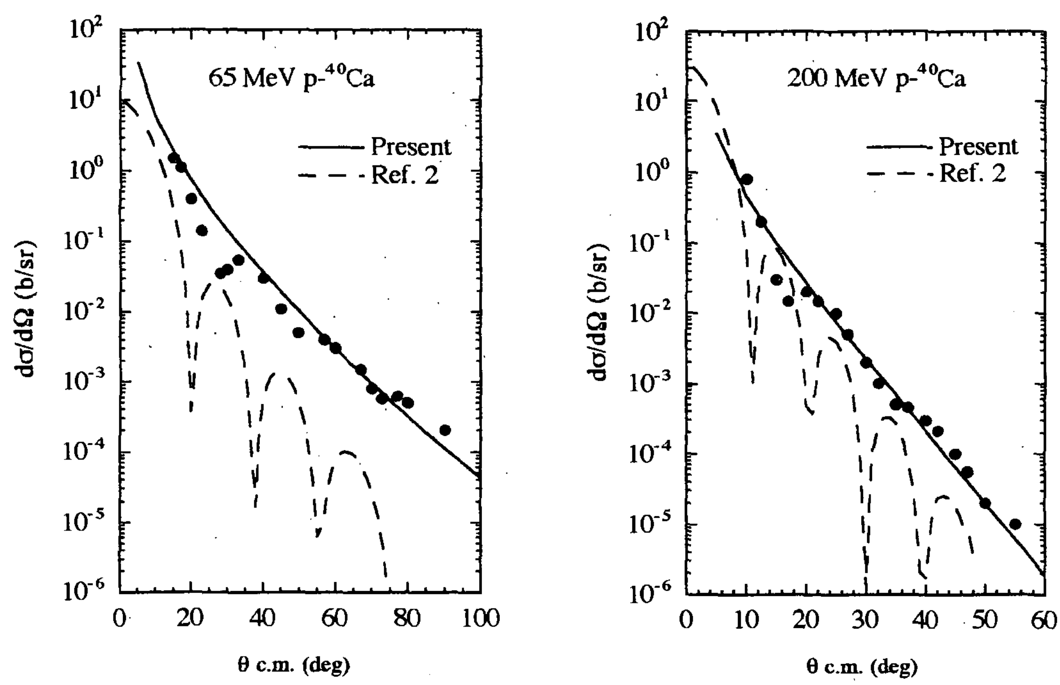

Fig. 3 Elastic scattering cross section. Closed circles are experimental, solid and broken lines are results of the present and Ref.[2], respectively.

The counter efficiency has been calculated under these conditions. Figure 4 shows the efficiency of detector in TRIUMF [5]. The present results are shown by solid lines.

The response of our detector was measured at RCNP using 350-MeV protons from the ring-cyclotron. Experimental procedures have been detailed in ref.[1]. In Table 1, the results are found to be in good agreement with the calculation.

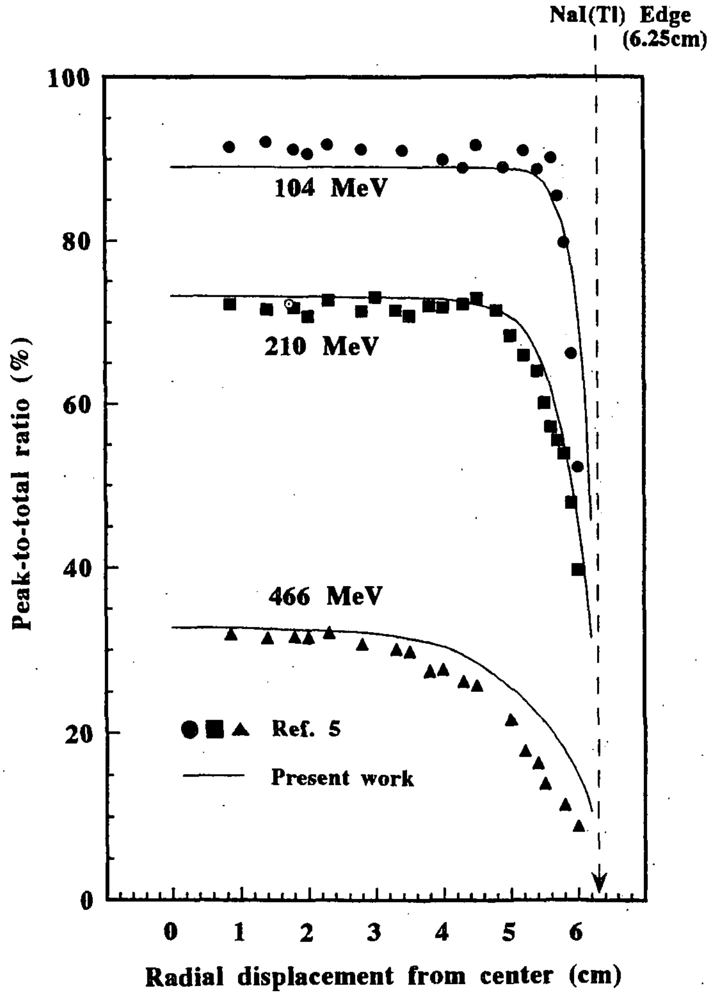

Fig. 4 Peak-to-total ratio of a detector in TRIUMF as a function of proton incident position

Table 1 Present measurement and calculation on peak-to-total ratios of the detector

	160 MeV		250 MeV	
	Experiment	Calculation	Experiment	Calculation
Ratio	79.5 %	80.9 %	53.3 %	53.9 %

References:

1) Y. Uozumi et al.: RCNP Annual Report in 1993 (1994)
   M. Yamashita: Master thesis, Kyushu Univ. (1994)
2) S. Pearlstein: Jour. Astrophys. 346 (1989) 1049
3) C.A. Goulding and J.G. Rogers: Nucl. Instr. Meth. 153 (1978) 511
4) R.E.L. Green et al.: Nucl. Phys. A405 (1983) 463
5) J.M. Cameron et al.: Nucl. Instr. Meth. 143 (1977) 399
6) S.E. Kuhn and G.E. Dodge: Nucl. Instr. Meth. A322 (1992) 88

B. Department of Energy Conversion Engineering

IV–B–1 U-238 Capture and Inelastic Scattering

Y.Kanda

A paper on this subject was published in Proc. of the 1992 International Symposium on Nuclear Data Evaluation Methodology, 12 – 16 Oct., Brookhaven National Laboratory, USA, p.88 with the following abstract:

The capture and inelastic scattering cross sections of ^{238}U have been left as the two important data of those which are agreed to be reevaluated in a nuclear data field. From a viewpoint of evaluation methodology, they are the extremes of conditions about experiments and theories. Concerning the capture cross sections, recently the reliable evaluation base on a few experiments has been done with a resonance analysis. The procedure of the evaluation is briefly reviewed. As contrasted with it, the evaluation of the inelastic cross setction should be performed on the fact that there are scarce and scattered experimental data and some theories can be applicable even though the parameters used in the theoretical evaluation are not decisive for ^{238}U yet. Referring the previous reports analyzing the inelastic scattering experiments for ^{238}U, the theory and parameter set applicable to the evaluation are searched. Both distorted wave Born approximation and coupled-channel model are suitable because the ^{238}U is strongly deformed. In practice, computing coast is important. The optical model parameters of Bruyeres group is used in all the previous report.

IV–B–2 Determination of Covariance of Calculated Cross Sections

Y.Kanda

A paper on this subject was published in Proc. of the 1992 International Symposium on Nuclear Data Evaluation Methodology, 12 – 16 Oct., Brookhaven National Laboratory, USA, p.673 with the following abstract:

The covariance of calculated cross sections have been generated with the method which are adopted by individual evaluators in order to express their understanding for the covariance. Three methods are briefly reviewed and compared quoting the results for Fe. The feature of the three are discussed connecting the result to the mutual differences are revealed to some extent.

A method to visualize a correlation matrix, called a graphical correlation matrix, is developed to compare easily each other. It is made definite that the method is considerably valid to clarify differences between correlation matrices. By using it, the characteristics of the correlation matrices depending on the parameters used in cross section calculation are examined to reach the method of covariance generation for calculated cross sections.

IV–B–3 Evaluation of ^{238}U Inelastic Scattering Cross Section

T.Kawano, N.Fujikawa, and Y.Kanda

A paper on this subject was presented at the 1993 Symposium on Nuclear Data, and published in JAERI-M 94-019, p.290, with the following abstract:

A new evaluation of ^{238}U inelastic scattering cross sections has been made. A coupled-channels model is adopted for calculation of direct inelastic scattering cross sections to the excited levels which belong to the vibrational bands of ^{238}U, as well as the ground state rotational band. The members of a certain vibrational band are coupled to the 0^+-2^+-4^+ triad of the ground state rotational band levels. A band coupling strength β is determined from the experimental inelastic scattering data below 3 MeV. Experimental double differential cross sections (DDX) are also taken into account in the β determination. The calculated level excitation cross sections and the calculated DDX reproduce consistently the experimental data.

IV–B–4 Covariance of the Nuclear Data

Y.Kanda

A paper on this subject was presented at the Specialists' Meeting on Covariance Data, 15 – 16, July, 1993, JAERI, and published in JAERI-M 94-068, p.1, with the following abstract:

There is an introductory review on the present status of covariance for evaluated nuclear data. The following articles are briefly discussed : Necessity of covariance for evaluated data, basic assumption of covariance production, dependency of produced covariance on methods, consistency of evaluated value and covariance, confirming of produced covariance and methods of comparing covariance matrices.

IV–B–5 Covariance Matrix Calculated from Nuclear Models

T.Kawano, K.Kamitsubo, T.Iwamoto, and Y.Kanda

A paper on this subject was presented at the Specialists' Meeting on Covariance Data, 15 – 16, July, 1993, JAERI, and published in JAERI-M 94-068, p.32, with the following abstract:

A production method of a covariance matrix from a nuclear model calculation is described. An optical model is used to estimate the covariance matrix of the ^{54}Fe total cross section, and a Hauser-Feshbach and a precompound models are used for the covariance matrices of ^{54,56}Fe(n,p) reaction cross sections. These matrices are calculated from the uncertainties of level density parameters, a precompound parameter, and the optical potential parameters for neutron, proton, and α-particle. The neutron optical potential parameters and their uncertainties are evaluated from the experimental total and elastic scattering data, while the other parameters and their uncertainties are evaluated from the experimental ^{54,56}Fe(n,p), (n,α), $(n,2n)$, (n,Xp) and $(n,X\alpha)$ reaction cross sections.

IV–B–6 Calculation of ^{238}U Inelastic Scattering Cross Sections to the Vibrational States with the Coupled-Channels Theory

T.Kawano, N.Fujikawa, and Y.Kanda

A paper on this subject was published in Engineering Sciences Reports, Kyushu Univ., vol.15, p.343, 1994, with the following abstract:

A coupled-channels model was adopted for calculation of inelastic scattering cross sections to the excited levels which belong to the vibrational bands of ^{238}U. The members of a certain vibrational band were coupled to the 0^+-2^+-4^+ triad of the ground state rotational band levels. Compound process contribution for the vibrational levels was calculated using a Hauser-Feshbach-Moldauer theory. A band coupling strength β was determined from the experimental inelastic scattering data below 3 MeV. Experimental double differential cross sections (DDX) were also included in the β determination.

Comparisons of calculated cross sections with the experimental data were made, and it was found that the coupled-channels calculation gave reasonable agreement with the DDX data at $E_n = 6.1$ MeV.

IV–B–7 Calculations of Double Differential Particle Emission Cross Sections for Nucleon-Induced Reactions on ^{12}C and Carbon Kerma Factors Using A Monte Carlo Method

Y. Watanabe, M. Harada, Y. Koyama, H. Kashimoto, H. Shinohara, and S. Chiba*

A paper on this title was presented at Int. Conf. on Nuclear Data for Science and Technology, May 9-13, 1994, Gatlinburg, Tennessee, U.S.A, with the following abstract:

A Monte Carlo based code is developed to calculate double differential particle emission cross sections of nucleon-induced reactions for 12C. Experimental data of neutron- and proton-induced reactions are analysed with particular attention to the 3 α breakup of ^{12}C. The code is also applied to the calculation of neutron kerma factors in the energy range from 10 to 80 MeV

* Japan Atomic Energy Research Institute

IV–B–8 Measurement of Double Differential Charged-Particle Emission Cross Sections For Reactions Induced By 26 MeV Protons and FKK Model Analysis

Y. Watanabe, A. Aoto, H. Kashimoto, S. Chiba*, T. Fukahori*, K. Hasegawa*, M. Mizumoto*, S. Meigo*, M. Sugumoto*, Y. Yamanouti*, N. Koori,** M.B. Chadwick+, P.E. Hodgson++

A paper on this title was presented at Int. Conf. on Nuclear Data for Science and Technology, May 9-13, 1994, Gatlinburg, Tennessee, U.S.A, with the following abstract:

Double differential charged-particle emission cross sections of proton-induced reactions have been measured for ^{nat}C, ^{27}Al, ^{nat}Si, ^{98}Mo, ^{106}Pd, ^{159}Tb and ^{181}Ta at energies around 26 MeV. Several (p,p') and (p,n) data for ^{98}Mo and ^{106}Pd in the incident energy range from 12 to 26 MeV are analysed in terms of the Feshbach-Kerman-Koonin model, in order to study preequilibrium nucleon emission from nucleon-induced reactions.

* Japan Atomic Energy Research Institute

** Faculty of Integrated Arts and Sciences, The University of Tokushima, Tokushima 770

\+ Nuclear Data Group, Lawrence Livermore National Laboratory, Livermore, California 94551, U.S.A

++ Nuclear Physics Laboratory, Physics Department, University of Oxford, Oxford, OX1 3RH, UK

IV–B–9 **Semiclassical Distorted Wave Model Calculation and Analysis of (p,p'x) Reactions at Intermediate Energies**

H. Shinohara, Y. Watanabe, and M. Kawai*

A paper entitled "A semiclassical distorted-wave model analysis of one-step process in proton inelastic scattering to continuum", written by Y. Watanabe and M. Kawai, was published in Nucl. Phys. **A 560** (1993) 43-56, with the following abstract:

The semiclassical distorted-wave model of one-step inelastic scattering recently developed is extended to include the effects of non-locality of distorting potentials and energy and angle dependence of two-nucleon scattering cross sections, and is applied to calculation of (p,p'x) cross sections for target nuclei ranging from ^{54}Fe and ^{209}Bi at incident energies ranging from 62 and 200 MeV. The model reproduces experimental cross sections, including the absolute magnitude, at forward angles and high energies of the outgoing protons. The effects of the corrections on the calculated cross sections, and comparisons with other models are discussed.

A paper entitled "Semiclassical distorted-wave model calculation of two-step direct process in (p,p'x) at intermediate energies" was submitted to Phys. Lett. B with the following abstract:

The cross section of two-step direct processes in (p, p'x) at intermediate energies is calculated by means of the recently developed semiclassical distorted wave model. The cross section supplements the one-step process which sharply decreases at large scattering angles and/or lower outgoing particle energies. The cross sections calculated without adjustable parameters are in good agreement with experimental data for small energy transfer, including the absolute magnitude. The calculation tends to overestimate the cross section for large energy transfer. Possible reasons for the discrepancy are discussed.

At present, some modification of this model is in progrss to improve the overestimation seen in the two-step cross sections. In this direction, we plan to use in-medium NN cross section[1] and calculate the similar cross section by using the effective N-N potential[2] derived on the basis of the reaction-matrix in nuclear matter.

References:

1) G.Q. Li and R. Machleidt, Phys. Rev., **C 48**, 1702 (1993); *ibid* **C 49**, 566 (1994).
2) N. Yamaguchi, Memoirs of the Faculty of Enginering, Miyazaki University, No. 18, February 1988.

* Department of Physics, Kyushu University

V. NAGOYA UNIVERSITY

A. Department of Nuclear Engineering

V-A-1 Measurement of Thermal Neutron Cross Section and Resonance Integral of the Reaction $^{99}Tc(n,\gamma)^{100}Tc$

Hideo Harada*, Shoji Nakamura*, Toshio Katoh and Yoshimune Ogata

A paper on this subject was submitted to J. Nuclear Science and Technology with the following abstract.

To obtain fundamental data for the research of the transmutation of nuclear waste, the thermal neutron cross section and the resonance integral of the reaction $^{99}Tc(n,\gamma)^{100}Tc$ has been measured by means of an activation method.

Ammonium pertechnetate targets containing about 370 kBq of ^{99}Tc were irradiated for 2 m. with reactor neutrons. Activation detectors of Co/Al and Au/Al alloy wires were irradiated for 10 m. to monitor the neutron flux and Westcott's epithermal index $r(T/T_0)^{1/2}$. The Tc samples and flux monitors were irradiated with and without a Cd capsule.
The gamma-ray spectra from the irradiated samples were measured with a high purity Ge detector. The thermal neutron cross section (2,200 m/s neutron cross section) and the resonance integral of the $^{99}Tc(n,\gamma)^{100}Tc$ reaction were found to be 22.7 ± 1.1 b and 395 ± 34 b, respectively. The thermal neutron cross section obtained is 14% larger than the value reported in 1977 by Lucas(20 ± 2 b) and the resonance integral is twice as larger the value reported by Lucas(186 ± 16 b).

---

* Power Reactor and Nuclear Fuel Development Corp

V-A-2 Measurement of Thermal Neutron Cross Section and Resonance Integral of the Reaction $^{137}Cs(n,\gamma)^{138}Cs$

Toshiaki Sekine*, Yuichi Hatsukawa*, Katsutoshi Kobayashi*, Hideo Harada**, Hisashi Watanabe** and Toshio Katoh

A paper on this subject was published in J. Nuclear Science and Technology 30,[11],pp.1099-1106(1993) with the following abstract.

To obtain fundamental data for the research of the transmutation of nuclear waste, the thermal neutron cross section and resonance integral of the reaction $^{137}Cs(n,\gamma)^{138}Cs$ have been measured by means of a modified Cd-ratio technique. Targets of about 0.4 MBq ^{137}Cs were irradiated with neutrons in the JRR-4 swimming pool reactor by using a pneumatic tube equipment with a movable Cd shield, and neutron fluxes and their epithermal neutron fractions were monitored with activation detectors(Co/Al and Au/Al) whose sensitivity to epithermal neutrons differed from each other. After irradiation, the ^{137}Cs samples were purified chemically and their gamma-ray spectra were measured with a high purity Ge detector.
The resulting yields of ^{138}Cs for different neutron spectra and the neutron flux data have yielded that the thermal neutron cross section(for 2,200 m/s neutrons) is 0.25 ± 0.02 b. and the resonance integral 0.36 ± 0.07 b. The results are consistent with the effective cross section($\hat{\sigma}$ = 0.250 ± 0.013 b) of our previous measurement. An uncertainty due to neglecting the production of the short-lived isomer of ^{138}Cs was calculated on the basis of the isomeric yield ratio given by the Huizenga and Vandenbosch model. A probable uncertainty was estimated to be +1.2% or +3.9%, depending om the spin of the compound nucleus produced in the s-wave neutron capture.

* Japan Atomic Energy Research Institute
** Power Reactor and Nuclear Fuel Development Corp.

V-A-3 Measurement of the Thermal Neutron Cross Section of the $^{90}Sr(n,\gamma)^{91}Sr$ Reaction

Hideo Harada*, Toshiaki Sekine**, Yuichi Hatsukawa**, Noriko Shigeta**, Katsutoshi Kobayashi**, Tsutomu Ohtsuki** and Toshio Katoh

A paper on this subject was published in J. Nuclear Science and Technology 31[3],pp.173-179(1994) with the following abstract.

To obtain fundamental data for the research of the transmutation of nuclear waste, the thermal neutron cross section of the reaction $^{90}Sr(n,\gamma)^{91}Sr$ has been measured by means of a radiochemical method. Strontium chrolide targets containing about 2 MBq of ^{90}Sr were irradiated for 10 m. with reactor neutrons. Activation detectors Co/Al and Au/Al alloy wires irradiated simultaneously to monitor the neutron flux and Westcott's epithermal index $r(T/T_0)^{1/2}$. The irradiated Sr samples were purified chemically and their gamma-ray spectra were measured with a high purity Ge detector. Since the targets included ^{85}Sr, a gamma-ray emitter and a tracer for ^{90}Sr, and a ratio of the amount of ^{85}Sr to that of ^{90}Sr was measured in advance, an effective cross section of the $^{90}Sr(n,\gamma)^{91}Sr$ reaction for a reactor neutron spectrum was determined from the ratio of radioactivities of ^{91}Sr and ^{86}Sr, and neutron flux data. the resonance integral was also measured by a modified Cd-ratio measurement. Considering an upper limit of the resonance integral to be 0.16 b., the thermal neutron cross section (2,200 m/s neutron cross section) of $^{90}Sr(n,\gamma)^{91}Sr$ reaction was found to be $0.0153 \pm ^{0.0013}_{0.0042}$ b.

The value obtained is only 1/50 of the value reorted by Zeisel(1966), and is in good agreement with the figure reported by McVey et al.(1983).

---

* Power Reactor and Nuclear Fuel Development Corp.
** Japan Atomic energy Research Institute

B. School of Engineering

V-B-1 Measurement of Activation Cross Section on Ta and W with 14 MeV Neutrons

Y. Kasugai, M. Asai, A. Tanaka, H. Yamamoto, I. Jun[1], T. Iida[2] and K. Kawade

A paper on this subject will be published in J. Nucl. Sci. Technol. in 1994.

Abstract

The cross sections of ^{181}Ta(n, p)^{181}Hf, ^{181}Ta(n, n'p)^{180m}Hf, ^{184}W(n, α)^{181}Hf, ^{186}W(n, n'p)^{185}Ta and ^{186}W(n, α)^{183}Hf reactions have been measured in the energy range of 13.4 and 14.9 MeV by the activation method. The intense 14 MeV neutron source facility (OKTAVIAN) at Osaka University was used for irradiation. The γ-rays emitted from the irradiated samples were measured with high-purity germanium (HPGe) detectors. All cross section values were obtained relative to the standard reaction cross section of ^{93}Nb(n, 2n)^{92m}Nb obtained by Nethaway. The cross sections of ^{181}Ta(n, n'p)^{180m}Hf reaction were measured for the first time. The present results were compared with previous data and the evaluated data of JENDL-3 and ENDF/B-VI, and the comparison showed that some significant discrepancies exist.

[1] UCLA, USA
[2] Osaka University

V-B-2 Beta Decay of ^{151}Pr into levels in ^{151}Nd

M. Shibata, T. Ikuta, A. Taniguchi, A. Osa, A. Tanaka, H. Yamamoto, K. Kawade, J. Ruan[1], Y. Kawase[2] and K. Okano[2]

A paper on this subject will be published in J. Phys. Soc. Japan in 1994.

Abstract

The β-decay of ^{151}Pr to levels in ^{151}Nd has been studied from the fission products of ^{235}U using an on-line isotope separator (KUR-ISOL). Gamma-rays and conversion electrons have been measured. Conversion coefficients have been determined for the first time. The precise decay scheme is proposed up to 2430 keV. The newly observed 65 γ-rays and 16 levels are incorporated in it. The deduced level scheme of ^{151}Nd was compared to the calculated level scheme on the basis of the rotation-vibration coupling model with a Nilsson potential. Low-lying levels were well reproduced by this model.

[1] Rikkyo University
[2] Research Reactor Institute, Kyoto University

VI. Osaka University

A. Department of Chemistry

VI-A-1 $^{238}U(p,f)$ Reaction at 17.9 MeV Excitation

A. Yokoyama, N. Takahashi, N. Nitani*, H. Baba, R. Kasuga, T. Yamaguchi, D. Yano, N. Shinohara*, K. Tsukada*, Y. Hatsukawa* and Y. Nagame*

Fission fragment yields were measured for the $^{238}U(p,f)$ reaction at 17.9-MeV excitation by combining the gas-jet transport system and ordinary radiochemical stacked-target technique with off-line Ge γ-ray spectrometry. The proton beam was obtained from the JAERI tandem Van de Graaff accelerator. For the measurement of short-life products with the half-lives from 30 min through subseconds we made use of a gas-jet transport system [1] installed in a course of the accelerator. Product nuclei recoiling out of the target were stopped in the reaction chamber filled with Ar gas and transported with the attached aerosol particles via a Teflon capillary of 17 m long to a tape collector system by the Ar gas flow using a mechanical pump. The product activities attached on aerosol particles were collected on the tape for an appropriate time and then moved to the position at which a Ge detector was set to acquire the γ-ray spectrum. The obtained data were subjected to the γ-ray spectrum analysis by the BOB code [2] and the decay analysis. The transport efficiency was deduced from the yield ratios of several common nuclides found in the gas-jet experiment and those of the stacked-target experiment. Cross sections for the production of γ-emitting nuclei were deduced from the analyzed results of the observed photopeak intensities for the growth-decay during and after the irradiation. The resulting formation cross sections are summarized in Table 1 together with the half-lives [3] and the total chain yields calculated with an appropriate charge distribution.

References:

1) K. Tsukada, T. Ohtsuki, K. Sueki, Y. Hatsukawa, H. Yoshikawa, K. Endo, H. Nakahara, N. Shinohara, S. Ichikawa, S. Usuda and M. Hoshi: Radiochim. Acta **51**, 77 (1990).

2) H. Baba, H. Okashita, S. Baba, T. Suzuki, H. Umezawa and H. Natsume: J. Nucl. Sci. Tech. (Tokyo) **8**, 703 (1971); H. Baba, T. Sekine, S. Baba and H. Okashita: JAERI report no. 1227 (1972).

3) U. Reus and W. Westmeier: At. Data and Nucl. Data Tables **29**, 1 (1983).

* Japan Atomic Energy Research Institute

Table 1. Formation cross sections of the product nuclides in the $^{238}U(p,f)$ reaction at 17.9-MeV excitation. The third column gives the results of the decay analysis only while the fourth and fifth columns respectively represent cumulative and independent yields corrected for the growth and decay during the irradiation. The total chain yields are summarized in the last column.

Nuclide	Half-life	σ_{obs} (mb)	σ_{cum} (mb)	σ_{ind} (mb)	chain yield
$^{83}\mathrm{Se}^{g}$	22.5m	0.78±0.08	0.77±0.08		>1.66±0.12
$^{84}\mathrm{Br}^{g}$	31.8m	1.89±0.12	2.32±0.17		2.76±0.21
$^{84}\mathrm{Br}^{m}$	6.0m	0.55±0.11		0.55±0.11	
$^{85}\mathrm{Kr}^{m}$	4.48h	2.55±0.15	2.31±0.15		>2.45±0.16
$^{87}\mathrm{Kr}$	76.3m	3.26±0.17	3.23±0.17		4.04±0.22
$^{88}\mathrm{Kr}$	2.84h	3.47±0.19	3.47±0.19		5.10±0.28
$^{89}\mathrm{Rb}$	15.4m	3.80±0.22	3.28±0.23	3.02±0.05	3.90±0.28
$^{91}\mathrm{Rb}$	58.4s	2.89±0.41	2.90±0.41		4.8±0.7
$^{91}\mathrm{Sr}$	9.52h	6.84±0.37	6.84±0.37	3.9±0.6	7.6±0.5
$^{91}\mathrm{Y}^{m}$	47.71m	0.24±0.08	6.13±0.33		>6.2±0.4
$^{92}\mathrm{Sr}$	2.1h	7.21±0.21	7.21±0.21		8.8±0.3
$^{92}\mathrm{Y}$	3.54h	1.86±0.35	6.22±0.38		6.4±0.4
$^{93}\mathrm{Sr}$	7.32m	6.2±0.9	6.3±0.9		9.0±1.3
$^{93}\mathrm{Y}$	10.1h	8.9±1.0	8.8±1.0	2.5±1.3	9.4±1.0
$^{94}\mathrm{Sr}$	74.1s	5.8±1.1	5.7±1.1		10.3±2.0
$^{94}\mathrm{Y}$	18.6m	6.42±0.37	6.42±0.37	1.6±0.8	7.4±0.5
$^{95}\mathrm{Sr}$	24.4s	4.47±0.46	4.40±0.46		10.6±1.2
$^{95}\mathrm{Y}$	10.3m	7.8±1.2	7.6±1.2	3.3±1.3	10.0±1.6
$^{95}\mathrm{Zr}$	64.03d	9.9±0.5	9.9±0.5	2.2±1.4	10.3±0.6
$^{96}\mathrm{Y}^{m}$	10.0s	0.83±0.14	3.14±0.15	0.24±0.15	>3.96±0.19
$^{97}\mathrm{Zr}$	17.0h	9.30±0.48	9.30±0.48		11.3±0.6
$^{98}\mathrm{Y}^{B}$	2.0s	0.43±0.10	1.31±0.25	0.43±0.10	>4.1±0.8
$^{98}\mathrm{Zr}$	30.7s	11.1±2.3	10.3±2.3		14.7±3.2
$^{99}\mathrm{Nb}^{m}$	26.0m	4.0±1.0	10.8±1.1	1.5±1.0	>12.3±1.3
$^{99}\mathrm{Mo}$	2.75d	11.6±0.6	11.6±0.6		11.8±0.6
$^{100}\mathrm{Y}^{B}$	0.94s	3.3±1.4			
$^{100}\mathrm{Nb}^{A}$	3.1s	5.5±1.1	6.7±1.1	5.5±1.1	>8.7±1.4
$^{101}\mathrm{Mo}$	14.6m	9.4±0.6	9.3±0.6		10.0±0.7
$^{101}\mathrm{Tc}$	14.2m	1.54±0.25	9.8±0.6	0.45±0.26	9.8±0.6
$^{103}\mathrm{Mo}$	67.5s	6.6±1.6	6.7±1.6		9.3±2.3
$^{103}\mathrm{Tc}$	54.2s	3.3±0.9	9.7±1.8	3.0±1.8	10.2±1.9
$^{103}\mathrm{Ru}$	39.25d	11.0±0.6	11.0±0.6	2.5±2.1	11.0±0.6
$^{104}\mathrm{Nb}^{A}$	4.8s	2.07±0.33	2.07±0.33		9.3±1.5
$^{104}\mathrm{Tc}$	18.4m	8.76±0.45	8.39±0.45		9.6±0.6
$^{105}\mathrm{Mo}$	36.7s	3.42±0.49	3.42±0.49		8.2±1.2
$^{105}\mathrm{Tc}$	7.7m	7.2±1.1	6.9±1.1	3.6±1.2	8.8±1.4

(continued)

Nuclide	Half-life	σ_{obs} (mb)	σ_{cum} (mb)	σ_{ind} (mb)	chain yield
$^{106}\mathrm{Tc}$	36s	5.9±0.8	5.8±0.8	4.0±0.9	8.9±1.3
$^{106}\mathrm{Ru}$	371.6d	6.5±0.7	5.6±0.7		6.6±0.7
$^{106}\mathrm{Rh}^{m}$	2.17h	2.46±0.27	5.48±0.48	2.46±0.27	>9.0±0.8
$^{107}\mathrm{Tc}$	21.2s	2.5±1.0	3.0±1.0	2.1±1.0	5.8±1.9
$^{107}\mathrm{Ru}$	3.75m	7.9±1.4	7.3±1.4	2.6±1.6	9.4±1.7
$^{108}\mathrm{Tc}$	5.4s	2.41±0.47	2.46±0.47		6.8±1.3
$^{108}\mathrm{Ru}$	4.55m	3.8±0.6	3.8±0.6	1.4±0.8	5.1±0.8
$^{108}\mathrm{Rh}^{A}$	16.8s	0.86±0.19	4.2±0.6	0.48±0.58	>4.5±0.6
$^{109}\mathrm{Ru}$	34.3s	3.09±0.43	2.96±0.43		5.0±0.8
$^{109}\mathrm{Rh}$	81.0s	4.1±0.6	4.2±0.6	1.5±0.7	4.8±0.7
$^{110}\mathrm{Ru}$	12.6s	0.84±0.13	0.84±0.13		2.04±0.32
$^{110}\mathrm{Rh}^{A}$	28.5s	0.90±0.13	2.8±0.8	1.7±0.8	3.8±1.2
$^{110}\mathrm{Rh}^{B}$	3.3s	1.86±0.79			
$^{111}\mathrm{Ag}^{g+m}$	7.45d	3.02±0.32	2.93±0.32		2.95±0.33
$^{111}\mathrm{Cd}^{m}$	48.6m	0.038±0.004	2.99±0.32		>2.99±0.32
$^{112}\mathrm{Pd}$	21.05h	3.20±0.19	3.20±0.19		3.40±0.21
$^{112}\mathrm{Ag}$	3.14h	0.30±0.06	3.33±0.19	0.13±0.19	3.35±0.20
$^{113}\mathrm{Ag}^{g}$	5.37h	2.95±0.16	2.94±0.16	2.13±0.21	>3.00±0.17
$^{114}\mathrm{Pd}$	2.48m	2.25±0.41	2.22±0.41		2.85±0.53
$^{115}\mathrm{Ag}^{m}$	18.5s	1.45±0.22	1.45±0.22		>1.60±0.25
$^{116}\mathrm{Pd}$	12.7s	1.42±0.42	1.42±0.42		2.9±0.9
$^{116}\mathrm{Ag}^{g}$	2.68m	2.57±0.36	2.45±0.45	1.0±0.6	2.95±0.45
$^{117}\mathrm{Ag}^{B}$	5.34s	0.95±0.15	2.12±0.17	0.52±0.16	>2.52±0.20
$^{118}\mathrm{Ag}^{g}$	3.7s	2.37±1.00	2.89±1.00		4.9±1.7
$^{119}\mathrm{Cd}^{g}$	2.69m	0.75±0.15	2.9±0.6		3.7±0.8
$^{119}\mathrm{Cd}^{m}$	2.20m	2.18±0.55			
$^{119}\mathrm{In}^{g}$	2.4m	0.75±0.12	0.77±0.12		>0.80±0.13
$^{120}\mathrm{In}^{C}$	47.3s	0.52±0.12	3.5±0.6	0.52±0.12	>3.8±0.7
$^{121}\mathrm{In}^{g}$	23.1s	1.43±0.21	1.43±0.21		>1.72±0.26
$^{124}\mathrm{In}^{A}$	3.21s	0.96±0.15	0.98±0.15		>2.20±0.34
$^{125}\mathrm{Sn}^{g}$	9.64d	0.55±0.16	3.25±0.30		3.4±0.4
$^{125}\mathrm{Sn}^{m}$	9.52m	1.70±0.25			
$^{126}\mathrm{Sb}^{g(+m)}$	12.4d	0.478±0.024	3.40±0.43	0.474±0.024	>3.40±0.43
$^{127}\mathrm{Sn}^{g}$	2.10h	2.69±0.15	3.56±0.20		4.20±0.24
$^{127}\mathrm{Sn}^{m}$	4.13m	0.87±0.13			

(continued)

Nuclide	Half-life	σ_{obs} (mb)	σ_{cum} (mb)	σ_{ind} (mb)	chain yield
^{128}Sn$^{g(+m)}$	59.1m	2.20±0.12	2.20±0.12		3.60±0.19
^{128}Sn^{m}	6.5s	0.31±0.07	0.46±0.07		
^{128}Sb^{g}	9.01h	1.86±0.11	1.59±0.11		>1.67±0.12
^{129}Sb	4.32h	3.96±0.34	3.84±0.34		4.30±0.38
^{130}Sb^{A}	40m	3.14±0.17	2.70±0.19		7.4±0.8
^{130}Sb^{B}	6.3m	2.81±0.57	2.99±0.58		
^{131}Sn^{A}	61s	2.1±0.6	2.1±0.6		>6.6±1.9
^{131}Sb	23.0m	6.8±1.2	6.5±1.2	0.7±2.0	9.5±1.7
^{131}Te^{g}	25m	0.68±0.24	8.1±0.5	2.22±0.48	9.8±0.7
^{131}Te^{m}	30h	3.65±0.19			
^{131}I	8.02d	10.34±0.36	9.63±0.38		9.7±0.4
^{132}Sn	40s	2.22±0.50	2.21±0.50		11.8±2.7
^{132}Sb^{A}	4.2m	2.38±0.36	7.8±0.9	5.6±1.0	13.5±1.5
^{132}Sb^{B}	2.8m	5.18±0.73		3.3±0.9	
^{132}Te	3.26d	8.2±0.7	8.2±0.7	1.4±1.1	9.6±0.9
^{132}I^{g+m}	2.30h	3.28±0.21	11.4±0.8	3.16±0.21	11.6±0.8
^{133}Te^{g}	12.5m	2.52±0.24	9.2±0.6		12.2±0.8
^{133}Te^{m}	55.4m	7.7±0.6			
^{133}I^{g+m}	20.8h	11.2±0.6	10.7±0.7	1.6±0.7	11.2±0.7
^{133}Xe^{g+m}	5.29d	2.2±0.7	10.9±0.9	1.7±0.7	11.0±0.4
^{133}Xe^{m}	2.19d	0.86±0.10		0.84±0.10	
^{134}Sb^{A}	10.4s	0.59±0.14	1.07±0.15	0.59±0.14	>4.4±0.7
^{134}Te	41.8m	4.84±0.29	4.84±0.29	4.14±0.32	8.0±0.5
^{134}I^{g+m}	52.6m	7.8±0.9	8.9±0.9	4.1±0.9	10.0±1.0
^{135}I	6.61h	9.2±0.8	9.2±0.8		11.3±1.0
^{135}Xe^{g+m}	9.08h	4.17±0.36	12.1±0.7	1.93±0.09	12.6±0.7
^{135}Xe^{m}	15.6m	1.42±0.13		1.37±0.13	
^{136}Te	21s	4.1±0.8	4.2±0.8	4.1±0.8	13.0±2.4
^{136}I^{A}	84.0s	0.43±0.22	6.0±0.9		7.7±1.1
^{136}I^{B}	45.0s	1.20±0.12			
^{136}Cs	13.16d	0.609±0.031		0.609±0.031	10.3±0.6
^{137}I	24.2s	3.9±2.0	4.0±2.0		7.2±3.5
^{138}Cs$^{g(+m)}$	32.2m	12.0±0.7	9.0±0.9		9.4±0.9
^{138}Cs^{m}	2.9m	1.40±0.47			
^{139}Ba	1.38h	10.7±0.6	9.5±0.5	0.77±0.13	9.6±0.6
^{140}Cs	63.7s	2.23±0.38	6.1±0.6	1.4±0.6	7.4±0.7

(continued)

Nuclide	Half-life	σ_{obs} (mb)	σ_{cum} (mb)	σ_{ind} (mb)	chain yield
^{140}Ba	12.75d	8.8±0.6	8.7±0.6	4.4±0.8	9.0±0.6
^{140}La	40.28h	0.227±0.027	8.9±0.6	0.197±0.027	9.0±0.6
^{141}Cs	24.74s	5.4±1.3	5.1±1.3		7.2±1.8
^{141}Ba	18.27m	7.95±0.42	7.81±0.42		8.3±0.5
^{141}La	3.92h	9.1±1.0	8.4±1.0		9.0±1.1
^{141}Ce	32.50d	8.82±0.45	8.77±0.46		8.8±0.5
^{142}Ba	10.7m	7.9±2.1	7.8±2.1		9.0±2.4
^{142}La	1.52h	8.74±0.46	8.20±0.48		8.3±0.5
^{143}Ba	14.5s	5.9±1.7	5.4±1.7		7.3±2.1
^{143}Ce	33.0h	7.16±0.36	7.11±0.36	0.01±0.62	7.4±0.4
^{144}Ba	11.9s	2.07±0.37	2.56±0.37		4.0±0.6
^{144}La	40.9s	4.0±0.6	4.0±0.6	1.6±0.7	4.3±0.6
^{145}La	25s	5.1±0.7	4.6±0.7		5.5±0.8
^{145}Ce	3.01m	4.6±0.7	4.9±0.7	0.6±0.9	5.0±0.6
^{146}Ce	13.52m	5.4±0.6	5.4±0.6	4.7±0.6	5.8±0.6
^{146}Pr	24.1m	1.07±0.14	5.7±0.6	0.42±0.16	5.7±0.6
^{147}La	4.48s	2.8±0.7	2.7±0.7		4.6±1.2
^{147}Pr	13.6m	3.5±0.7	3.7±0.7	1.1±0.8	3.8±0.7
^{147}Nd	10.98d	4.02±0.21	4.02±0.21	0.3±0.8	4.02±0.21
^{148}La	1.19s	0.62±0.28	0.62±0.28		1.4±0.7
^{148}Ce	48s	1.0 ±0.8	1.0±0.8		1.3±1.0
^{148}Pr^{A}	2.27m	2.24±0.33	2.57±0.34	0.5±0.6	>2.70±0.36
^{149}Ce	5.0s	2.0±0.9	2.0±0.9		2.9±1.3
^{149}Pr	2.25m	2.7±0.8	2.7±0.8	0.8±1.2	3.0±0.8
^{149}Nd	1.73h	2.65±0.14	2.60±0.14		2.61±0.14
^{151}Nd	12.4m	1.36±0.22	1.38±0.22		1.45±0.24
^{151}Pm	28.4h	1.57±0.14	1.56±0.14	0.17±0.26	1.56±0.14
^{152}Nd	11.4m	1.57±0.43	1.59±0.43		1.80±0.49
^{156}Sm	9.4h	0.464±0.035	0.464±0.035		0.48±0.04

VI-A-2

Fragment Mass and Kinetic Energy Distributions in the Fission of Actinide Nuclei Measured by the Double-Energy Method

T. Hakoda, T. Miyauchi, S. Watanabe, D. Yano, A. Yokoyama, T. Saito, N. Takahasi, Y. Nakagome*, T. Tamai*, and H. Baba

The fragment mass and kinetic energy distributions were measured in the fission of some actinide nuclei by the double-energy method using silicon surface barrier(SSB) detectors. We have performed the experiments on the $^{233}U(n_{th},f)$, $^{235}U(n_{th},f)$ and $^{239}Pu(n_{th},f)$ reactions at the Super-Mirror Neutron-Guide-Tube Facility of Kyoto University Reactor. The neutron flux was about $6\times10^7 n/cm^2/s$. The uranium and plutonium targets were prepared by making very thin nitrocellulose films in which organic uranium and plutonium compound were suspended, respectively. The thickness of these targets were between about 1 and $13\mu g/cm^2$. The experiment on $^{252}Cf(sp,f)$ was carried out at Radioisotope Center of Osaka University. The californium target was prepared by electrodeposition on a $80\mu g/cm^2$ nikel fiol. The thickness of californium was $13ng/cm^2$. The coincident complementary fragments were measured with two SSBs and the fragment kinetic energy was determined by the method of Schmitt.[1)] The number of prompt neutrons was referred to the compilation by Wahl.[2)] By iterative calculations the primary mass and kinetic energy of complementary fragments were obtained.

Figure 1 shows the primary fragment mass distribution for each fissioning system. The symmetirc mass yield increases when going from $^{233}U(n_{th},f)$ to $^{252}Cf(sp,f)$. The average kinetic enegy(MKE) of a single fragment and the total kinetic energy(TKE) as functions of fragment mass are indicated in figure 2 and 3, respectively.

References:

1) J.H. Neiler, F.J. Walter, and H. Schmitt, Phys. Rev. **149**, 894 (1966).

2) A. C. Wahl, At. Data Nucl. Data. Tables **39** (1988) 1.

---

* Research Reactor Institute, Kyoto University

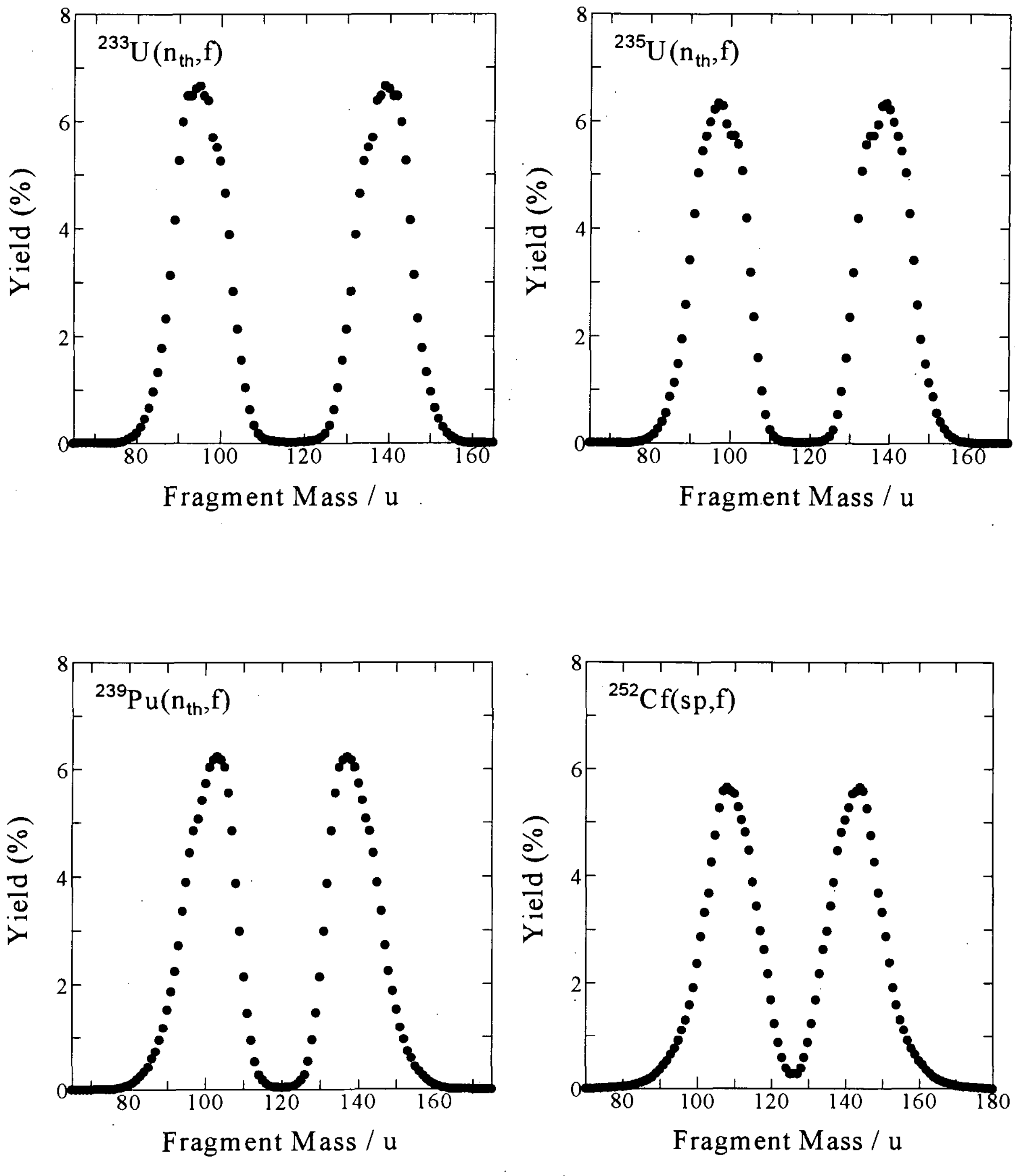

Fig.1. The Primary fragment mass distributions for the various fissioning systems.

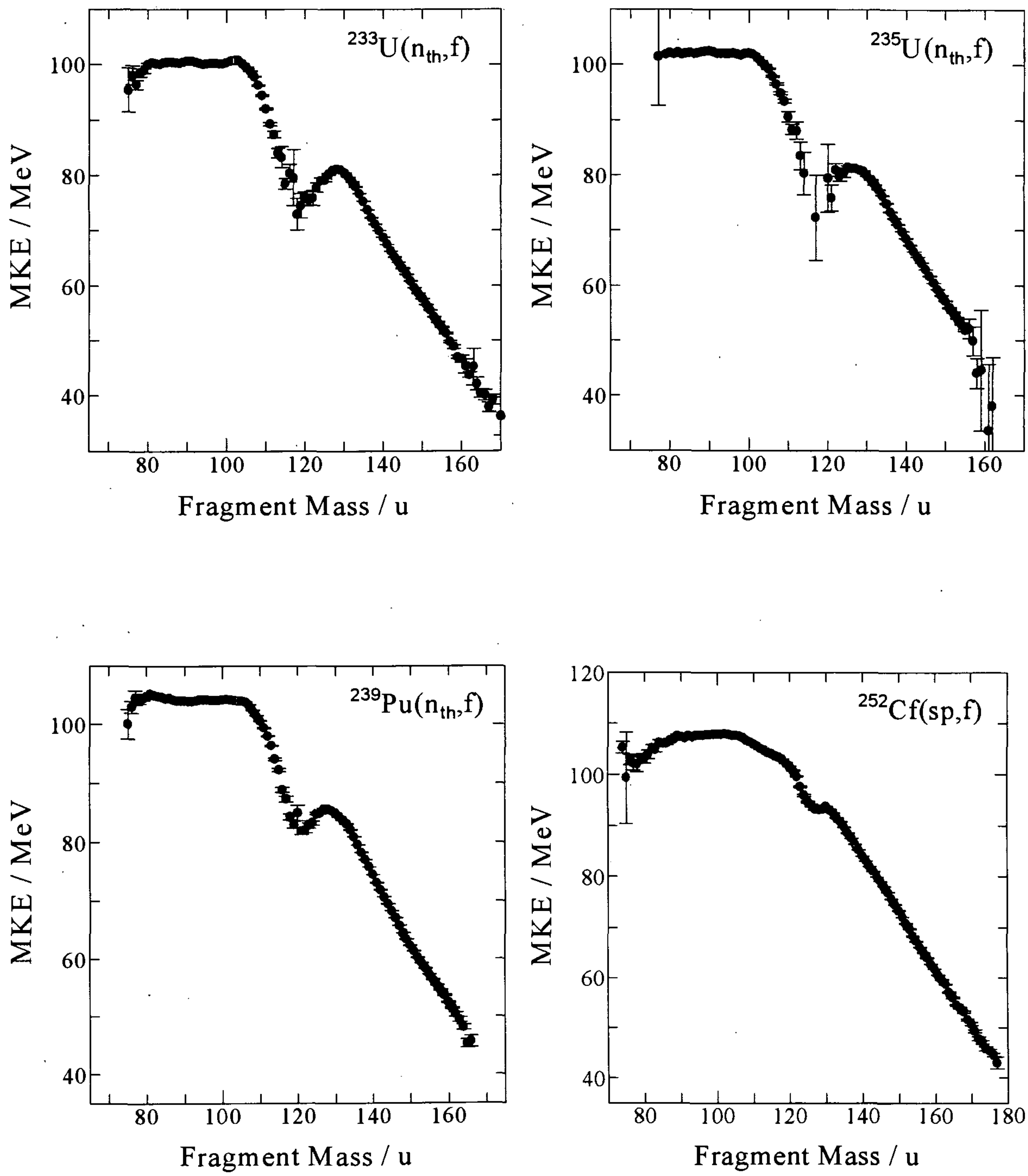

Fig.2. The single-fragment kinetic energy distributions measured for fragments from various fissioning systems.

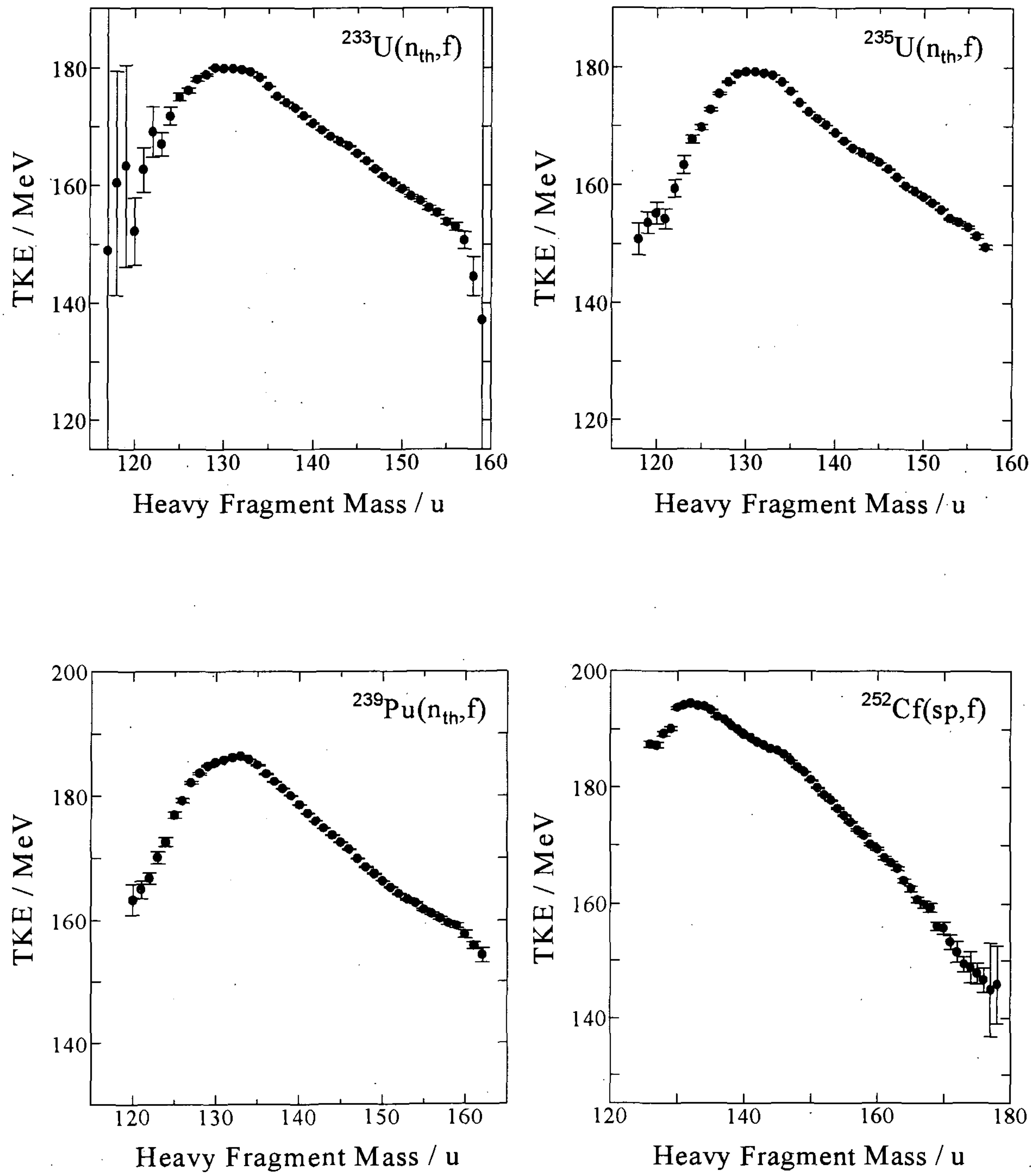

Fig.3. The total kinetic energy distributins measured for fragments form various fissioning systems.

B. Department of Nuclear Engineering

VI-B-1

Double Differential Charged Particle Emission Cross Sections by 14.1 MeV Incident Neutrons

Akito Takahashi, Hiroshi Nishizawa and Takehiro Kondoh

A brief summary of works on this subjective was presented at the Nuclear Data Conference in Gatlinburg[1]. Using a pulsed D-T neutron source(1.5 ns pulse width and 2 MHz repetition frequency) of OKTAVIAN, double differential cross sections for proton and alpha-particle emissions with 14.1 MeV incident neutron energy have been measured for several elements (Fe, Ni, Co, Ti, Be et al.) which are interested in fusion applications. The experimental method is based on the two-dimensional E-TOF (pulse height and time-of-flight) analysis of emitted particles from a several micrometers thick target foil of sample in vacuum, which are detected with a 2 mm thick CsI(Tl) scintillator. To separate proton, alpha and gamma signals, the pulse shape discrimination technique is very successfully applied. An example of DDX data for Ni(n, xa) reaction is shown in Fig.1. Measurements are under way for structural elements (Nb, Zr, Cu and so on) and light elements (C and Li). Measured DDX data have been compared with evaluated nuclear data (ENDF/B-VI and JENDL3) and some nuclear model calculations.

1) Akito Takahashi: "Japanese Activities in Nuclear Data Measurements for Fusion Applications", submitted to Proc. Int. Conf. Nuclear Data for Science and Technology, Gatlinburg USA, May 1994.

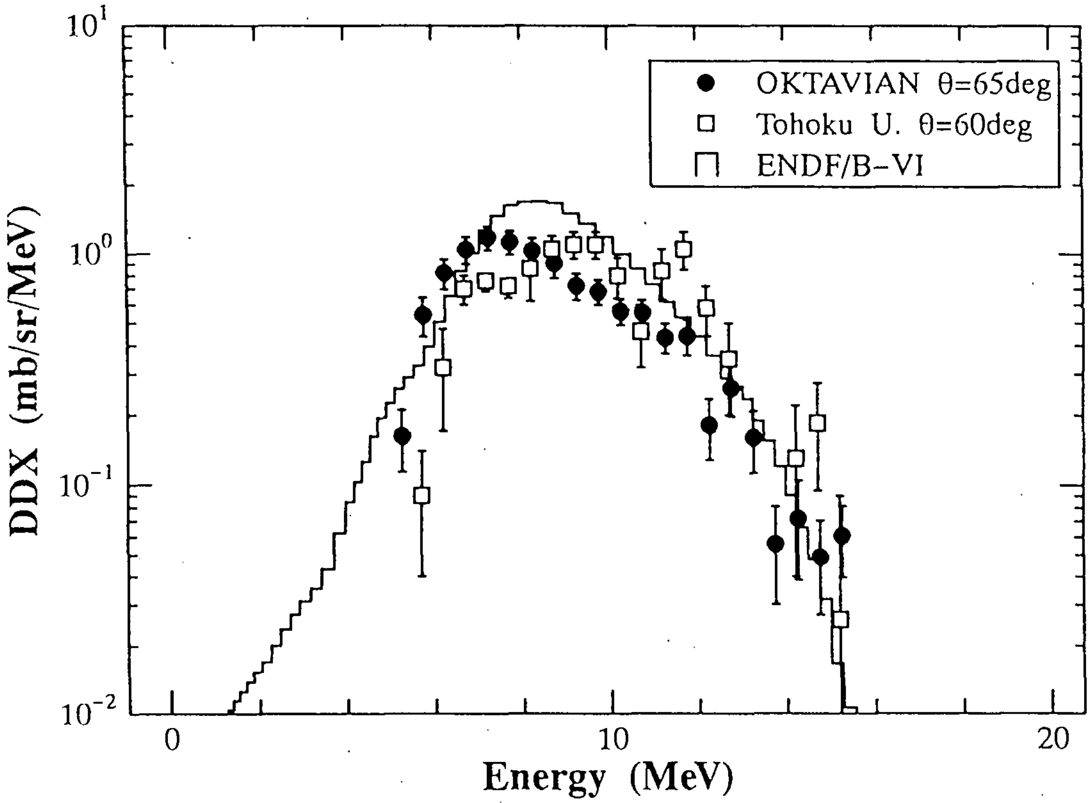

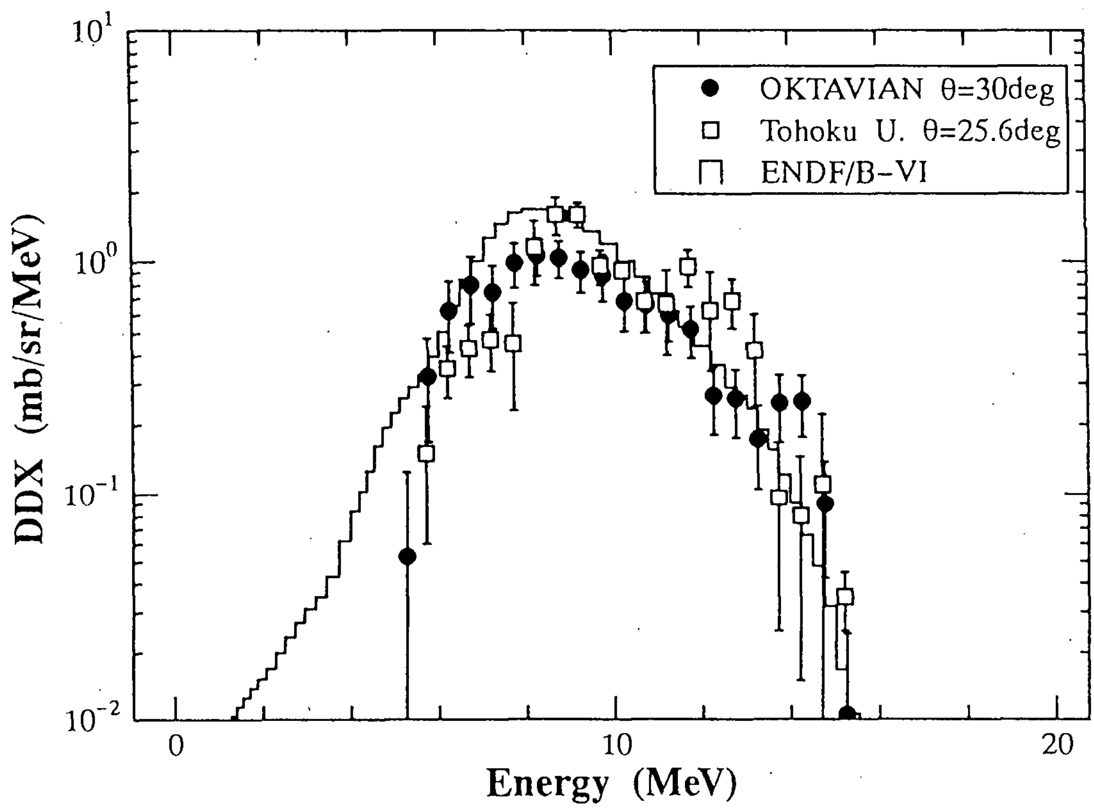

Ni (n , xα)

Fig.1 : Double differential alpha-particle emission cross sections at En = 14 MeV, for nickel

VI-B-2 Integrated Data Testing of JENDL3 and ENDF/B-VI by Leakage Neutron Spectra from Spherical Piles

Akito Takahashi and Yo Makita

Within the framework of IAEA activities on "Improved Evaluations and Integral Data Testing for FENDL", a series of calculational analyses on previously measured leakage neutron and gamma-ray spectra from spherical piles of various materials interested in fusion applications has recently started.

A one dimensional Sn code with DDX data base, NITRAN and a three dimensional Monte Carlo code MCNP are comparatively used for calculation. Data source for FENDL, namely JENDL3 and ENDF/B-VI are processed and used for transport calculations to be compared with experimental data. An example of analyses is shown in Fig.1 for Zr sphere.

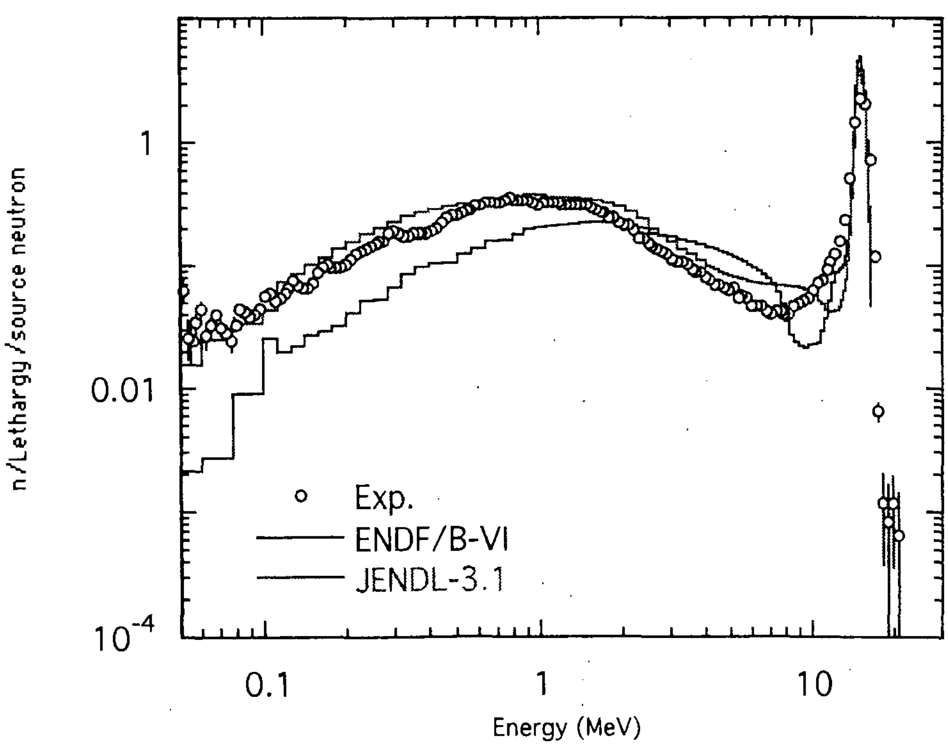

Fig.1 Comparison of Measured and Calculated Spectra of Zr Sphere by NITRAN

VII. Rikkyo (St. Paul's) University

A. Institute for Atomic Energy

VII-A-1

Measurements on effective total macroscopic cross sections of materials and effective energies of cold and thermal neutron beams.

Hisao Kobayashi

Two papers are related to this subject, and were submitted to the Proceedings of The Forth Asian Symposium on Research Reactors,[1] and to the Forth International Conference on Applications of Nuclear Techniques.[2]

Recently, an effective total macroscopic (ETM) cross section has been suggested instead of a total macroscopic (TM) cross section at the velocity of 2200m/s for continuum thermal neutron beams[3]. It has been shown[4] that the ETM cross section depends on spectral shape of thermal neutron beams from different irradiation facilities as well as of cold neutron beams from guide tubes. In the two papers,[1,2] a relation between ratios of ETM cross sections $R=\langle\Sigma_{Ti}(E_m)\rangle/\langle\Sigma_{Pb}(E_m)\rangle$ and mean energies E_m of known spectra was studied for beams of one thermal and two cold neutron beams whose spectra have been measured by a TOF method[5,6] or known by a theoretical calculation.[7] Titanium and lead were used for R measurements to determine the effective energy of unknown neutron beams. Measured R values of the three beams are plotted as a function of mean energies E_m with a regression line assumed as a functional form $R\propto E_m^{\ a}$ in Fig. 1 (dotted broken line). Where parameter a was found to be -1.00 ± 0.04 within the energy range from ~4meV to ~50meV. Results are compared with a solid curve of the TM ratio $\Sigma_{Ti}(E)/\Sigma_{Pb}(E)$ for a monochromatic beam given by BNL 325.[8] Measured three R values agree with that of BNL 325 within 27 %. The discrepancy may be resulted by a distortion of spectral shapes from a Maxwell distribution and by a difference of solid state characteristics of samples from characters of materials used in the BNL such as an uncertainty of mass density and an undefined crystallographic character of materials particularly for Pb. Here, we can define the effective energy as an inverse function of R, $E_{eff}\sim R^{-1}$.

Table 1 Summary of NR facilities used in this experiment.

Facility(Power)	ϕ(n/(cm^{2}s))	N. Source	Filter	Cd ratio	E_m(meV)	Ref.
RUR/N2(100kW)	3.2×10^6	Graphite-Tang.	none	2	---	(9)
R3/TF2(20MW)	1.5×10^8	D_2O(29°C)-Tang	none	130	*1 47.2	(10,11)
KUR/E2(5MW)	1.2×10^6	D_2O(50°C)-Tang.	none	400	---	(12)
UTR(1W)	1.4×10^4	Graphite-Tang.	none	4.3	---	(13)
KUR/CN3(5MW)	1.4×10^7	Graphite-liq.D_2O	Super mirror G.T. (λ_c=1.2Å)	---	---	(14)
KUR/CN2(5MW)	1.1×10^7	Graphite-liq.D_2O	Ni mirror G.T.(λ_c=2.6Å)	---	*2 7.2	(15)
R3/C2(20MW)	1.6×10^8	D_2O-liq.H_2O	Ni mirror G.T.(λ_c=4Å)	---	*2 4.6	(10,11)

*1 Estimated from computed energy spectrum.

*2 Estimated from measured energy spectrum using a TOF method.

Table 2 Estimated effective neutron energies for various NR facilities

Facility	Cd ratio	*1 E_m (meV)	$\langle\Sigma_{Ti}\rangle/\langle S_{Pb}\rangle$	*2 E_{eff} (meV)	*3 E_{eff} (meV)
Rikkyo U: RUR/N2	2	---	1.71 ± 0.02	48.4 ± 0.6	55.2 ± 1.0
JRR3M: R3/TF2	130	47.2	1.74 ± 0.06	47.5 ± 0.8	53.6 ± 2.1
Kyoto U: KUR/E2	400	---	1.73 ± 0.03	47.8 ± 0.9	53.3 ± 1.6
Kinki U: UTR	4.3	---	1.87 ± 0.10	44.2 ± 2.4	47.8 ± 3.8
Kyoto U: KUR/CN3	---	---	9.92 ± 0.55	8.4 ± 0.5	6.6 ± 0.3
Kyoto U: KUR/CN2	---	7.2	12.10 ± 0.78	6.8 ± 0.5	6.1 ± 0.6
JRR3M: R3/C2	---	4.6	17.31 ± 0.52	4.8 ± 0.2	4.2 ± 0.2

*1 Estimated from energy spectrum (see text).

*2 Determined using $\langle\Sigma_{Ti}\rangle/\langle S_{Pb}\rangle$ and the regression curve (see Fig.1).

*3 Determined using $\langle\Sigma_{Ti}\rangle/\langle S_{Pb}\rangle$ and the curve based on BNL 325 (see Fig.1).

The method was examined seven neutron beams from research reactors in Japan: Four thermal (RUR/N2 in Rikkyo University,[9] JRR-3M/TNRF2 in JAERI [10,11]), KUR/E2 in Kyoto University[12]), and UTR in Kinki University[13]) and three cold neutron beams (KUR/CN3[14] and KUR/CN2[15] and JRR-3M/C2-3[10,11]). Results are summarized in Table 1 and 2.

A beam quality indicator will be proposed near future as a device to determine the effective energy for continuum neutron beams with spectra less than 0.1eV. The device will be applied to test five thermal neutron beams without filter, six with filters, a cold neutron beams with cooled filter, and three cold neutron beams from guide tubes in the world[16].

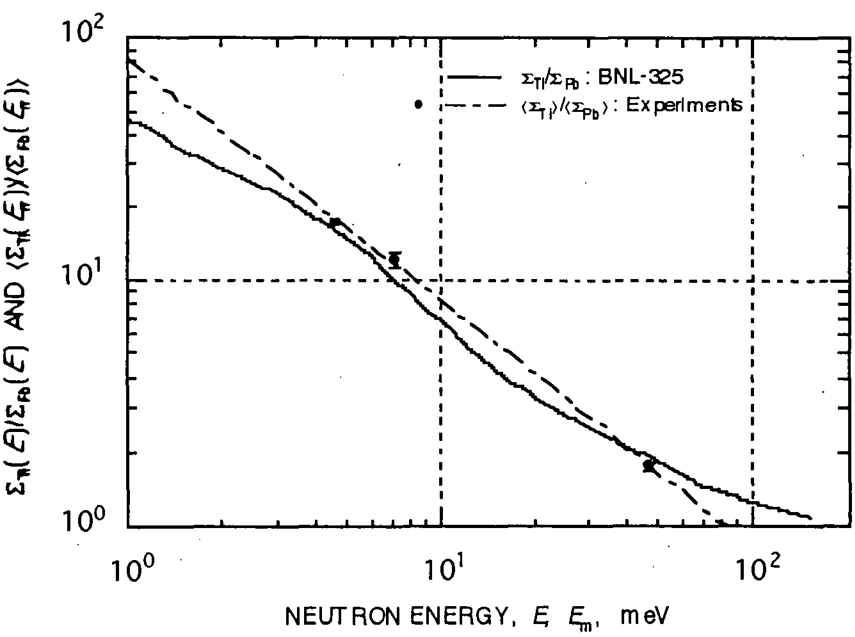

Figure 1 Ratio of TM cross section of Ti to Pb given by BNL325 as a function of monochromatic energy E (solid curve), and measured ratios of ETM cross sections versus mean energy E_m for the JRR-3M TF2 thermal, the JRR-3M C2-3 cold, and the KUR CN2 cold beams (solid circles). Regression line for ETM cross section ratio is shown as a dotted broken line.

References:

1) H. Kobayashi, "A qualification of neutron radiograms", Proc. 4th Asian Symposium on Research Reactors, (Beijing, 1993) p.175-183.
2) H. Kobayashi, "Effective energy determination of neutron beams by transmittance measurements", 4th Int. Conf. on Applications of Nuclear Tech., – Neutrons and Their Applications, June 12-18, 1994 (to be published on March 1995).
3) H. Kobayashi, H. Wakao, Y. Ikeda, K. Ohokubo, and A. Tsuruno, "Macroscopic cross section measurements and defect detection in materials using neutron radiography technique", J. Nucl. Sci. Tech., **29**, No.11, 1045-1053 (1992).
4) H. Kobayashi, Ir. Sri. Wardani, H. Wakao, K. Yoneda, S. Fujine, M. Matsubayashi, and A. Tsuruno, "Efficacy of cold neutron radiography", Neutron Radiography (4), ed. J. P. Barton, (Gordon Research Sci. Publ., 1994) p.403-412.
5) T. Kawai and M. Sugiyama (private communication).
6) Y. Kawabata et al., J. Nucl. Sci. Tech. 30, No.10, (1993) 84.
7) J. Iwasaki et al., "Neutronics calculation of upgraded JRR-3", JAERI Report M 85-062 (JAERI, Tokai, 1985) (in Japanese).
8) D. I. Garber and R. R. Kinsey, "Neutron Cross Sections, Vol.II, Curves", 3rd ed. BNL 325 (BNL, 1976).
9) H. Kobayashi, "Neutron radiography research in Rikkyo reactor", Proc. 1st Asian Symp. on Res. Reactors, (Tokyo, Nov. 1987) 360.
10) A Tsuruno et al., "Description of JRR-3 neutron radiography facility plan", ibid. 81.
11) M. Matsubayashi and A. Tsuruno, "JRR-3 neutron radiography facility", Neutron Radiography (4), ed. J. P. Barton, (Gordon and Breach Sci. Publ., Pennsylvania, 1994) 415.
12) S. Fujine et al., "Visualization on gas-liquid two-phase flow in a narrow rectangular duct", Neutron Radiography (3), (Kluwer Academic Press, Dordrecht, 1990) 513.
13) H. Kawai et al., "Neutron radiography facility using low power reactor of Kinki University", ibid. 101.
14) K. Yoneda (private communication).
15) K. Yoneda, et al., "Cold neutron beam hole in KUR and its radiography test", Neutron Radiography System Design and Characterization, eds. G. M. MacGillivray and J. S. Brenizer, (Canadian Nuclear Society, Tront, 1994) 32.
16) H. Kobayashi et al., "Characterization of thermal and cold neutron beams", 6th European Conference on Non Destructive Testing, Nice, Oct. 24-28, 1994.

VIII. Tohoku University

A. Department of Nuclear Engineering

VIII–A–1

Large Solid Angle Spectrometer for the Measurements of Differential (n,charged-particle) Cross Sections

N.Ito+, M.Baba, S.Matsuyama, I.Matsuyama, N.Hirakawa

A paper of this subject was published in Nuclear Instruments and Methods in Physics Research **A337** 474(1994) with the following abstract:

A charged-particle spectrometer with a large solid angle close to 4π has been developed for studies of fast neutron induced charged-particle emission reactions. On the basis of a high-pressure gridded ionization chamber employing high-Z structural elements, the spectrometer permits the measurements of energy-angular distribution of secondary charged-particles with very high geometrical efficiency and a good signal -to-noise ratio. It has been applied successfully for the measurements of double -differential cross sections of (n,xα) reactions for incident neutrons up to 14 MeV, and of (n,p) reactions up to 6 MeV by use of the data reduction and particle selection methods developed in this study. The present spectrometer proved to be an efficient means for studies of differential (n,charged-particle) cross sections.

+ Present Address: Japan Atomic Energy Research Institute

VIII-A-2

Differential (n,α) Cross Sections of Fe and Ni for 4.3 to 14.1 MeV Neutrons

M.Baba, N.Ito+, I.Matsuyama, S.Matsuyama, N.Hirakawa
S.Chiba*, T.Fukahori*, M.Mizumoto*, K.Hasegawa* and S.Meigo*

A paper on this subject was published in Journal of Nuclear Science and Technology **31(7)** 745(1994) with the following content:

Double-differential (n,xα) cross sections of Fe and Ni have been measured in the neutron energy range between 4.3 and 14.1 MeV using a specially developed gridded ionization-chamber (GIC) and monoenergetic neutrons provided by Tohoku University 4.5 MV Dynamitron accelerator and JAERI 20 MV tandem accelerator. Owing to very high efficiency of GIC, new systematic data have been obtained for α-emission spectra and the integrated α-production cross sections. This work was undertaken as a part of IAEA Research Coordinated Program for (n,α) cross sections.

+ Present Address: Japan Atomic Energy Research Institute
* Japan Atomic Energy Research Institute

VIII-A-3

Measurements of Double-Differential Neutron Emission Cross Sections of Nb, Mo, Ta, W and Bi for 14 and 18 MeV Neutrons

M.Baba, S.Matsuyama, T.Ito+, T.Ohkubo and N.Hirakawa

A paper on this subject was accepted for publication in Journal of Nuclear Science and Technology **31(8)** (1994) with the following abstract:

Double-differential neutron emission cross sections have been measured for Nb, Mo, Ta, W and Bi at 14.1 MeV incident energy, and for Nb and Bi at 18 MeV using Tohoku University Dynamitron TOF spectrometer. The experimental results indicated problems in current evaluations both for energy spectra and angular distributions. Angle-integrated neutron emission spectra and angular distributions of secondary neurons were analyzed, respectively, by the statistical multi-step model code EXIFON and the systematics by Kalbach-Mann, and by Kalbach. The energy spectra were reproduced successfully by EXIFON except for Bi, and the angular distributions were followed by the systematics over wide range of outgoing energy and target mass if the emission spectra calculated by EXIFON were employed for generation of angular distributions.

+ Present Address: Nuclear Fuel Industries, Ltd.,

VIII-A-4 Measurement of Double-Differential (n,α) Cross sections of Fe, Ni, Cu and ^{50}Cr for 4.5 - 14.1 MeV Neutrons

M.Baba, N.Ito+, I.Matsuyama, S.Matsuyama, N.Hirakawa
S.Chiba*, T.Fukahori*, M.Mizumoto*, K.Hasegawa*, S.Meigo*

A paper on this subject was presented at the International Conference on Nuclear Data for Science and Technology (May 9-15 Gatlinburg USA) with the following abstract:

We have measured doubly-differential (n,xα) cross sections of Fe, Ni, Cu, ^{50}Cr for 4.3 to 14.1 MeV neutrons using a high-efficiency gridded ionization chamber and obtained energy-angular distributions and integrated α-production cross sections.

---

* Japan Atomic Energy Research Institute
+ Present Address: Japan Atomic Energy Research Institute

VIII-A-5 Application of $^{15}N(d,n)^{16}O$ Neutron Source for Neutron Scattering Cross Section Measurements

S.Matsuyama, D.Soda, M.Baba, T.Ohkubo, N.Hirakawa

A paper on this subject was presented at the International Conference on Nuclear Data for Science and Technology (May 9-15, Gatlinburg USA) with the following abstract:

We investigated the $^{15}N(d,n)^{16}O$ reaction (Q=9.885 MeV) as a neutron source around 11 MeV and applied to scattering cross section measurements for secondary neutron energy range down to around 5 MeV using a 4.5 MV Dynamitron accelerator of Tohoku University. The $^{15}N(d,n)^{16}O$ neutron source proved to be useful for the scattering cross section measurements. Typical results are shown for carbon and lead.

VIII–A–6

Characterization and Application of 20-90 MeV ^{7}L(p,n) Neutron Source at TIARA

M.Baba, T.Kiyosumi, T.Iwasaki, M.Yoshioka, S.Matsuyama, N.Hirakawa, T.Nakamura*, Su.Tanaka**, R.Tanaka**, Shu.Tanaka***, H.Nakashima***, S. Meigo***

A paper on this subject was presented at the International Conference on Nuclear Data for Science and Technology (May 9-15, Gatlinburg USA) with the following abstract:

Using the mono-energetic neutron source facility of TIARA, JAERI, we have measured 1)the spectrum of the ^{7}Li(p,n) neutron source for 43 and 67 MeV protons, and 2)the double-differential cross sections of C(n,xp), (n,xd), (n,xt) reactions at En=40 and the 64 MeV.

* Cyclotron Radioisotope Center, Tohoku University
** Takasaki Establishment, Japan Atomic Energy Research Institute
*** Tokai Establishment, Japan Atomic Energy Research Institute

VIII–B–1

Spectrometry of Several Tens MeV Neutrons Penetrated through Concrete and Iron Shields Using Organic Liquid Scintillator

N. Nakao, T. Nakamura, M. Takada
Cyclotron and Radioisotope Center, Tohoku University, Sendai, Japan
Shun. Tanaka, H. Nakajima, Y. Sakamoto, Y. Nakane
Tokai Establishment, Japan Atomic Energy Research Institute, Tokai, Japan
Su. Tanaka
Takasaki Establishment, Japan Atomic Energy Research Institute, Takasaki, Japan
K. Shin
Department of Nuclear Engineering, Kyoto University, Kyoto, Japan

For shielding design of accelerator facility, estimation of high energy neutron attenuation through shielding material is essentially important. There have been several shielding experiments of neutrons having continuous energy, but very scarce for monoenergetic neutrons in the energy range above 15 MeV, because of the lack of available monoenergetic neutron beam line for shielding experiment.

We are now doing a systematic experiment on the penetration of quasi-monoenergetic neutrons in the energy range of 20 to 90 MeV through several shielding materials in the neutron beam line established at the AVF cyclotron of TIARA (Takasaki Ion Accelerator for Advanced Radiation Application) facility, Japan Atomic Energy Research Institute(JAERI). This study is one thema of 5-year cooperative research project on basic data for accelerator shielding between Universities and JAERI. In the present stage, we made an experiment on the penetration of 40.5 and 64.0 MeV quasi-monoenergetic neutrons through concrete and iron. These neutrons were produced from 3.6 mm and 5.2 mm thick ^{7}Li targets bombarded by 43 and 67 MeV protons which were extracted from the cyclotron, respectively. Protons passed through the Li target were bent down to the beam dump by a clearing magnet and neutrons ejected in the forward direction were extracted toward the experimental hall through the 220 cm thick concrete wall with a 10.9 cm diam collimator. The neutron beam was injected into 120 cm by 120 cm concrete slab of 25 to 200 cm thickness and 120 cm by 120 cm iron slab of 10 to 130 cm thickness, which were fixed in contact with the collimator exit located at 4 m from the target.

The spectra of neutrons without shield and penetrated through shield were measured with a 12.7 cm diam by 12.7 cm long organic liquid scintillator, BC-501A (Bicron Co. Ltd.), by coupling with the neutron-photon pulse shape discrimination technique. The scintillator was just set behind the rear shield surface on the neutron beam axis and at 20 and 40 cm off the beam axis. In advance to the spectrum analysis, the response function of this scintillator was measured with the TOF method using neutrons from Li and ^{9}Be targets bombarded by 65 MeV ^{3}He particles and 135 MeV protons. The experiments using 65 MeV ^{3}He particles and 135 MeV protons were done at the AVF cyclotron of Cyclotron and Radioisotope Center, Tohoku University and the Separate Sector cyclotron of Institute of Physical and Chemical Research, respectively. Figure 1 exemplifies the measured response functions comparing with the calculated ones.

The measured response functions were arranged into a matrix form of 1 MeV energy interval and compared with those calculated by the Monte Carlo code, SCINFUL[1]. The comparison showed good agreement below 20 MeV, but some discrepancy above 20 MeV, mainly at the light output corresponding to deuterons and alpha particles produced by ^{12}C(n,d) and ^{12}C(n,n'3α) reactions, owing to the inaccurate nuclear reaction model and light yields of charged particles.

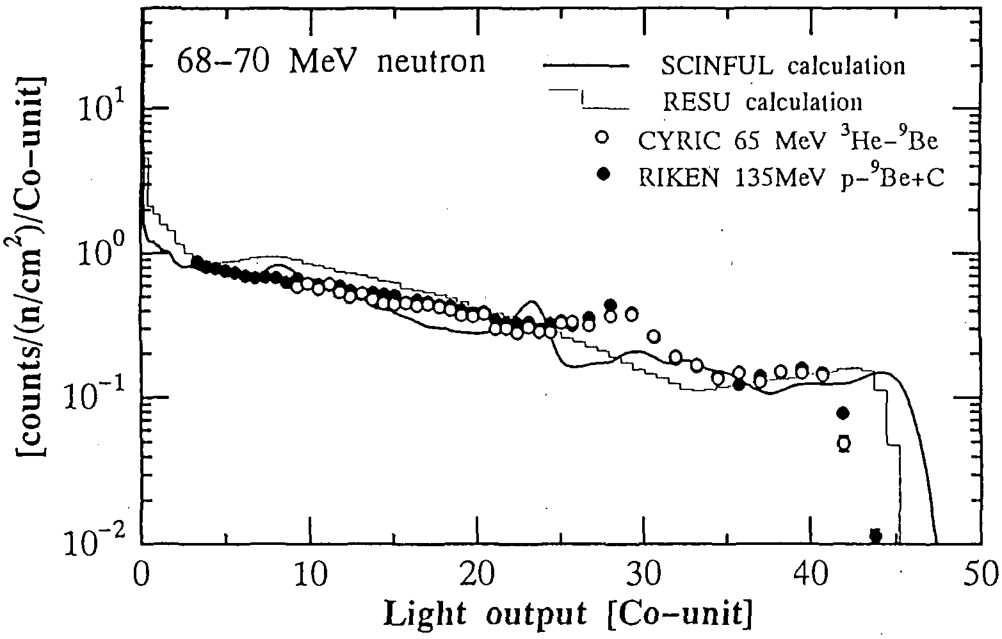

Fig.1 Neutron Response Function of BC501A in E_n=68–70 MeV

By using the measured response functions, we obtained the neutron spectra in the energy range above 3 MeV through the FERDOU[2)] unfolding code. Figure 2 and 3 exemplify the measured neutron spectra transmitted through concrete and iron, respectively, comparing with the calculated spectra. The measured energy spectra clearly give the exponential decrease of the monoenergetic peak neutrons and the energy spread of the peak width with penetrating the thick shield due to multiple small angle scattering. For concrete shield, the 1/E-shaped slowing-down spectra can be seen in the energy lower than about 20 MeV beyond 100 cm thickness, while on the other hand, the neutron spectra through iron shield show steep decrease down to several MeV.

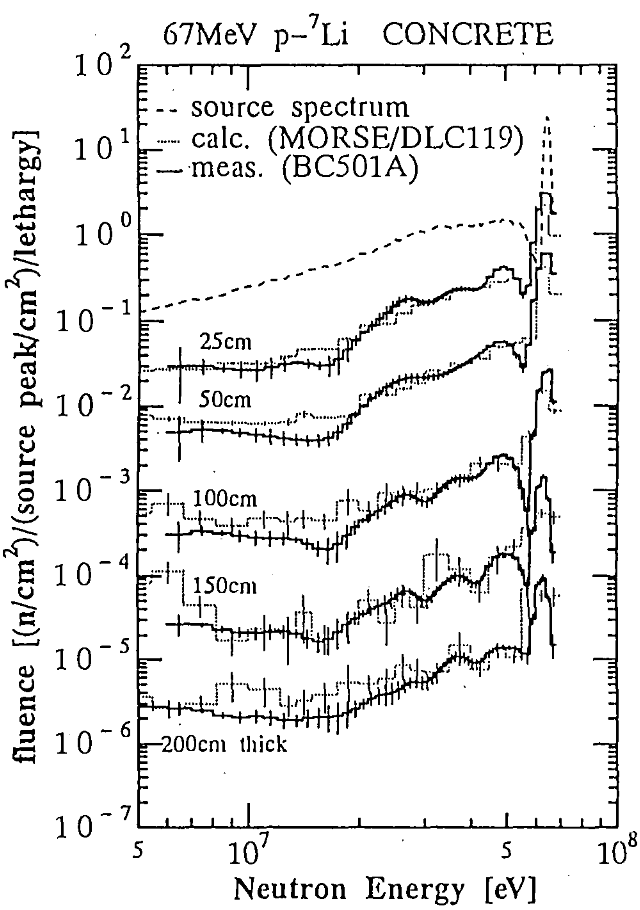

Fig.2 Neutron spectra transmitted through concrete shield using 67MeV p-^{7}Li neutron source

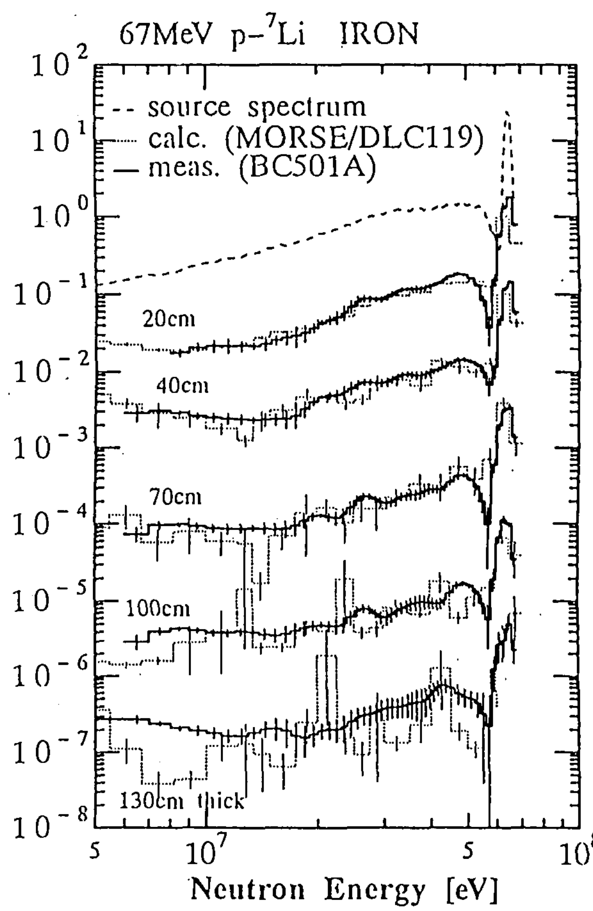

Fig.3 Neutron spectra transmitted through iron shield using 67MeV p-^{7}Li neutron source

The measured neutron spectra were compared with the MORSE[3] Monte Carlo calculation using the DLC-119/HILO86[4] group cross section library. The comparison revealed that the calculated spectra are in good agreement with the measured spectra, especially on the beam axis, excluding around the monoenergetic peak, since the DLC-119 cross sections have a group structure of 5 MeV interval above 30 MeV, on the contrary to the measured spectra given at every 1 MeV interval. From the measured results, the attenuation profiles in iron and concrete shields could be clarified for various neutron energies.

1) J. K. Dickens, ORNL-6463, Oak Ridge National Laboratory (1988)
2) K.Shin et al., Nucl. Technol., Vol. 53, 78 (1981)
3) G. R. Straker et al., ORNL-4585, Oak Rigde National Laboratory (1970)
4) R. G. Alsmiller Jr. et al., ORNL/TM-9801, Oak Rigde National Laboratory (1986)

VIII-B-2

Measurement of $^{12}C(n,2n\ \alpha)^{7}Be$, $^{27}Al(n,2n\ \alpha)^{22}Na$, $^{209}Bi(n,xn)^{20m}Bi$ Reaction Cross Sections in the Energy Range of 20 to 120 MeV

T.Nakamura, A.Konno, E.Kim, N.Nakao, M.Takada
Cyclotron and Radioisotope Center, Tohoku University
Y.Uwamino*, M.Imamura, T.Shibata, S.Shibata
Institute for Nuclear Study, Unversity of Tokyo

Successively with the neutron activation cross section measurements for various samples [1) 2)], we measured the $^{12}C(n,2n\ \alpha)^{7}Be$, $^{27}Al(n,2n\ \alpha)^{22}Na$ and $^{209}Bi(n,xn)^{20m}Bi$ cross sections in the energy range of 20 to 120 MeV. The quasi-monoenergetic neutrons were produced by $^{7}Li(p,n)$ reaction in the following three cyclotron facilities. At the Institute for Nuclear Study (INS), University of Tokyo, the five quasi-monoenergetic neutrons of 17.6 21.8, 27.6, 32.8 and 38.1 MeV peak energies were obtained by using the respective 20, 25 30, 35 and 40 MeV proton beam bombardment on 2mm-thick Li target backed by 12 mm thick carbon target. At the Takasaki Research Establishment (TIARA), JAERI, the three quasi-monoenergetic neutrons of 40.5, 55.5 and 64.5 MeV peak energies were obtained by 43 58.2 and 67 MeV protons , respectively. The neutron beam was collimated into 10 cm diameter through 220 cm concrete wall and the protons passed through the target were bent down to the beam dump by a clearing magnet. At the Institute of Physical and Chemical Research (RIKEN) the protons of 90, 100, 110 and 120 MeV energies were extracted from the Ring Cyclotron and injected into 1 cm thick Li target, and the protons passed through the target were also bent down to the beam dump. The neutrons produced in the forward directon were extracted through 22cm × 22cm in aperture and 1.2 m long concrete collimator which was fixed 7.2 m behind the target. the neutron spectra in these fields were measured by the TOF method using the BC501A and NE-213 liquid organic scintillators and the peak neutron fluence during sample irradiation was determined from the ^{7}Be yield produced in the target by the transition to the ground and the first excited states of ^{7}Be due to $^{7}Li(p,n)^{7}Be$ reaction. The activities induced in carbon, aluminum and bismuth samples which were irradiated in these neutron fields were measured with the HP-Ge detector to identity the produced radionuclides and their radioactivities. We are now analyzing our measured results. Table 1 shows the examples of identified radionuclides and their physical quantities. Some cross section data obtained in our experiments are shown in Fig.1, together with the calculated results by Fukahori [3)].

Reference:

1)T.S.Soewarsono : "Development of p-Li Monoenergetic Neutron Field and Measurement of Neutron Activation Cross Sections" Doctor Thesis, Department of Nuclear Engineering, Tohoku University (1993)

2)Y.Uno : "Measurement of Activation Cross Sections Using 15-40 MeV Quasi-Monoenergetic Neutrons" Master Thesis, Department of Nuclear Engineering,Tohoku University (1993)

3)T.Fukahori : ENDF／B-VI

---

*Present Address: Institute of Physical and Chemical Research

Table 1 : Examples of Identified Radionuclides and Their Physical Quantities

Reaction	Nuclide	Half life	Thesehold energy [MeV]	Photon energy [MeV]	Intensity [%]
$^{209}Bi(n,3n)^{207}Bi$	^{207}Bi	32.2y	14.4	0.569 1.063	97.8 74.9
$^{209}Bi(n,4n)^{206}Bi$	^{206}Bi	6.24d	22.6	0.803 0.881	98.9 66.2
$^{209}Bi(n,5n)^{205}Bi$	^{205}Bi	15.3d	29.6	0.703 1.764	31.1 32.5
$^{12}C(n,2n\,\alpha)^{7}Be$	^{7}Be	55.3d	28.5	0.478	10.4
$^{27}Al(n,2n\,\alpha)^{22}Na$	^{22}Na	2.60y	23.5	1.275	99.9

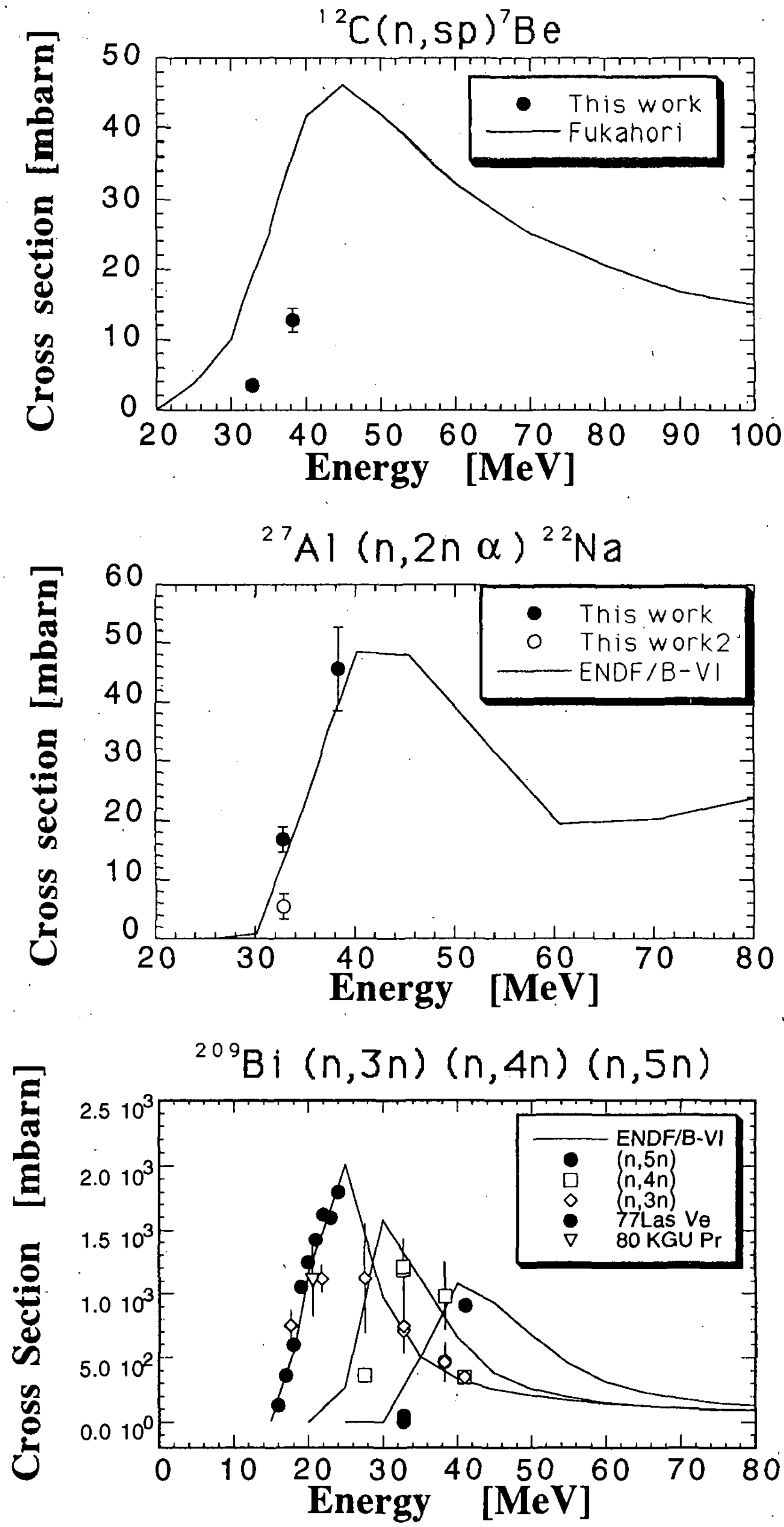

Fig. 1 Measured and calculated cross section data of $^{12}C(n,2n\ \alpha)^{7}Be$

$^{27}Al(n,2n\ \alpha)^{22}Na$, $^{209}Bi(n,3n)$, (n,4n), (n,5n) reactions

C. Laboratory of Nuclear Science

VIII–C–1 Study of the reactions ^{6}Li(e,e'p) and ^{6}Li(e,e't)

T. Hotta, T. Tamae, T. Miura, H. Miyase*, I. Nakagawa, M. Sugawara,
T. Tadokoro, A. Takahashi, E. Tanaka and H. Tsubota*

^{6}Li(e,e'p) and ^{6}Li(e,e't) cross sections have been measured using a134MeV continuous electron beam at energy transger between 27 and 37 MeV and momentum transfer of 61MeV/c on an average. Scattered electrons were measured at 26°. Charged particles emitted from the target were detected with Si-solid-state detectors arranged out of the scattering plane (ϕ=–45° and ϕ=–135°).

In the ^{6}Li(e,e'p) reaction, events corresponding to the protons emitted from the p-shell (E_m=2-8MeV) and the s-shell (E_m=20-23MeV) are identified as two peaks in missing-energy spectra (Fig. 1). There exist the events corresponding to the three-body a-p-n final state between those peaks. Measured angular distributions fitted with Legendre polynomials for each reaction channels are shown in Fig. 2. No remarkable difference is observed among those angular distributions. There exists a large component of $P_3(\cos\theta)$ in all cases. The result of the fitting suggests that higher multipoles than E1 contribute to these reactions.

In the ^{6}Li(e,e't) reaction, the angular distribution corresponding to the two-body t-^{3}He final state is shown in Fig. 3. The result indicates a strong C1(E1) contribution to this reaction. There is little $P_3(\cos\theta)$ component in the polynomials. An inteference between C1(E1) and C0 or M1 components is presumed to produce the asymmetric angular distribution. The multipolarities for this reaction is expected to be sensitive to different cluster model description of the ground state of ^{6}Li and the reaction mechanism itself.

We have carried out the ^{6}Li(e,e'x) experiment at higher energy and momentum transfer regions and also the ^{7}Li(e,e'x) experiment at energy transfer between 7 and 37 MeV. The data analysis is now underway.

*Department of Physics, Tohoku University

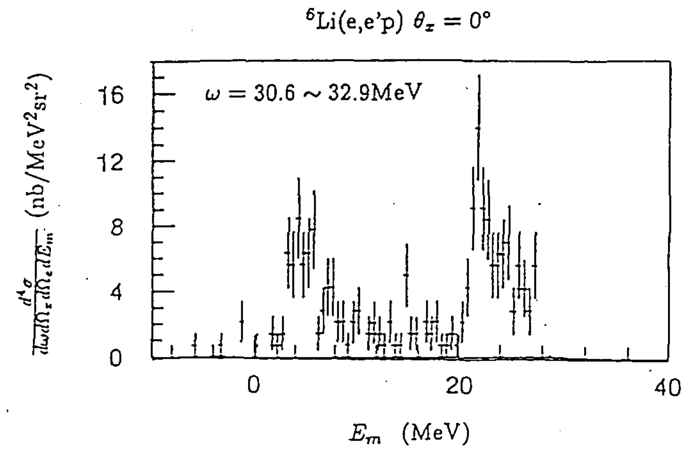

Fig. 1. Missing-energy spectrum for the ^{6}Li(e,e'p) reaction at $\theta = 0°$

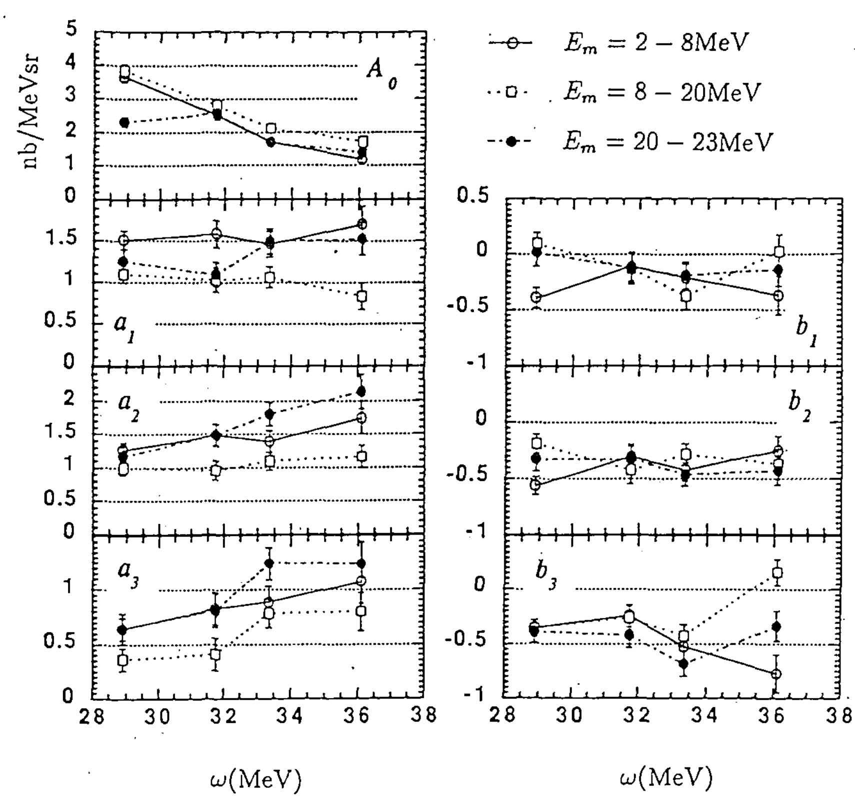

Fig. 2. The angular distributions for the ^{6}Li(e,e'p) reactions.

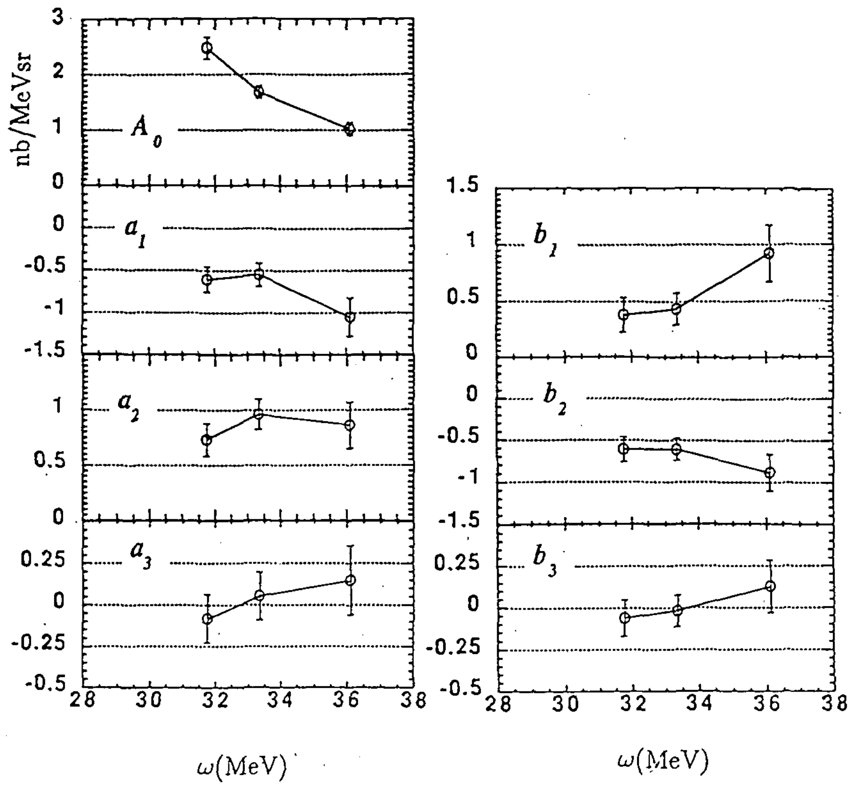

Fig. 3. The angular distributions for the ^{6}Li(e,e't)^{3}He reaction.

VIII–C–2 The ^{92}Mo(e,e'p) coincidence cross section in the giant resonance region

T.Miura, E.Tanaka, T.Hotta, H.Miyase*, I.Nakagawa, M.Sugawara, T.Tadokoro, A.Takahashi, T.Tamae and H.Tsubota*

In order to obtain infomation for the isospin splitting and multipolarities of giant resonances, the cross section and angular distributions for the reaction ^{92}Mo(e,e'p) were measured at transfered energies from 12 to 37 MeV and transfered momentum q~ 0.29 fm^{-1}. An enriched ^{92}Mo target (98.3% purity) was bombarded with a 129 MeV continuous electron beam, and scattered electrons were measured at θ_e= 26°. Emitted protons were detected with six detector telescopes set at an azimuthal angle ϕ= -90°, each of which consists of three or four Si-diode detectors. Their polar angles are 0°, 30°, 60°, 90°, 180° and 210°

An analysis in the excitation energy range of 17-27 MeV has been carried out so far, and a missing energy spectrum is shown in fig.1. One of two narrow peaks corresponds to a doublet of the ground state (9/2$^+$) and the 1st-excited state (0.10 MeV;1/2$^-$), another to a triplet of the 4th- (1.32;3/2$^-$), 5th- (1.62;3/2$^-$) and 6th- (1.85;5/2$^-$) excited states of ^{91}Nb, respectively. A broad peak probably due to a statistical decay process is also observed. In fig.2, the values of the Legendre fitting parameter A_0 for two narrow peaks are shown with open circles, and the A_0 values of the (e,e'p_{total}) reaction with closed circles. The shape of the cross section are smooth over the entire energy region, in contrast to the (γ,p) cross section (solid line in the figure) measured by Shoda *et al.*[1] using the yield curve method.

Reference:

1) K. Shoda *et al*. : Nucl. Phys. A239, 397 (1975).

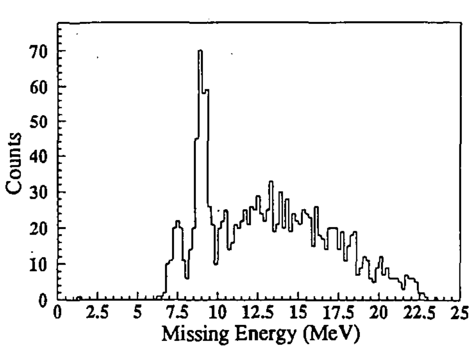

Fig.1 Missing energy spectrum of the ^{92}Mo(e,e'p) reaction.

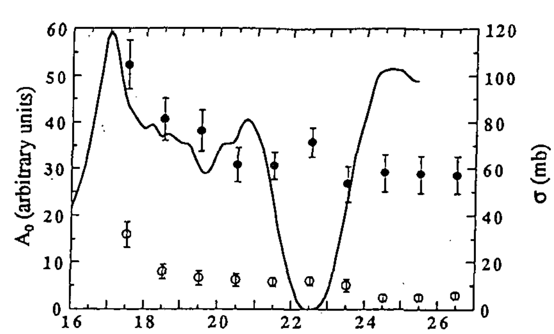

Fig.2 Cross sections for the ^{92}Mo(e,e'p) and ^{92}Mo(γ,p) reactions. Closed circles : (e,e'p_{total}), open circles : (e,e'p_{1-6}), solid line : (γ,p).

*Department of Physics, Tohoku University

VIII-C-3

Angular distribution for the $^{16}O(e, e'n_0)^{15}O$ reaction in the giant resonance region

Y. Suga, T. Saito, M. Oikawa, T. Tohei*, T. Nakagawa*,
K. Abe** and H.Ueno***

A theoretical analysis of proton and neuron coincidence electron scattering reactions on ^{16}O at low momentum transfer were performed by Cavinato et al. in the frame-work of a self-consistent random-phase approximation theory in the energy continuum.[1] In their calculation, the $^{16}O(e, e'p_0)$ and $^{16}O(e, e'n_0)$ angular distributions show the characteristic feature corresponding to interference between a T=0 and a T = 1 resonant amplitudes, viz. the proton angular distribution is forward peaked, while the neutron angular distribution is backward peaked.

Angular distributions for the $^{16}O(e, e'n_0)$ reaction has been measured using ten NE-213 liquid-scintillators and a continuous electron beam from the 150 MeV pulse stretcher ring. The angular distribution at $\omega = 21$ MeV is shown in Fig. 1. The experimental angular distribution is forward-backward symmetric peak against backward-peak prediction (solid line). The dashed line shows multipole expansion fit. Calculation is normalized at 30° of the fitting curve.

Reference:

1) M. Cavinato et al. : Phys. Rev. C37, 1823 (1988).

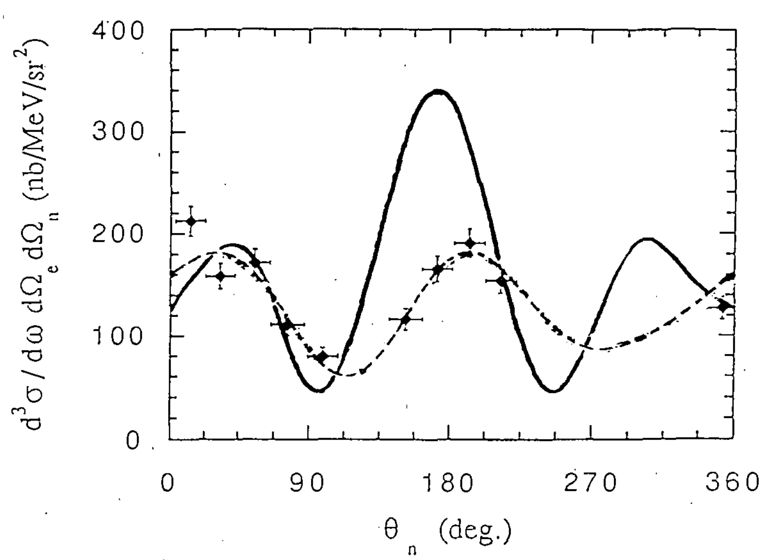

Fig. 1 Angular distribution for the $^{16}O(e, e'n_0)$ reaction at $\omega = 21$ MeV. Solid and dashed lines are RPA prediction and multipole expansion fit, respectively.

*Department of Physics, Tohoku University
**Department of Nuclear Engineering, Tohoku University
***Department of Physics, Yamagata University

VIII–C–4 Observation of the giant quadrupole resonance in $^{13}C(\gamma,n)$ reaction

S.Ito, H.Itoh, O.Konno, K.Maeda* H.Matsuyama, T.Murakami**, T.Sasaki,
T.Suda*, M.Takeya and T.Terasawa

Isovector Giant Quadrupole Resonance (IVGQR) has been studied by observing the forward-backward asymmetry in (γ,n) and (γ,p) reactions and their inverse reactions .The asymmetry ($A = \{(d\sigma/d\Omega)_{55^o}-(d\sigma/d\Omega)_{125^o}\}/\{(d\sigma/d\Omega)_{55^o}+(d\sigma/d\Omega)_{125^o}\}$) caused by interference between E1 and E2 transition gives a sensitive information of the E2 excitation. Especially, the (γ,n) reaction has been considered to be one of the most elegant tool to study E2 resonances, because the E2 effective charge of a neutron is much smaller than that of a proton.

We have carried out the $^{13}C(\gamma,n)$ experiment in an excitation energy range of E_x = 17~72 MeV by using the tagged photon facilities at Laboratory for Nuclear Science, Tohoku University. Neutrons following the $^{13}C(\gamma,n)$ reaction were measured by newly developed large volume liquid-scintillation detectors which were placed at θ_{lab} = 55^o, 90^o and 125^o. We deduced the asymmetries (A) of the neutron groups, $n_{(g.s.)}$and $n_{(15.1)}$,leaving around the ground (T=0, $J^\pi=0^+$) and the excited 15.1 MeV (T=1, $J^\pi=1^+$) states in ^{12}C, respectively (Fig. 1).

Closed and open circles represent A of $n_{(g.s.)}$and $n_{(15.1)}$ respectively. Solid and dashed lines are the results of direct-semidirect model calculation by employing the computer code HIKARI. The locations and the widths of E1 resonances are Ex= 11.5 MeV Γ= 5.0 Mev, and Ex= 20.2 Γ=3.5 MeV. Assumed parameters are the location of the IVGQR at 25 MeV and the width of 12 MeV (solid line), and at 38 MeV and of 12 MeV (dashed line). The isospin splitting of the IVGQR might be suggested. The excitation functions for $n_{(g.s.)}$ and $n_{(15.1)}$ are also deduced, and the E_x dependence of them show different behavior.

*Department of Physics, Tohoku University
**Department of Physics, Kyoto University

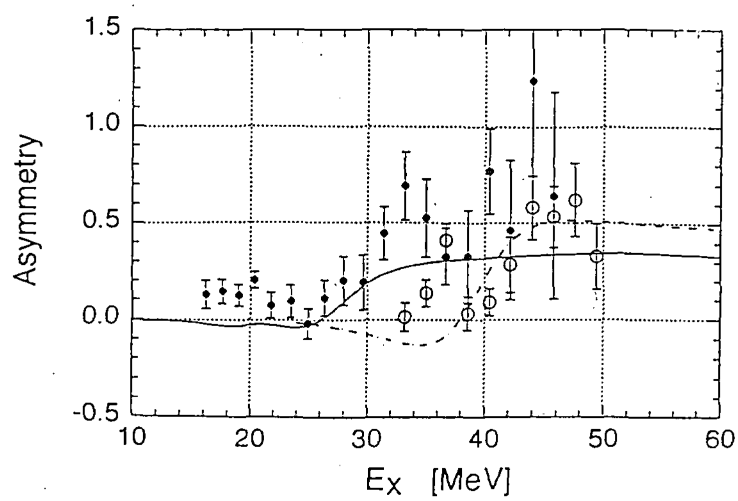

Fig.1 The E_X dependence of the forward-backward asymmetry in the $^{13}C(\gamma,n)^{12}C$ reaction. Closed and open circles represent the neutron groups leading to the ground and 15.1 MeV states in ^{12}C. Curves represent the results of direct-semidirect model caluculation.

VIII–C–5 The $^{28}Si(\gamma, \pi^{\pm})^{28}Al$ Reaction

H. Tsubota*, T. Taniuch, H.Yamazaki, K. Shoda, T. Yamaya* and M. Saito*

Pion energy spectra and angular distributions of the $^{28}Si(\gamma, \pi)^{28}Al$ reaction near the threshold have been measure with 200 MeV electrons. New strong spin-isospin flip transitions leaving residual excited states at around 4.0, 7.0, and 10.0 MeV in ^{28}Al are found in the spectra. The angular distributions for E_X=4.0 and 7.0 MeV states are shown in the figures. Although the experimental errors are large, the angular distributions are almost isotropic, indicating complexity of these transitions. DWIA calculations with shell model wave functions by Donnelly and Walker[1] are made using Ohtsubo code, where M2, M4, and M6 transitions are included. The results multiplied by a reduction factor n are shown in the figures by solid curves. All calculations overestimate. The additional experiment has been carried out and the data in analysis. More detailed experimental data and theoretical discussions will be given in time.

Reference:
1) T. W. Donnelly and G. E. Walker: Annals of Phys. 60, 207 (1970).

*Department of Physics, Tohoku University

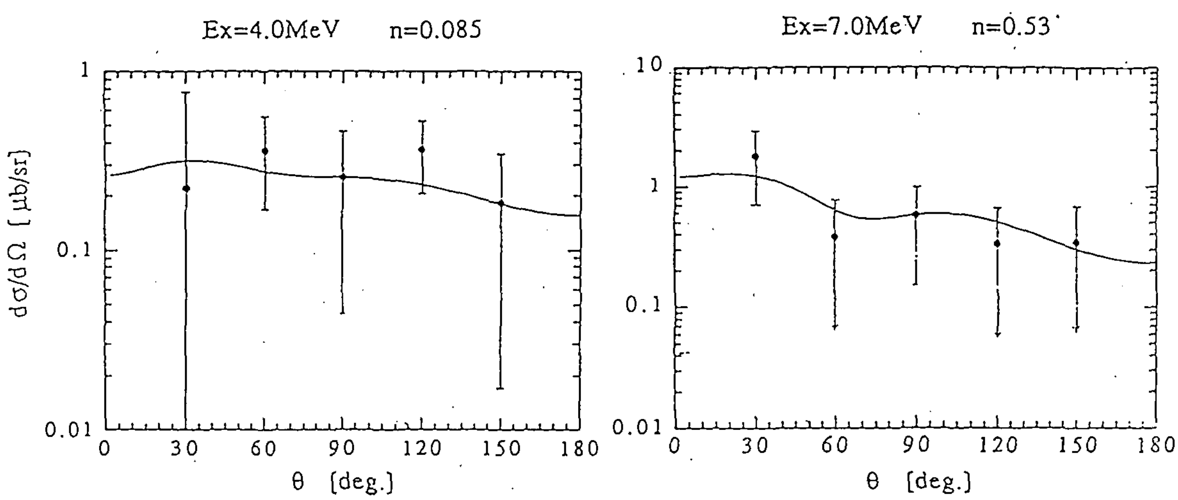

Fig. 1 Angular distributions of $^{28}Si(\gamma, \pi^{+})^{28}Al$ cross sections.

IX. The University of Tokushima

A. Department of Mathematical and Natural Sciences

IX–A–1 Elastic Proton Scattering from Boron Isotopes

N. Koori, K. Ichiba, Y. Watanabe⁺, H. Shinohara⁺, T. Michibata⁺, H. Ijiri⁺,

K. Sagara⁺⁺, H. Nakamura⁺⁺, K. Maeda⁺⁺, and T. Nakashima⁺⁺

We have been studying experimentally and theoretically the mechanism of proton-induced reactions on light and medium-heavy nuclei, paying special attention to the continuum in the energy spectra of emitted particles[1-4]. In our program of polarized proton experiments covering the energy range 12-16 MeV, several data on elastic and inelastic proton scattering have also been accumulated for the 1p-shell nuclei. These data are analyzed on the basis of the optical model and the coupled channel (CC) method and are compared with available neutron data. Among these results, the analyses of elastic proton scattering from ^{10}B and ^{11}B with the spherical optical model (SOM) are described in this report.

Recently we have measured differential cross sections and analyzing powers for elastic and inelastic scattering from ^{10}B and ^{11}B. Figure 1 shows, as examples, the measured angular distributions of the elastic scattering from ^{11}B at 14 MeV. The SOM fitting by means of the ECIS88 code was carried out to the present data for ^{10}B and ^{11}B. The parameter sets of Dave

⁺ Department of Energy Conversion Engineering, Kyushu University.
⁺⁺ Department of Physics, Kyushu University.

and Gould[5] were used as the initial parameter set of the search in the code, after correction to the Coulomb force. As similarly to Woye et al.[6], the search have been done finally for the parameters including the imaginary part of the spin-orbit term; the results are shown in Table I. The results of SOM fits for ^{11}B are shown by solid lines in Fig.1; the angular distributions of cross section and analyzing power are well reproduced by the parameters.

It is interesting that W_{SO} were obtained to be a negative small value, as found in the table. Brieva and Rook[7] have estimated theoretically the ratio W_{SO} / V_{SO} is to be - 0.05, if the real and imaginary spin-orbit terms are taken into account in the optical model. The presently obtained values for the ratio are similar (- 0.03 for ^{11}B and - 0.06 for ^{10}B) to the proposed one. Further analyses will be necessary to investigate the effect in detail.

References

[1] N. Koori et al., JAERI-M 89-167 (1989).
N. Koori et al., JAERI-M 91-009 (1991).
N. Koori et al., JAERI-M 92-029 (1992)

[2] Y. Watanabe et al: Proc. 1990 Symp. on Nuclear Data, JAERI-M 91-032 (1991) p.336.

[3] Y. Watanabe et al., Proc. Int. Conf. on Nuclear Data for Science and Technology

[4] Y. Watanabe et al., Proc. XXth Int. Symp. on Nuclear Physics, Nuclear Reaction Mechanism, p.151 (1990).

[5] J.H. Dave and C.R. Gould, Phys. Rev. C **28**, 2212 (1983).

[6] E. Woye et al. Nucl. Phys. **A394**, 139 (1983).

[7] F.A.Brieva and J.R. Rook, Nucl. Phys. A307, 493 (1978).

Table I. Optical potential parameters for ^{11}B and ^{11}B at 14 MeV.

	V_R (MeV)	r_R (fm)	a_R (fm)	W_D (MeV)	r_I (fm)	a_I (fm)	V_{SO} (MeV)	W_{SO} (MeV)	r_{SO} (fm)	a_{SO} (fm)
^{11}B	63.44	1.046	0.642	8.41	1.478	0.360	9.63	-0.28	0.828	0.551
^{10}B	57.54	1.193	0.679	16.85	1.384	0.176	3.63	-0.23	1.172	0.478

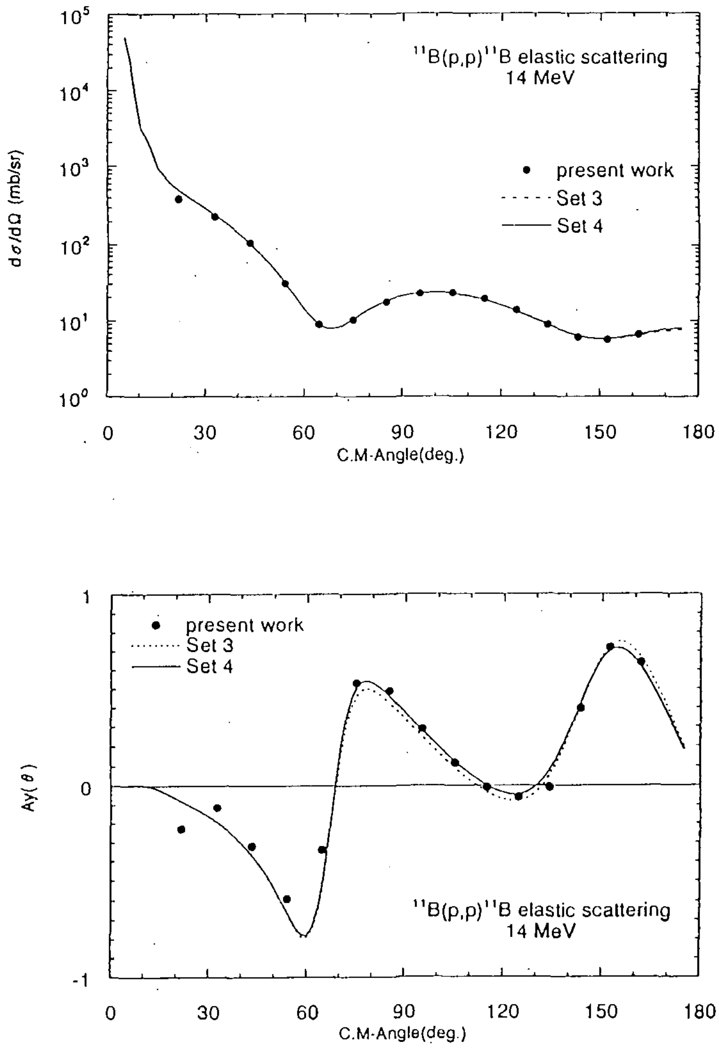

Fig.1. Comparison of experimental differential cross sections and analyzing powers of ^{11}B(p,p) elastic scattering at 14 MeV with the SOM fits. Solid lines (Set 4) show the result calculated by the parameters given in Table I.

IX–A–2 Elastic and Inelastic Scattering of Protons from Oxygen-16

N. Koori, Y. Watanabe+, H. Hane+, Kashimoto+, A. Aoto+, H. Ijiri+,

K. Sagara++, H. Nakamura++, K. Maeda++ and T. Nakashima++

A paper on this subject was published as JAERI-M 94-011 (1994) with the following abstract:

Double differential cross sections of the $^{16}O(p,p'x)$ reaction and differential cross sections and analyzing powers of polarized proton elastic and inelastic scattering were measured at 14 and 16 MeV. The optical potential parameter set, which was derived for ^{16}O from the spherical optical model analysis, reproduces the elastic scattering data fairly well. Large differences are found in the potential depths of the imaginary and spin-orbit terms between 14 and 16 MeV. This may be due to strong resonance structure in the compound nucleus of ^{17}F.

+ Department of Energy Conversion Engineering, Kyushu University.
++ Department of Physics, Kyushu University.

X. Tokyo Institute of Technology

X-A-1 Neutron Effective Charge for E1 Transitions from Broad Neutron Resonance in p-Shell and sd-Shell Nuclei

H. Kitazawa

A paper on this subject has been accepted by Nuclear Physics A for publication.[1)]

Strong retardation of p→d and d→p single-particle transitions, previously observed for primary E1 transitions from broad neutron resonances on p-shell (^{9}Be) and sd-shell (^{24}Mg) nuclei,[2)] are found to be well explained by using a renormalized neutron effective charge $e_f(E1)$ which takes account of the coupling between those single-particle motions and the giant-dipole resonance excitation in the target nucleus :

$$e_f(E1) = -\frac{Z}{A} e \left(1 - \frac{1}{2} v_1 \alpha \frac{\langle j_2 | rf(r) | j_1 \rangle}{\langle j_2 | r | j_1 \rangle} \frac{E_R}{E_R^2 - \Delta E_{21}^2}\right),$$

where E_R is the GDR energy, ΔE_{21} is the single-particle transition energy, v_1 is the symmetry-potential strength, and f(r) is a Wood-Saxon potential form factor. The reduction factor α is related to the non-energy weighted sum rule for the isovector-dipole mode.

In the capture process, the dipole-transition moment may receive an appreciable contribution from the external region of the nucleus, and thus the polarization effect depends on a residual form factor for the dipole field. In the 1d→1p transition in the ^{10}Be nucleus, however, the effect is not so sensitive to the form factor, because the radial wave functions of the initial and final single-particle states have no node in the nuclear internal region. For the 2p→1d transition in the ^{25}Mg nucleus, a more refined radial form factor is used to explain the observed E1 retardation.

References:

1) H.Kitazawa, M.Igashira, S.Shibata, K.Tanaka, H.Takakuwa, and K.Masuda, Nucl. Phys. A575, 72-84(1994).
2) H.Kitazawa and M.Igashira, Proc. 8th Int . Symp. on Capture Gamma-Ray Spectroscopy and Related Topics, Fribourg, Switzerland, 1993(World Scientific, 1994) p.558.

XI. Toshiba Corporation

A. Nuclear Engineering Laboratory

XI-A-1 High Energy Nuclear Data Calculation on Si and Cu using ALICE-F

Tadashi IKEHARA , Kazuki HIDA, and Tadashi YOSHIDA

Neutron and proton induced cross sections have been evaluated for silicon and copper in the energy range 20 MeV to 1 GeV using the ALICE-F code system[1]. The results are in good agreement with experimental values, and have been compiled and stored in the ENDF-6 format.

Introduction

Recently, the need for nuclear data in the high energy region has been increased in many fields, including spallation neutron sources, accelerator shielding design, and space radiation on astronauts and their equipment. Such high energy data, however, have not been available in a satisfactory form for users. The purpose of this study is to test the validity of the ALICE-F code system[1] in evaluating proton and neutron nuclear data in the energy range 20 MeV to 1 GeV for silicon and copper. The results obtained are compiled and stored in the ENDF-6 format. These data are particularly useful in analyzing the effects of cosmic rays on electronics devices.

The ALICE-F code system consists of the ALICE-F code for calculating cross sections, and a postproccesing code, PEND6F. ALICE-F is based on the evaporation and pre-equilibrium models, and is applicable to nuclear reaction calculations in the MeV and GeV energy range. PEND6F compiles the results calculated by ALICE-F in to the ENDF-6 format. Moreover, PEND6F can also produce values for total cross sections, non-elastic cross sections, and elastic cross sections through use of systematics[2] and then overlay the ALICE-F results with these values.

Model Parameters

To obtain reliable results, it is necessary to search for the best ALICE-F parameters by comparing the calculated results with experimental data. However, recommended values chosen to reproduce general experimental data for the range from light to heavy elements are prepared as defaults. In the this work, therefore, the search and adjustment is limited to the following four parameters:

1. OMP, sharp cut-off model, systematics: for inverse reaction cross section models
2. HM, GDH: for pre-equilibrium process models
3. (MP, LDOPT)=(2, 1), (0, 0), (3, 0): for level density formulas
4. a=A/7, A/9, A/11: for the level density parameters

Default values are selected for the rest of the theoretical parameters. The above parameters were chosen by comparing the calculated results with experimental data for ^{63}Cu(p, x) reactions, and the following set is selected: OMP, GDH, MP=2, LDOPT=1, a=A/9.

Calculated results

By using the parameter set selected above, nuclear data for ^{28}Si, ^{29}Si, ^{63}Cu, and ^{65}Cu were calculated. Some of the results are shown here.

The total and non-elastic cross sections for ^{28}Si and ^{63}Cu were calculated. The results with both the ALICE-F code and Pearlstein's systematics are compared with the ^{nat}Si and ^{nat}Cu experiments in Figs. 1 and 2. Although, the systematics reproduces the experimental data well, the ALICE-F code underestimates the experimental values.

Other calculations for double differential cross sections and reaction cross sections were also performed, and the results mostly reproduced the experimental data. An example of a ^{65}Cu(p, x) reaction cross section is shown in Fig. 3.

References

1) T. Fukahori, "ALICE-F calculation of Nuclear Data up to 1 GeV", Proc. Specialists' Mtg. on High Energy Nucl. Data, JAERI-M 92-039 (1992).
2) A. J. Koning, "Review of High Energy data and Model Codes for Accelerator-Based transmutation", Report NEA/NSC/DOC(92)12, (1992) OECD-NEA
3) Auman, M. et al., Phys. Rev., C5 (1972) 1, Culler, V. et al., Phys. Rev., 99 (1955) 740, and Larson, D. et. al., Proc. 1980 BNL Conf., p. 277
4) Culler, V. et al., Phys. Rev., 99, Larson, D. et. al., Proc. 1980 BNL Conf., p. 277, Bowen, P. H. et. al., Nucl. Phys., 22 (1961) 640, Franz, J. et. al., Nucl. Phys., A490 (1988) 667, Schimmerling, W., Phys. Rev., C7 (1973) 248, Taylor A. E. and Wood E., Phil. Mag., 44 (1952) 95, Schneider R. J. at al., Nucl. Phys. A119 (1968) 197, Ashmore A. et. al., PPS, A70 (1957), and De Juren J. et. al., Phys. Rev., 80 (1950) 27
5) Pulfer, P. :no reference available except EXFOR database, Albouy G. et. al., JPR (1962) 1000, and Meadows J. W. et. al., Phys. Rev., 91 (1953) 885

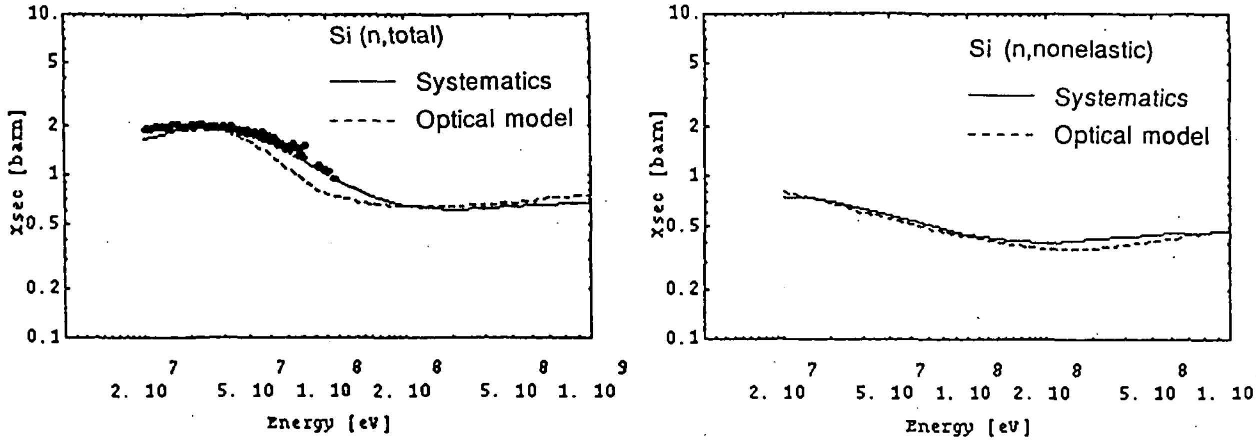

Fig. 1. Total and non-elastic cross sections for Si compared with experimental data[3)]

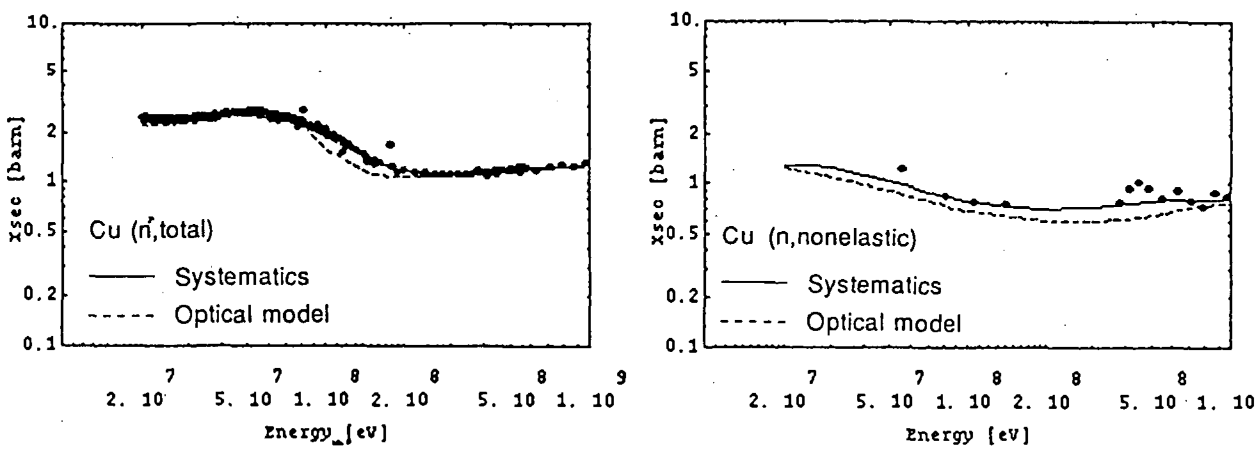

Fig 2. Total and non-elastic cross sections for Cu compared with experimental data[4)]

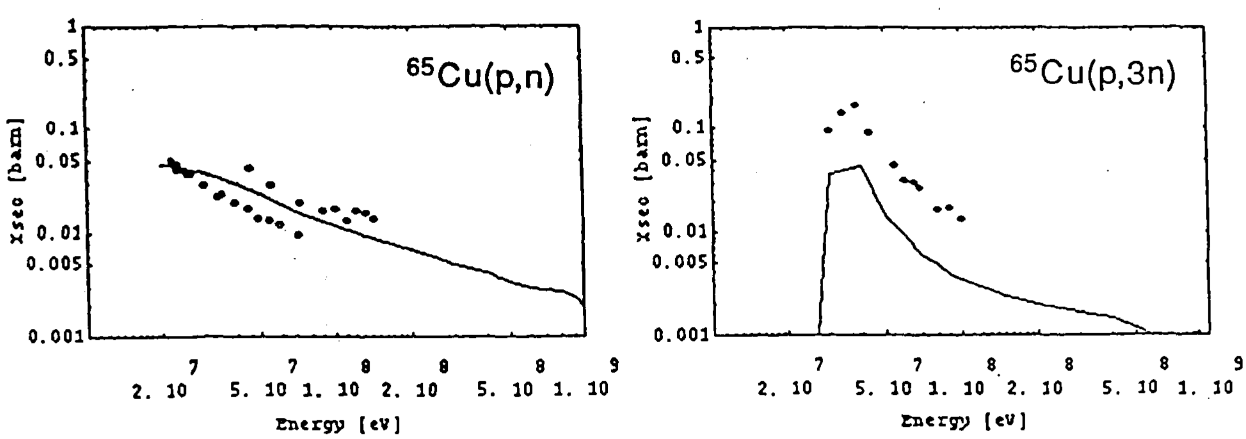

Fig3. ^{65}Cu(p, x) reaction cross sections compared with experimental data[5)]